Macromolecules

Perspective

pubs.acs.org/Macromolecules

# *50th Anniversary Perspective*: Polymer Crystals and Crystallization: Personal Journeys in a Challenging Research Field

Bernard Lotz,[†] Toshikazu Miyoshi,[‡] and Stephen Z. D. Cheng*[,‡]

[†]Institut Charles Sadron (CNRS − Université de Strasbourg), 23, Rue du Lœss, 67034 Strasbourg, France

[‡]Department of Polymer Science, College of Polymer Science and Polymer Engineering, The University of Akron, Akron, Ohio 44325, United States

**ABSTRACT:** Analyzing and understanding the structure and morphology of crystalline polymers has been and remains to be a major challenge. Some of the issues have resisted analyses for decades. The present account illustrates how individual contributions help build a body of knowledge that must cover length scales ranging from submolecular features to morphology and correlates them with bulk properties. Emphasis is put on structures and morphologies as formed spontaneously. Possible extension of the research area to connected fields is illustrated with a development on supramolecular crystals.

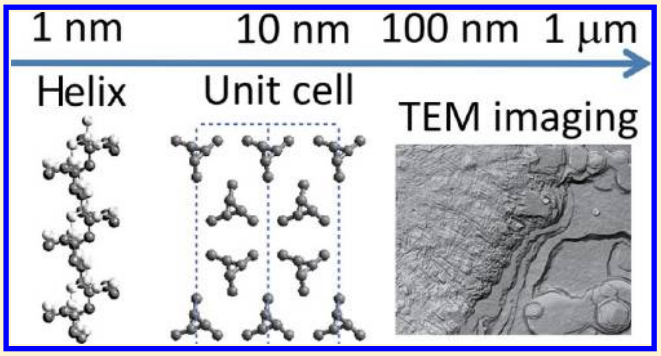


## INTRODUCTION

Polymer crystal and crystallization were initially discussed in cellulosic and bio-related natural polymers in the first half of the past century. Mostly in its second half, many synthetic polymers were invented and successfully commercialized. Summarizing this field, Andrew J. Lovinger stresses the importance of these different synthetic polymers, the majority of which are crystalline. Scientific investigation of crystalline polymers has quickly developed, which has been described as a "big bang" over 60 years ago. "This started the discovery of polymer single crystals, lamellae, and chain folding. Explosive growth followed in the ensuing few decades based on the detailed studies of crystallization, annealing, and melting, the determination and control of molecular conformations, crystal structures, and morphologies, the heated debates over crystal-growth models and the validity and extent of chain folding, the elucidation and exploitation of mechanical, optical, and other physical properties."[1]

"Frequently, however, something new and revolutionary may become so successful that it ends up eventually being taken for granted." "Crystalline polymers are still so critically important—after all, 70% of all commercial polymers are crystalline—including an enormous number and variety of materials in our daily lives and in all kinds of high-technology applications. Crystalline polymers have become so pervasive that we just take them for granted. Polymer researchers have moved on to newer areas of more current appeal (for example, block copolymers, hybrids, nano-everything, bio-, ...)."[1]

"But—have the major questions in crystalline polymers been solved? Has it been time to move on? No, not by a long shot. What happened is that some of the unsolved problems have led to intense controversies or dead ends, and researchers in crystalline polymers have focused their attention more and more on ever narrower problems and ever more specialized materials. Most of us have been cultivating our own 'trees of knowledge', working on our favorite polymers, properties, or techniques. Sometimes our efforts extend beyond these individual 'trees' and build a little 'groove' as we address, for example, families of related polymers or properties of greater breadth. But, as the saying goes, we generally keep missing the forest for the trees."[1]

The purpose of this Perspective is certainly not to cover all the important topics in polymer crystals, their crystallization processes, and properties. We will merely report on some interesting and challenging topics we have faced during the past several decades in our own research "grooves", taking this opportunity to summarize some major points of current understanding of crystalline polymers and to indicate possible future directions in this field.

## CRYSTAL STRUCTURE DETERMINATION

Crystalline polymers are first and foremost characterized by their crystal structures at the unit cell level. The structure determination relies mostly on wide-angle X-ray fiber diffraction and techniques such as infrared, Raman, and nuclear magnetic resonance spectroscopies. The diffraction principle and methodologies to determine crystalline lattice are well established since the early years of the past century—Bragg's law, crystallographic symmetry and space groups, Fourier transformation of a real space to a reciprocal space, etc. The advent of synchrotron X-ray diffraction widens the range of accessible wavelengths; since using shorter wavelengths

**Received:** May 2, 2017
**Revised:** July 24, 2017
**Published:** August 22, 2017





DOI: 10.1021/acs.macromol.7b00907
*Macromolecules* 2017, 50, 5995−6025

makes it possible to access a wider part of the reciprocal lattice; and using electron diffraction and titling diffraction techniques to determine unit cell structures of lamellar single crystals with only a few tenths of a nanometer thick crystals; development of more sensitive cameras makes it possible to follow kinetics of phase transformations, and many others. With solid developments in knowledge of macromolecular crystallography, phase structures, and morphologies, a significant contribution stems from the technical availability of user-friendly data analysis, modeling, and energy minimization software—the Cerius 2 program—which is at present used in or as a complement to virtually every polymer structure determination.

Whereas a large number of crystal structures have been established in the past, these technical improvements not only help in analyzing crystalline structures in newly synthesized crystalline polymers but also provide new approaches in recognizing ever more complex materials or the impact of structural or chemical defects—side chains as in linear low-density polyethylene (PE)—and stereodefects in other crystalline polymers as well as recognizing polymorphisms.

This can be best illustrated by a recent investigation of the structure of the alpha phase of poly(L-lactic acid) ($\alpha$-PLLA).[2] The $\alpha$-PLLA phase has an irrational helix made of ten residues in three turns, with a helix repeat distance of nearly 3 nm. Two antiparallel helices are housed in an orthorhombic cell, the symmetry of which differs from that of the helix, that is thus deformed. The use of a high-energy beam from a synchrotron source with a wavelength 0.0328 nm has helped record nearly 700 reflections at −150 °C (Figure 1a). A deuterated sample

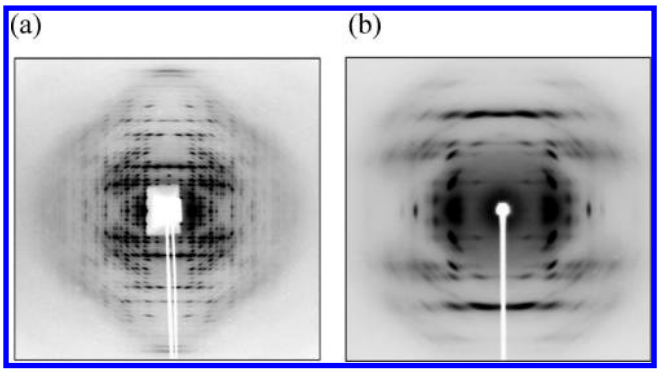


**Figure 1.** (a) Fiber X-ray diffraction pattern of PLLA in its ordered $\alpha$-PLLA phase and (b) its disordered $\alpha'$ phase. The patterns have been taken with synchrotron radiations of wavelength 0.032 nm (a) and 0.071 nm (b). The right pattern (b) corresponds to the center of the left pattern (a). Note the diffuseness of the reflections indicating a structural disorder. Part a: reproduced with permission from ref 2. Part b: reproduced with permission from ref 3. Copyright 2011 Elsevier.

was also investigated with neutron diffraction, which helped locate the hydrogen atoms. Analysis of these data, after small corrections of the initial model to retrieve more standard bond lengths and geometries, led to a structure in which the 90 atoms are located and the departures from strict helix symmetry characterized. It is fair to acknowledge, however, that Wasanasuk and Tashiro's earlier structure determination using the Mo K$\alpha_1$ $\lambda$ of 0.071 nm had caught the major features of this structure[3] as well as, for that matter, the earlier structure determination made by Sasaki and Asakura (made with the Cu K$\alpha$, 0.154 nm) (Figure 1b).[4] Nevertheless, this study illustrates the level of sophistication that has been reached in the structure analysis of polymers.

Out of a number of possible topics, of particular interest in the present context are the recognition of a polymer structure with nonparallel chains and the concept of frustrated polymer crystal structures These two advances result from the very belated analysis (30 and 35 years after their initial observation) of two metastable structures of isotactic polypropylene (it-PP), the gamma ($\gamma$-it-PP), and the beta ($\beta$-it-PP) phases. A third, more specific but highly illustrative issue deals with the impact of chain folding on the crystal structure—an issue that exists only in polymer science. The analysis of structural disorder, a pervasive feature of crystalline polymers, is also briefly illustrated.

**A Structure with Nonparallel Chain Axes: $\gamma$-it-PP.** The $\gamma$-it-PP phase is (or more exactly was considered to be) a minor component that grows on the lateral edges of parent $\alpha$-it-PP crystals. Its structure determination stems from the analysis of a specific morphological feature of the $\alpha$-it-PP phase: a lamellar branching in which daughter lamellae initiated also on the lateral *ac* growth faces are at an 80° angle to their mother lamellae (Figure 2a).[5] This phenomenon has been analyzed as resulting from an occasional "stumble" in the crystallographic alternation of layers made of right-handed helices and of left-handed helices along the *b*-axis of the cell. The interaction between two isochiral *ac* layers results in an unconventional orientation of the chains parallel to the *a*-axis (and not the *c*-axis) of the substrate (Figure 2b). This is a rotation twin or a homoepitaxy favored by the near identity (0.65 nm) of the *a* and *c* parameters of the unit cell.[6]

The $\gamma$-it-PP phase structure described by Brückner and Meille results from the systematic repetition of this unconventional interaction of isochiral layers: the rotation twin axis becomes a symmetry element of the (large) $\gamma$-it-PP unit cell.[7] The structure is made of double layers of right- and left-handed helices with the helix axes oriented about roughly 80° or 100° apart (Figure 2c),[8] a feature that could be confirmed by electron diffraction of single crystals of tilted $\gamma$-it-PP phase.[9,10] This phase had been considered as a mere curiosity for many years. It has gained considerable interest in recent years. Copolymers of propylene and olefins with longer side chains (e.g., pentene, hexene, etc.) produced by metallocene catalysis can be obtained in virtually pure $\gamma$-it-PP phase[11] and have been the subject of intense structural investigations.[12,13] Because the near-orthogonal orientation of the helices makes the unit cell optically nearly isotropic, these copolymers are used to produce clarified it-PP, with the additional help of highly dispersed nucleating agents or clarifying agents. In a different context, the unique features of $\gamma$-it-PP phase make it an excellent test material that helps confirm or challenge theories and/or models of polymer crystal growth. Indeed, as developed in a later section (Polymer Crystallization Mechanisms) the near-orthogonal orientation of the stems precludes any polymer "preorganization" such as liquid-crystal type prior to the deposition of the stems on the growth face.

**Frustrated Polymer Crystal Structures.** The concept of geometrical frustration was introduced in materials science in 1977 by Toulouse.[14,15] It describes a situation in which pair–pair interactions are incompatible with e.g. packing considerations. This geometrical frustration is best illustrated by the impossibility to combine hexagonal close packing of balls of two different colors with the additional requirement that any one ball is surrounded by six balls of the other color. For


DOI: 10.1021/acs.macromol.7b00907
*Macromolecules* 2017, 50, 5995−6025

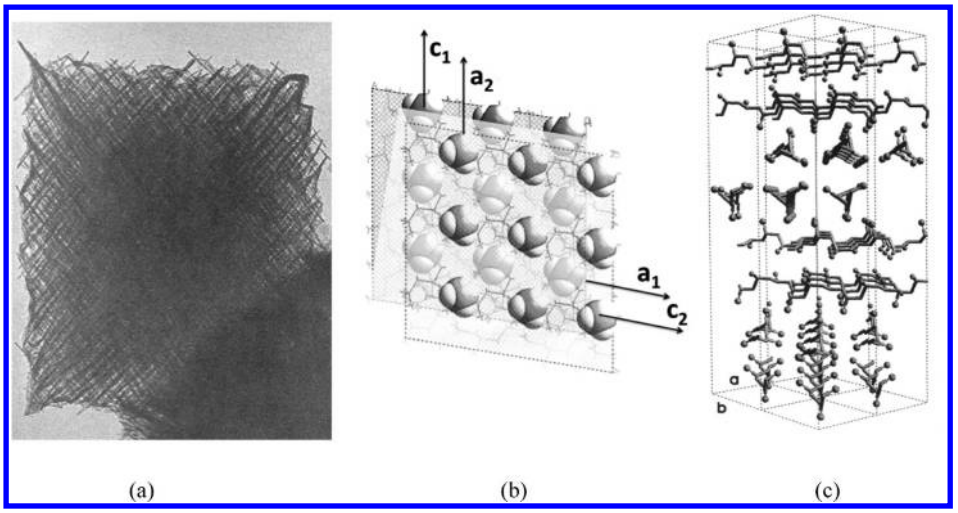


**Figure 2.** (a) Lamellar branching of $\alpha$-it-PP generates "quadrites" made of edge-on elongated crystal laths of $\alpha$-it-PP. Reproduced with permission from ref 5. Copyright 1966 National Institute of Standards. (b) Its molecular interpretation. The two superposed *ac* layers are made here of right-handed helices. The methyl groups face each other. Satisfactory interdigitation of the methyl groups requires rotation and alignment of the $a_1$- and $c_1$-axes with the $c_2$- and $a_2$-axes. (c) Crystal structure of $\gamma$-it-PP phase as established by Brückner and Meille.[7] Reproduced with permission from ref 8. Copyright 1999 Kluwer Publishers.

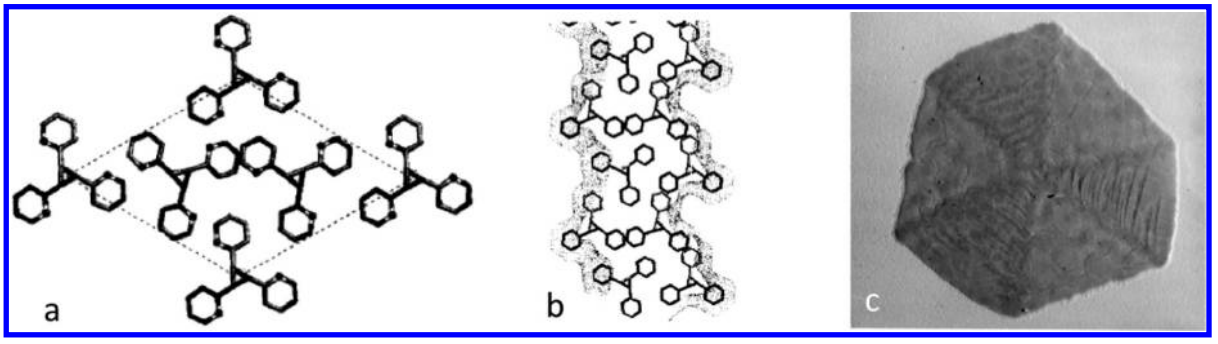


**Figure 3.** (a) Crystal structure of isotactic poly(2-vinylpyridine) determined by Puterman et al. in 1977.[17] (b) Growth faces topography as seen along the chain axis that illustrates two features: the asymmetry of the different front and back topographies that explain the different characteristics of opposing growth sectors in the single crystal and the left versus right asymmetry of the (here right) growth front that explains the asymmetric growth of that face.[18] (c) Single crystal of it-P2VP grown in thin films. Note the three thicker growth sectors with "tilted" growth fronts and the ripples in these sectors indicating lamellar thickening after the initial growth.[18] Parts a–c: reproduced with permission from ref 18. Copyright 1999 Elsevier.

polymers with a 3-fold symmetry packed on a hexagonal lattice, favorable interactions may be established between three out of the six neighbors. These favorable interactions propagate through the lattice and generate a honeycomb network of helices that share favorable interactions. This honeycomb leaves aside one helix located at the place of the honey in the honeycomb. This helix adapts to its different, less favorable environment by a rotation and translation along its axis. The frustrated structure is thus characterized by a trigonal unit cell in which the three helices are crystallographically independent.[16]

As indicated, frustration was introduced in 1977.[14] Coincidentally, at the same time, the crystal structure of isotactic poly(2-vinylpyridine) (it-P2VP) was determined and published (Figure 3a).[17] It illustrates a very clear case of frustrated structure and was analyzed in great detail. In particular, the helices were recognized as being isochiral and "independent" since they are not related by any unit cell symmetry element. The frustration is further illustrated by a rare single crystal habit: the growth faces are tilted in three of the growth sectors (Figure 3c). This tilt indicates that the "lateral spread" is not equal on the growth face, as a result of its "asymmetric" topography (Figure 3b). However, the possible wider applicability of this new and original packing scheme was not recognized. This development had to wait for nearly 20 more years before being rediscovered.[19,20] It helped analyze or reanalyze and correct several earlier crystal structure determinations.[16] The frustrated packing scheme is very widespread in polymers but also in biopolymers and, surprisingly, applies in some cases for helices that do not have 3-fold symmetry. In fact, it is surprising that parallel but separate routes were followed for so many years in the synthetic polymers field and the biopolymers field even though very similar problems were under investigation. Crystal structures of poly(L-glutamic acid) esters ($\alpha$-helices with 18 residues in 3 turns) and of concentrated phases of DNA ($10_1$ double helices) display frustration even though their frustrated nature had not been described as such in the initial analyses.[21,22] Frustration appears to be favored when interhelix interactions are relatively weak. In the DNA case, it exists only in a narrow window of relatively concentrated phases but not in condensed phases. Very detailed experimental and



DOI: 10.1021/acs.macromol.7b00907
*Macromolecules* 2017, 50, 5995–6025

conceptual analyses of these features have been developed.[23] The favorable interactions overcome the packing energy penalty introduced by the frustrated element: although the three chains contribute to various extents to the total packing energy, the resulting structure is a viable crystal phase. For many polymers, among which the widespread it-PP and PLLA, the frustrated structure is a metastable phase. In other cases, as for it-P2VP, the frustrated packing corresponds to the stable crystal structure.

**Impact of Chain Folding on the Crystal Structure.** The third conceptual advance deals with the impact of the folds on the crystal structure or, more exactly, on the unit cell symmetry. Although highly specific, it illustrates the level of insight that can be—and in the present case has been—reached in the structural analysis of polymers.

Chain folding of polymers with a chemical sense such as polyamide 6 implies that stems linked by a fold are antiparallel. A subtle differentiation affects stems linked by a fold in helical isotactic polyolefins. In these systems, helices can be antichiral (right-handed versus left-handed) and anticline (up- versus down-orientation). Anticline helices have the same conformation but differ, although only marginally, by the position of the atoms in the unit cell (the side chains orientation relative to the helix axis results in slightly different chain axis projections). As demonstrated by Petraccone et al.,[24] the trick is that conformational constraints on the succession of trans and gauche bonds in the folds impose that stems of isotactic polyolefins linked by a fold cannot be *both* antichiral and anticline. Packing of such antichiral and anticline stems in a unit cell would, however, be preferable since it takes advantage of a center of symmetry that links the two helices. Because of the constraints on the fold, the crystal structure must settle for some lower crystal structure symmetry that allows for the packing of for example isocline right- and left-handed helices. This lower symmetry shows up in electron diffraction patterns of single crystals by the presence of additional weak spots. These reflections are observed in one of the numerous crystal forms of isotactic poly(4-methyl-pentene-1).[25] This is a clear example of the impact (limited but real) of the folds on the crystal structure at the unit cell level.

**Structural Disorders: Shifts along the Chain Axis and Lateral Stacking of Chains.** Chain folding is the most familiar source of structural disorder in polymer crystals at the level of the lamella. However, the crystalline cores themselves experience several types of disorder—mostly packing disorders. With the modern diffraction techniques that allow collection of more complete and better quality experimental data, the high symmetry crystal structures are frequently questioned and "downgraded" to lower symmetry. A recent example is provided by the work of Tashiro et al. on the familiar structure of isotactic poly(1-butene), it-PBu, form I′.[26] The newly proposed, lower symmetry $P\bar{3}$ allows for azimuthal settings of the helices in the unit cell different from the initial more "constrained" *R*3*c* space group.

Disorder is manifested by loss of resolution and sharpness of the diffraction pattern and by the formation of streaks. These are usually analyzed from fiber diffraction patterns (cf. Figure 1b). In it-PBu form I, epitaxial crystallization made it possible to get single crystal type data as indicated by its (right−left) asymmetry, an asymmetry that is lost in fiber patterns. The streaks result in this case from up−down disorder and a small stagger along the chain axis by as little as 0.05 nm (Figure 4).[27]

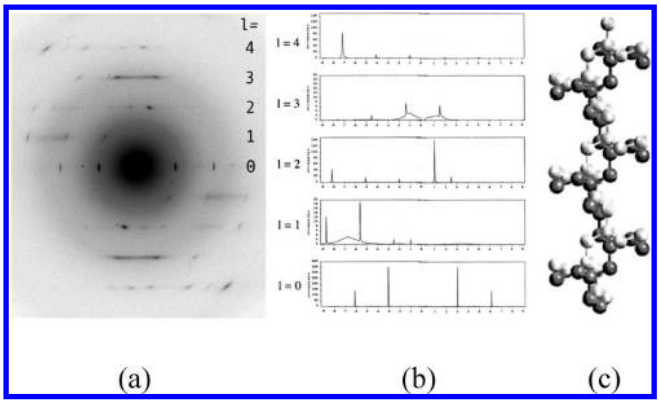


**Figure 4.** Up−down and translational disorder along the chain axis in it-PBu. (a) The diffraction pattern is from an epitaxially crystallized sample. Its asymmetry indicates a single crystal-type organization, different from a fiber orientation. (b) Calculated intensity profile of the sharp reflections and the streaks for the equator ($l$ = 0) and the four first layer lines (top of part a) that reproduces the asymmetry in part a assuming (c) a shift of up- and down-pointing helices along the *c*-axis by 0.5 Å (shown as light and dark, respectively). Reproduced with permission from ref 27. Copyright 2001 Elsevier.

More important positional disorder may exist when two different but related packing modes are possible for related chain conformations or even larger structural elements. Referring to the structure of the $\alpha$ and $\gamma$ phases of it-PP, these phases are built with the same sheets made of either all right- or all left-handed helices (R and L). They differ only by the sequence of stacking: regular RLRLRL... alternation in $\alpha$-it-PP, regular R*RLLRRLLRR* alternation in $\gamma$-it-PP (the different stem orientations in successive layers are shown in normal and italic characters). "Mixed" phases are therefore perfectly conceivable and have been documented and analyzed.[12] The impact of helix conformation is clearly illustrated by the crystals of syndiotactic polypropylene (st-PP). The stable crystal structure is orthorhombic and houses four helices. Any one helix has helices of opposite hand along the *a*- and *b*-axes. This "ideal" structure is formed at high crystallization temperatures. At lower crystallization temperatures, the helix chirality selection is less operative and helices of the "wrong" hand are incorporated in the crystal, but they are shifted along the *b*-axis by half an interhelix distance. This packing defect generates shifts of whole layers along the *b*-axis. This structural disorder is revealed by a streaked single crystal diffraction pattern, and its impact increases as crystallization temperature decreases (Figure 5).[28,29]

As already indicated, crystal structure determination of polymers rests on a set of well-established conceptual tools. Most crystal structures have been established with a reasonable accuracy in the early days of polymer science, sometimes with rather primitive means. In this mature field, one difficulty remains with metastable phases that are unstable to stretching and are not therefore amenable to "classical" fiber science. As seen next, one means to overcome these difficulties is to rely on single crystals investigated by electron diffraction and epitaxial crystallization (a "mild" orientation process). At present, polymer crystallography as a research field is no longer widespread in our community. The major and more regular contributions are due to Japanese and Italian colleagues, a situation that reflects the legacy of the early "giants" in this field (e.g., Tadokoro and Corradini).



DOI: 10.1021/acs.macromol.7b00907
*Macromolecules* 2017, 50, 5995−6025

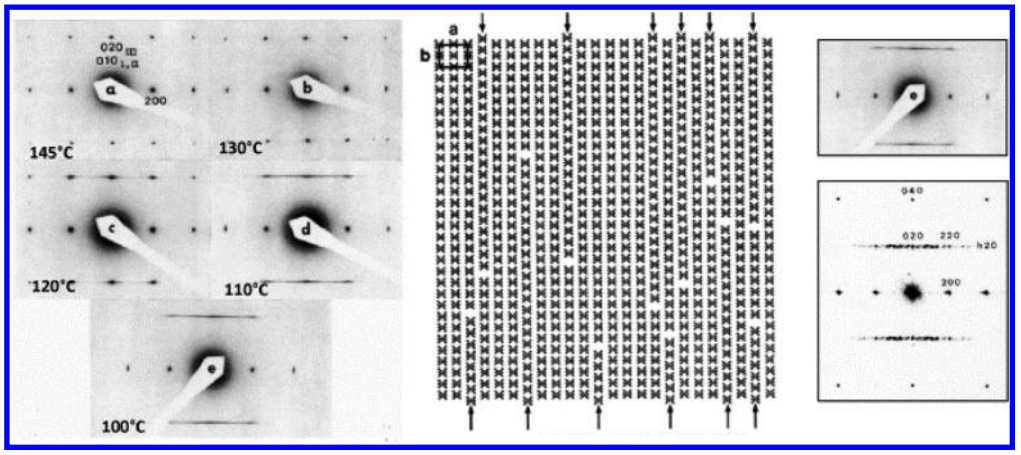


**Figure 5.** Structural disorder in single crystals of st-PP. Right: the single crystal *hk*0 diffraction patterns obtained at different crystallization temperatures. Middle: the structural model with the defects inducing shifts of parts of layers by half an interstem distance along the *a*-axis (vertical) and its optical transform with the resultant streaking (lower right) that affects the *h*20 layer line only. Reproduced with permission from ref 28.

## POLYMER SINGLE CRYSTALS

Single crystals provide a welcome, simple material to investigate crystallization processes and crystal features over the whole structure hierarchy and length scales, from the crystal unit cell structure to the lamellar morphology. Their contribution to our general understanding of polymer crystals and crystallization processes is truly invaluable. They are of great help—together with epitaxially crystallized films—in the crystal analysis of metastable phases that, when mechanically unstable, transform on stretching and are not therefore amenable to fiber science. The investigation by dark field imaging—a technique in which only the diffracted electrons are used to produce the image and therefore "sees" and provides an image of the crystal interior—reveals processes that take place during crystal growth and crystal−crystal transformation. In all cases, the sample investigated must have a crystal structure (cell geometry, symmetry, etc.) suited to the problem investigated. Even though the details of such analyses may be specific, the insights provided have general validity.

**Polymer Single Crystal Habits.** In the mid-1950s, Jaccodine, Keller, Till, and Fischer reported their experimental observations of PE lamellar single crystals grown in dilute solution with crystallographically defined, faceted habits via optical microscopy and transmission electron microscopy.[30−33] In the past 60 years, a majority of crystalline polymers have been reported to form single crystals in certain crystallization conditions in dilute solution, in the melt, or in thin films. In some cases, they form single crystals under specific environments or conditions such as at elevated pressures or epitaxial growth. In this Perspective, only a few selected illustrations of the insights, either historical or relatively recent, gained with the help of single crystals are described here.

With the large number of lamellar single crystals observed and their crystal unit cell dimensions and symmetry groups determined, polymer single crystals display a variety of habits ranging from elongated ribbon-like (kinetically anisotropic) to square or hexagonal shaped (kinetically isotropic), in both the melt and solution.[34−39] The formation of anisotropic single crystal morphologies implies that the growth rate along one specific crystallographic direction is faster than the others. Therefore, the nucleation barrier for polymers to crystallize on specific crystallographic planes is different. The isotropic single crystal habit is generated by identical growth rates along the normal direction of the same set of crystallographic planes, and thus, growths possess the same nucleation barrier. In general, the single crystal habit is critically associated with the crystal unit cell symmetry. Namely, a low rotational symmetry along the *c*-axis results in an anisotropic shape of single crystal. For example, a $2_1$ rotational symmetry about the *c*-axis in the unit cell gives rise to elongated single crystal habits. A high rotation symmetry about the *c*-axis ($3_1$, $4_1$, or $6_1$) results in regular polygonal single crystal habits. Experimental results on PE (orthorhombic with $2_1$ rotational symmetry versus hexagonal with $6_1$ rotational symmetry forms in Figures 6a and 6b, on it-

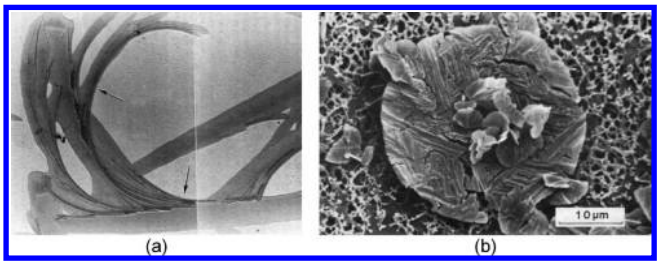


**Figure 6.** Elongated single crystals of (a) polyethylene with an orthorhombic lattice crystallized from thin film melt and (b) isotropic single crystal habit of polyethylene with a hexagonal lattice crystallized at elevated pressure and temperature. Part a: reproduced with permission from ref 43. Part b: reproduced with permission from ref 44. Copyright 1990 Elsevier.

and st-PP, poly(vinylidene fluoride) (PVDF), isotactic and syndiotactic polystyrene (PS), and poly(ε-caprolactone)) illustrate this conclusion.[40] Furthermore, a quantitative analysis based on unit cell symmetry to predict single crystal shapes has also been carried out by Shcherbina and Ungar.[41,42]

The slowest growing crystallographic plane determines the habit of a polymer single crystal because the faster growing planes are exhausted first during crystal growth. We are specifically interested in the formation of these anisotropic single crystal habits. One of the central issues in this respect is that single crystal habits may change with crystallization temperature. If the crystal growth is nucleation controlled, this change in habit indicates that not only the nucleation barriers at each crystallographic plane are different and that all of them decrease with increasing supercooling but also that the supercooling dependence of these barrier heights is different


DOI: 10.1021/acs.macromol.7b00907
Macromolecules 2017, 50, 5995−6025

and specific for each crystallographic plane. One typical example is PE single crystals grown in solution (Figure 7)[45−50] and in the bulk (Figure 8).[51−53]

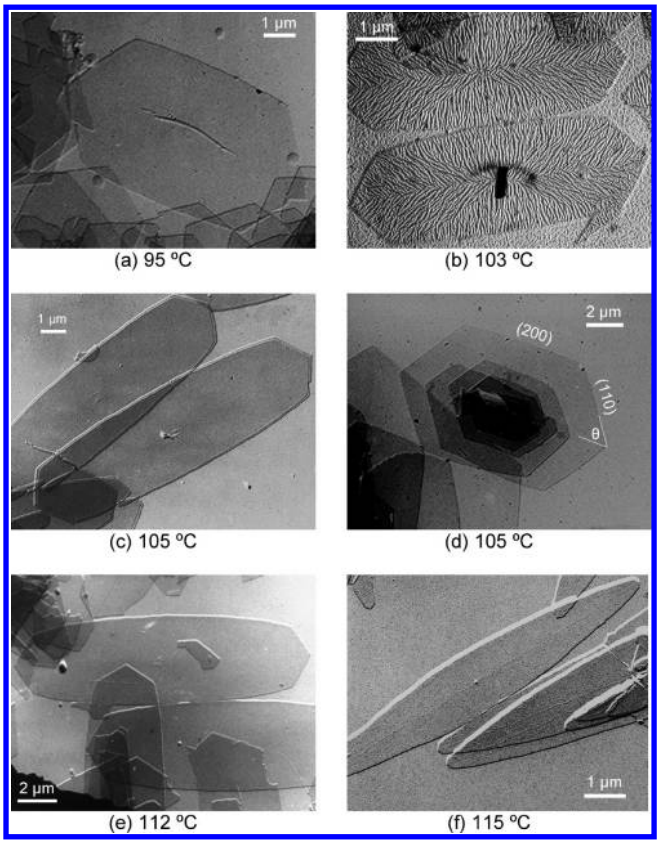


**Figure 7.** Set of polyethylene single crystals grown from dilute solutions at different crystallization temperatures in two solvents. The polyethylene fraction has a number-average molecular weight of 11.4K g/mol and a polydispersity of 1.19. Parts a−c are the single crystal habits obtained in heptyl acetate (a better solvent), and parts d−f are obtained in dodecanol (a poorer solvent). The crystal habit changes can be characterized by the aspect ratio between the dimensions along the *b*- and *a*-axes. In part b, polyethylene decoration has been performed on the single crystal surface to illustrate the chain folding direction (see Figure 12) (courtesy of Dr. F. Khoury).

Polyethylene single crystals crystallized in xylene at relatively low crystallization temperatures are bounded by four (110) crystallographic planes (see Figure 11a). When single crystals are grown in heptyl acetate (that is, a good solvent) between 95 and 115 °C (Figures 7a−c), the (200) crystallographic plane starts to appear and the crystal habit changes from lozenge to truncated lozenge. When polyethylene single crystals are produced in dodecanol (that is, a poorer solvent), the aspect ratio between the *a*- and *b*-axes increases with decreasing supercooling. The truncated lozenge shape turns into an almost lenticular habit (Figures 7d−f). In Figure 7d, an angle $\theta$ between the (110) plane and the *b*-axis (the long axis of the growth) can be defined.[54] Using this angle helps to calculate the single crystal growth rate along the (110) plane normal when measuring the size increase along the *b*-axis with time.

When PE single crystals are grown *in the melt* at different supercoolings as illustrated in Figure 8,[51−53] the single crystal habit changes from truncated lozenge to lenticular-shaped with a continuous increase of the aspect ratio. For the single crystals

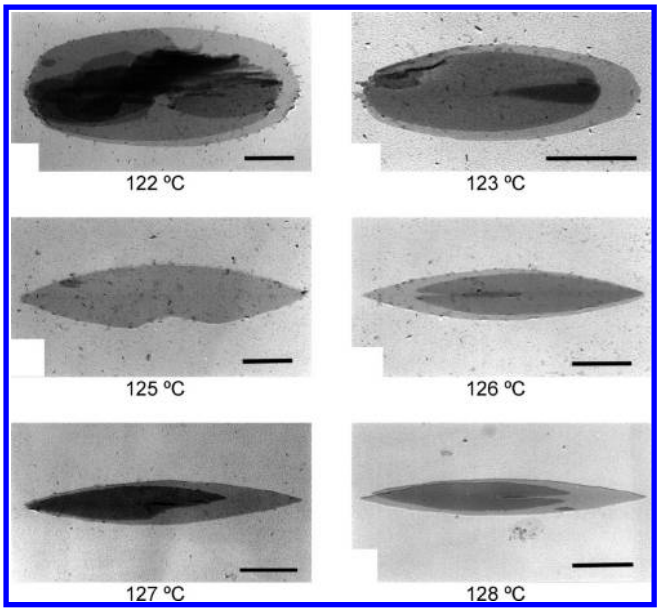


**Figure 8.** Set of polyethylene single crystals grown from the melt at different crystallization temperatures (from 122 to 128 °C). The polyethylene fraction had an average number molecular weight of 1.1K g/mol and a polydispersity of 1.16. The crystal habit changes from truncated lozenge to lenticular shape with increasing temperature. Reproduced with permission from ref 52. Copyright 1993 Royal Society of Chemistry.

grown in the melt, the lozenge-shaped single crystals are predicted to grow at very high supercooling in a range where the single crystals of polyethylene cannot be grown: only sphelurites can be formed.

The supercooling dependent variation in single crystal habits of other polymers[40] has also been investigated. Most spectacular habit changes have been documented for poly(ethylene oxide) (PEO) fractions of medium and low molecular masses, as a consequence of integer chain folding[55−60] and other polymers.

**Crystallization Processes of Single Crystals: Extent of Lateral Spread.** We are interested in a specific case to utilize the growth of twinned single crystal to investigate the lateral spread in polymer crystallization in a nucleation-controlled process. The conventional nucleation and growth scheme of crystallization involves a so-called "secondary (or surface) nucleation" in which a stem is deposited on the surface of a growth face. The face is then "filled in" by lateral deposition of additional stems until the strip formed reaches the crystal edge or is stopped when it impinges with its neighbor strips. The observed overall growth rate is easily measured and results from the contributions of both secondary nucleation and lateral spread. The relative contributions of secondary nucleation and lateral spread are very difficult to differentiate: few depositions and extensive lateral spread or many depositions and limited lateral spread may result in the same overall growth rate. No direct visualization of the process seems conceivable: as soon as a stem is deposited on a crystal face, it becomes part of the crystal and cannot be differentiated from its neighbors or from that crystal.

Direct visualization of the extent of lateral spread has been possible nevertheless in one specific case, namely, in solution grown, *twinned* single crystals of isotactic poly(vinylcyclohexane) (it-PVCH).[61] This polymer is a high


DOI: 10.1021/acs.macromol.7b00907
*Macromolecules* 2017, 50, 5995−6025

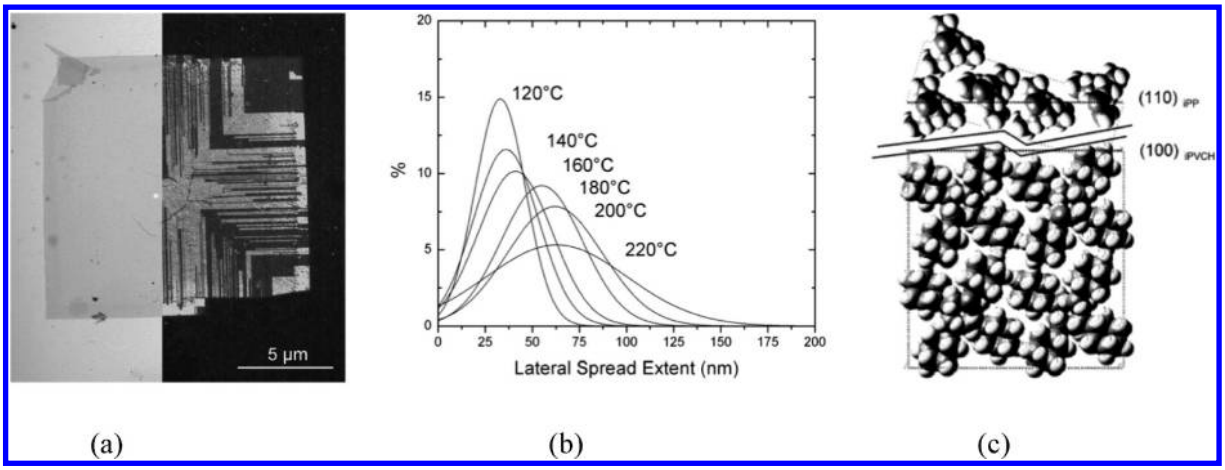


**Figure 9.** Evaluation of lateral spread by dark field electron microscopy in single crystals of it-PVCH. (a) Illustration of the composite structure revealed by dark field imaging (right part) in an apparently featureless crystal when examined by bright field imaging (left part). (b) Distribution of domain widths (or total lateral spread) at different crystallization temperatures. Since each it-PVCH stem is 1 nm wide, the scale expresses also the number of stems. (c) Illustration of the topographic matching between it-PVCH, a polymer nucleating agent for it-PP alpha phase. The it-PVCH part illustrates the tilted setting of the 4-fold helices relative to the *a*- and *b*-axes that makes it possible to image the twinned parts in part a. Parts a and b: reproduced with permission from ref 61. Part c: reproduced with permission from ref 62.

melting polyolefin that is also a nucleating agent for it-PP.[62] The twinned parts have identical tetragonal unit cell parameters and orientations. They differ only by the symmetric, tilted setting of the helices in the unit cell (cf. Figure 9c), which is a minor disturbance. In dark field imaging and by selecting appropriate diffraction spots, the different twinned parts appear as dark or bright elongated domains or mini-sectors normal to the growth faces (Figure 9a). The width of these domains corresponds to the lateral spread. They are formed only occasionally when a secondary nucleation stem deposits in twinned orientation on the substrate crystal. Lateral spread maintains this twinned orientation, and growth of additional layers maintains the substrate stem orientation, i.e., continues as a twinned mini-sector. The lateral size of these mini-sectors, that is, of lateral spread, ranges from roughly 60 stems at 220 °C to about 25 stems at 120 °C (Figure 9b). In other words, the density of secondary nucleation increases at lower crystallization, as is expected for a nucleation and growth mechanism.

**Analysis of Crystal−Crystal Transformations.** Many polymers display crystal polymorphism that may result in crystal−crystal phase transformations. Metastable phases are formed more easily than stable phases but may experience a delayed transformation into the stable phase. Numerous examples have been reported. A very early and best known one is the transformation of it-PBu form II into form I. It involves a change in chain conformation (from a $11_3$ helix to a $3_1$ helix) as well as a change of unit cell symmetry (from tetragonal to trigonal). In spite of the large crystal modifications (cell geometry, density of packing, anisometric crystal contraction/extension), one major feature characterizes this solid-state transformation: the helix chirality is maintained during the transformation even though the helix conformation changes from $11_3$ to $3_1$.[63,64]

A similar change of chain conformation exists for the extended form III to the helical form I of st-PP. Interestingly, the transformation of a crystal phase with an extended chain conformation to a helical one is a chiral process: neighbor chains adopt the conformations of their neighbors.[65] In the st-PP case, the initial structure determination was made on an extended and annealed/relaxed fiber that had experienced such a crystal transformation: the crystal phase thus determined (phase I) is chiral whereas the stable crystal structure obtained by crystallization from solution or at high crystallization temperature is made of right- and left-handed helices alternating along both the *a*- and *b*-axes of the unit cell.[28]

These examples deal with delayed or controlled crystal−crystal transformations. However, such processes may also take place spontaneously on much shorter time scales, possibly even during crystal growth. At low crystallization temperatures between ∼90 °C and ∼120 °C, PLLA crystallizes in an $\alpha'$-PLLA crystal phase with up−down helix orientation disorder, whereas at higher crystallization temperatures an ordered $\alpha$-PLLA is formed (orthorhombic phase with two antiparallel stems per cell; see Figure 1).[3,66] This structure change is accompanied by larger growth rates[67] and lamellar thicknesses[68,69] than expected from an extrapolation of values recorded for the ordered $\alpha$-PLLA phase. These differences may be explained by the formation at low crystallization temperatures of a transient frustrated phase.[67] Evidence for such a process came in a recent analysis of partly transformed single crystals of the frustrated $\beta$-PLLA. With its three stems in the unit cell, no regular up−down chain orientation is possible in the frustrated phase formed first, a disorder that is maintained during the solid-state transformation.[70]

A more detailed scenario of the crystal−crystal transformation process is revealed by the $\beta$ to $\alpha$ transformation taking place in single crystals of poly(ethylene-*alt*-carbon monoxide) (POK).[71] Both phases are orthorhombic but differ by their chain azimuthal settings and shifts and lattice parameters. When single crystals are deposited on a carbon film, the transformation starts preferentially near the crystal edges and propagates inward, along the $\beta$ phase *b*-axis. The uneven lattice contractions limit the transformation after some distance. The inner edges of the transformed domains have an arrowhead shape (Figure 10). The planes that bound this arrowhead have a very clear structural origin: they are the invariant strain planes of the transformation. In these planes, the transformation is easiest since it involves only a mere


DOI: 10.1021/acs.macromol.7b00907
*Macromolecules* 2017, 50, 5995−6025

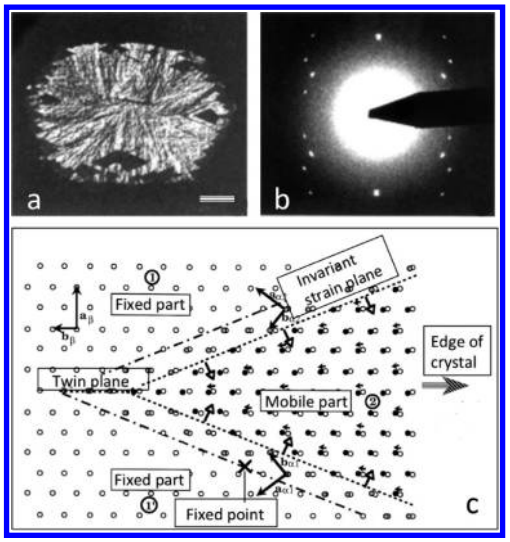


**Figure 10.** Crystal transformation of POK $\beta$ phase to POK $\alpha$ phase. (a) Dark field image of a single crystal in $\beta$ phase (bright) with domains transformed to $\alpha$ phase, in black. Scale bar: 1 $\mu$m. (b) Diffraction pattern of the single crystal. The eight weaker spots are of the transformed $\alpha$ phase and indicate twinned domains symmetric to the horizontal twin plane. (c) Origin of the arrowhead shape of the transformed domains. The oblique limits at 23° to the twin plane correspond to the invariant strain plane of the transformation. The unit cell orientations of the $\alpha$ and $\beta$ phases are indicated. Reproduced with permission from ref 71.

rotation around and/or shift along the *c*-axis but no lateral translations.[71]

## CHAIN FOLDING IN POLYMER CRYSTALS

Since polymer single crystals were observed in the 1950s, the questions immediately arose: with a polymer single crystal a few tens of nanometers thickness, how can a polymer chain (usually a few micrometers long) be accommodated in the crystal? Figure 11a shows a bright field transmission electron

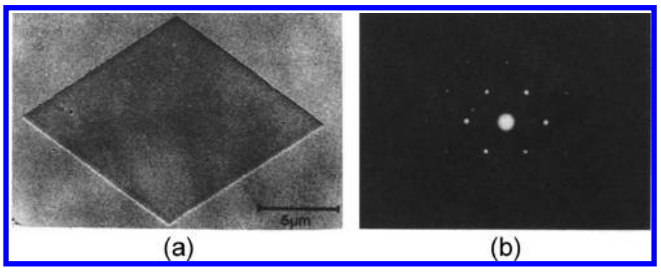


**Figure 11.** Single crystal of polyethylene grown in dilute solution. Its *c*-axis is perpendicular to the single crystal (a). Its corresponding electron diffraction with the *c*-axis is a zone direction (b) (courtesy of S. J. Organ and A. Keller).

micrograph of PE single crystals grown in dilute solution. Electron diffraction provided direct experimental evidence of the way the long chain molecules crystallize in a lamellar form (Figure 11b). The concept of chain folding was proposed at that time by Keller,[31] whereas the origin of this concept can be traced back to Storks.[72] This concept is widely accepted today despite some controversies about the folding process itself. At the same time, the observation of polymeric spherulites in the melt,[73−77] indicated that the chain folded lamellar crystals are also the building blocks of these spherulites[78,79] and, more generally, of polymer crystal aggregates.

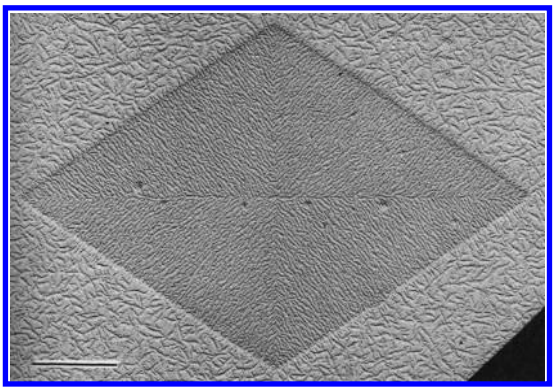

**Figure 12.** Bright field transmission electron microscopy image for the decoration of a PE single crystal grown in solution. The scale bar represents 1 $\mu$m. Reproduced with permission from ref 81. Copyright 1985 John Wiley & Sons.

The clearest experimental evidence in support of the chain folding principle is the surface decoration method proposed by Wittmann and Lotz.[80−82] This is a kind of morphological epitaxy process that uses PE vapor-deposited onto the PE single crystal basal surfaces. The vapors (of low molecular mass of ~1000 g/mol) crystallize and form short rod-shaped crystals as shown in the electron micrograph of Figure 8. This is a soft epitaxy technique in which the epitaxial growth relies only on the molecular orientational order at the surface of the material. When the chain folds are along a given (*hkl*) plane, the rod-like PE crystals are oriented with their *c*-axis parallel to the chain-folded direction grown in solution (along that {*hkl*} plane). Four sectors of the single crystal can be clearly identified by the different orientation of these short rod crystals, and the long axis of the short rod PE crystals is oriented perpendicular to the (110) planes of the basal faces, indicating that the chain folding direction of the solution grown PE single crystal is along the (110) plane. This lamellar decoration technique can detect the surface topography down to a length scale of about 1 nm.[80,81]

This lamellar decoration method has also been utilized on other polymer crystals to identify chain folding directions in their single crystal forms, such as it-PP,[81] PEO,[83] a series of chiral nonracemic polyesters,[84−86] and others. A few examples on melt-grown single crystals as well as spherulites have been found to induce oriented polymer decoration, which indicates oriented chain folding.[81] With the advent and the progress of atomic force microscopy, direct imaging of chain folding has become accessible. Kumaki[87] and Hobbs et al.[88] observed folds in isotactic poly(methyl methacrylate) (Figure 13a) and PE films using torsional tapping atomic force microscopy (Figure 13b). It has also been reported that chain conformations in the crystal and at the crystalline−amorphous interface can be monitored at single-chain resolution.[89]

The near-ubiquitous observation of chain folding raises an immediate question; namely how rigid should a chain molecule be to prevent the chain folding? For crystalline polymers with semi-rigid conformations, many reports indicate that chain folding is quite general. Polyether−ketones[90] and poly(3-alkylthiophenes)[91,92] basically follow the chain folding principle. Even detailed information about how the chains


DOI: 10.1021/acs.macromol.7b00907
Macromolecules 2017, 50, 5995−6025

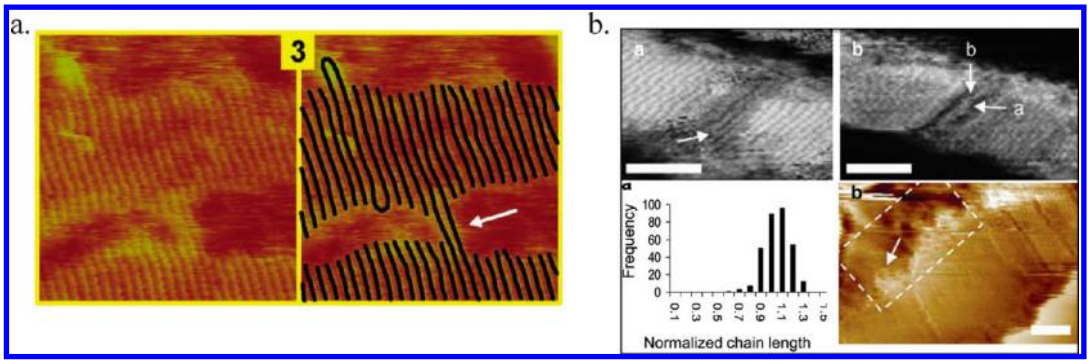


**Figure 13.** Torsional tapping atomic force microscopic observations of (a) isotactic poly(methyl methacrylate) chain folds on two-dimensional mica and (b) polyethylene chain folds in lamellar crystals. Part a: reproduced with permission from ref 87. Part b: reproduced with permission from ref 88. Copyright 2011 American Physical Society.

fold and the structure of the fold can be imaged to a significant level. For example, by use of scanning tunneling microscopy to investigate thin films of the $\pi$-conjugated polythiophenes, the folds were found to link stems 1.3−1.4 nm apart or even 1.9−2.0 nm apart (for hexyl- and dodecyl-substituted thiophenes, respectively); that is, the folds span the wide gap generated by the crystalline alkyl side chains.[85]

Quantitative information on the structure of folds has also been obtained by solid-state NMR spectroscopy and $^{13}C$ selective isotope labeling by Miyoshi et al.[93−102] Hong et al. found that it-PBu solution-grown hexagonal single crystals have a nearly full adjacent re-entry structure, i.e., almost exclusively sharp folds.[96,97] In melt-grown crystals formed under slow crystallization as well as after melt-quenching into icy water, it-PBu chains still adopt adjacent re-entry structures with mean adjacent folding number of ∼2.[94,97] Similarly, it-PP chains in the mesomorphic form prepared by melt-quenching also possesses an adjacent reentry-rich structure. The mean value of its adjacent re-entry number is close to that observed in $\alpha$-it-PP crystallized at high temperature (150 °C).[98−100]

These experimental data indicate that polymer concentration and entanglements significantly influence long-range order in adjacent re-entry sequence whereas this order can hardly be modified by the experimentally accessible kinetics. These results indicate that chain folding is a natural consequence of polymer rearrangement on crystallization. They further invite us to revisit the open issue of "when does chain folding occur?" Chain-level analysis of semicrystalline polymers quenched into the glassy state may provide an answer to such a question. In a different approach, chain-folding analysis was used to understand the deformation behavior of semicrystalline polymers at the molecular level. Kang et al. investigated the response of folded it-PP chains under hot drawing. They showed that the folded chains transform into locally extended chain conformations under large deformation.[101]

The stereocomplex of PLLA with poly(D-lactic acid) (PDLA) has by design an original folding pattern and process, essentially different from intramolecular packing in flexible homopolymers. PLLA stems alternate with PDLA stems. An "intermolecular packing" is the leading process during crystallization. Since every stem of a given chirality is surrounded by antichiral stems, sharp folds connecting neighbor helices are excluded. The folds must link by necessity second-nearest-neighbor stems, and two kinds of polymer chains occupy the fold surface, which may influence the folding patterns and crystal morphology. Chen et al. prepared two types of PLLA (with molecular mass of 84K g/mol)/PDLA (with molecular masses of 2.9 and 120K g/mol, respectively) stereocomplex crystals in amyl acetate solution.[102] The low molecular mass PDLA has a chain length comparable to the single crystal thickness of ∼10 nm and crystallizes mostly as extended stems in the triangular crystals that are formed. PDLA thus allows the counterpart PLLA chains to fold regularly. The PLLA adopts nearly full-adjacent re-entry patterns as similarly observed in homopolymer single crystals, in spite of the slightly longer interstem distance. By contrast, high molecular weight PDLA/PLLA complex forms multilayered stacked crystals. The PLLA chains cannot fold in a regular fashion. This result clearly indicates that anomalous densities at the fold surfaces significantly influence chain-folding patterns and thus crystal habits in the case of stereocomplex.

## ■ LAMELLAR TWISTING AND SPHERULITES

Spherulites are ubiquitous in materials science. Spherulites are known in many low molecular weight systems with (usually) relatively high viscosity.[103] Investigation of their structures has been for years a nightmare. In the early days of polymer morphology, the tangential orientation of chains was recognized in spherulites, but it made sense only after the chain folding and lamellar structure of crystalline polymers were recognized: broadly speaking, the polymer spherulites are made of radial lamellae in which chain folding generates the tangential orientation of chains that appeared so puzzling. Rationalizing the structure of bulk systems in the broader concept of chain folding and the resultant lamellar structure is probably one of the major added contributions of the early investigations of polymer single crystals.[33−38]

These new insights did not settle all the issues. As a matter of fact, investigation of polymers in the bulk remains an active field up to these days. Some structure/morphology problems considered in this section were answered sometimes only after years or even decades of effort.

Spherulites are made of lamellae of constant thickness that must fill an opening space. The multiplication of lamellae is mostly achieved via screw dislocations and noncrystallographic branching. Such mechanisms cannot generate any regular, crystallographic filling-in of the available space: the spherulites are by design geometrically frustrated systems. Yet, many spherulites display regular extinction patterns under the polarizing microscope, which indicate some cooperativity in their buildup. The most spectacular and, for a long time,



DOI: 10.1021/acs.macromol.7b00907
Macromolecules 2017, 50, 5995−6025

puzzling feature is the cooperative lamellar twisting. As a rule, this optical banding is observed more systematically for polymers with low-symmetry unit cells that form elongated, thin lamellae. The twisting gives rise in polarized optical microscopy to concentric extinction bands (see Figure 15c) that have been explained in the early 1950s.[73−77] It also gives rise to concentric rings made of C-shaped stacks of lamellae on the surface of the spherulites, as best seen in scanning electron microscopy (cf. Figure 15b).[104]

The origin of the lamellar twisting has been an issue since the very early investigations on spherulites in the early 1900s and is usually explained—but by no means only—by the existence of surface stresses in the lamellae. The problem has been revived with the observation of twisted lamellae in polymer spherulites. Although stresses and twisting are ubiquitous in materials science and in biology—they intervene in the opening of seedpods[105]—investigation of polymer crystals has provided a number of new insights. For a large part these advances stem from the fact that the fold surface of polymer lamellae is structurally different from the crystalline core. It can be investigated in its own right and modified on purpose. For example, in statistical copolymers, bulky side chains are segregated in the folds, a segregation that changes the volume of the folds. Also, since the folds are molecularly connected to the crystalline core, constraints of composition, conformation, etc., may be imparted by the crystal stems to the fold: knowing the crystal structure can help analyze the fold. Such chemical manipulation of the folds and such transfers of information between the crystal core and the folds do not exist for nonpolymeric systems.

Many and diverse hypotheses have been put forth to explain this lamellar twist, as reviewed recently by Kahr and co-workers.[106] In an earlier review, two of the present authors evaluated critically these various hypotheses.[107] Most of them are too specific and target, or focus on, only one specific lamellar morphology. The diversity of lamellar shapes created sometimes under the same crystallization conditions but for different crystal polymorphs rules out such scenarios. In 1984, Keith and Padden came up with a hypothesis that has more general validity. They pointed out the role of surface stresses, and more specifically of imbalanced surface stresses, on the shape of the thin polymer lamellae.[108] This explanation, first put forth to explain the lamellar twist of polyethylene spherulites, has been confirmed in several later studies and accounts for most of or for all the diverse lamellar shapes observed in polymer spherulites.

The existence and impact of the surface stresses linked with chain folding had been established early on in single crystals of PE (but without reference to their balance or imbalance between opposite fold surfaces). The folds induce a deformation of the orthorhombic unit cell of PE into a monoclinic one such that the cell is expanded in the direction normal to the fold and is compressed parallel to it (Figure 14a).[109] This deformation is documented with electron microscopy observations. The dark field images of the different growth sectors depend on whether the fold orientation is parallel or not to the diffracting planes. In much enlarged diffraction patterns of such lozenge-shaped PE single crystals, the diffraction spots are found to be actually doublets.[109]

The mere existence of surface stresses does not explain lamellar twisting. As developed by Keith and Padden in 1984,[108] these stresses must be *different on opposite sides* of the lamella. In their analysis, initially developed for the twisting

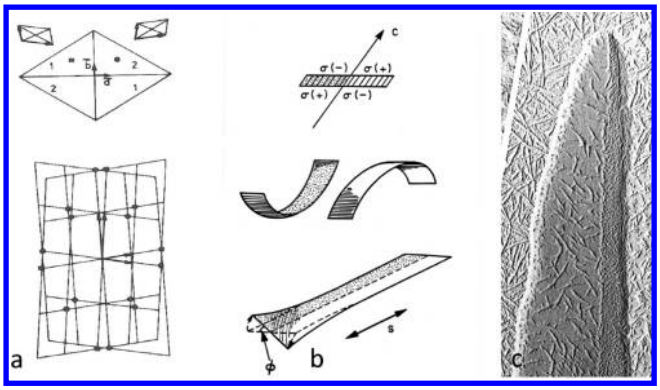


**Figure 14.** Existence of surface stresses associated with chain folding and role of unbalanced surface stresses on the lamellar twist of PE. (a) Schematic (and exaggerated) deformation of the PE orthorhombic unit cell in the PE single crystals growth sectors (top) as deduced from the splitting of the single crystal electron diffraction spots (bottom). (b) The proposal of unbalanced surface stresses due to Keith and Padden.[108] The crystal is seen along its radial growth direction. The different surface stresses [$\sigma(+)$ and $\sigma(-)$] result from the stem tilt; the bending of half-lamellae and the twist of lamellae with connected halves.[108] (c) Tip of a flat-on single crystal of PE grown at 130 °C and decorated with PE vapors. The different decoration patterns on the two sides of the growth axis confirm that the surface (fold) layer differs in opposite growth sectors.[43] Note the different size of the growth sectors on opposite sides of the growth axis. This difference is linked with the chain tilt and the growth on a flat surface (cf. part b, top). Part a: reproduced with permission from ref 109. Copyright 1980 Elsevier. Part b: reproduced with permission from ref 108. Copyright 1984 Elsevier. Part c: reproduced with permission from ref 43.

lamellae of the achiral polyethylene, the imbalance results from the fact that in bulk crystallized polyethylene the stems are tilted in the lamellae, which creates an acute and an obtuse angle at opposite ends of the stem when this stem reaches the lamellar surfaces (Figure 14b). The existence of lamellar twist would then imply that the fold conformation or structure differs at these acute and obtuse angled locations, creating different degrees of overcrowding. In the reasoning, illustrated in Figure 14b, Keith and Padden also pointed out that unbalanced surface stresses should result in the bending of half-lamellae in opposite directions.[108] Since these half-lamellae are linked, the whole lamella twists in order to relieve the opposite bending tendencies of its two halves.

Experimental support for the unbalanced surface stresses is difficult to gather: the fold surface is a poorly organized layer only one or two molecular cross sections thick. In such a case, the PE decoration technique is useful, since the decoration pattern highlights even minor differences that exist in the substrate surface.[81] When applied to PE single crystals grown in thin films at high crystallization temperatures, two very distinct decoration patterns are observed on different sides of the crystal axis (Figure 14c).[43] Although qualitative, this technique confirms that the underlying fold surface is different on opposite lamellar surfaces in these lamellae. The additional suggestion made by Keith and Padden that half-lamellae should bend was confirmed by an unexpected feature: the tilted stems occasionally "fall" on the glass substrate and act as seeds for the crystallization of half-lamellae growing edge-on. These lamellae are indeed bent (see Figure 6a). Similar lamellar bending has been investigated for many other polymers by inducing "forced" nucleation of edge-on lamellar


DOI: 10.1021/acs.macromol.7b00907
*Macromolecules* 2017, 50, 5995−6025

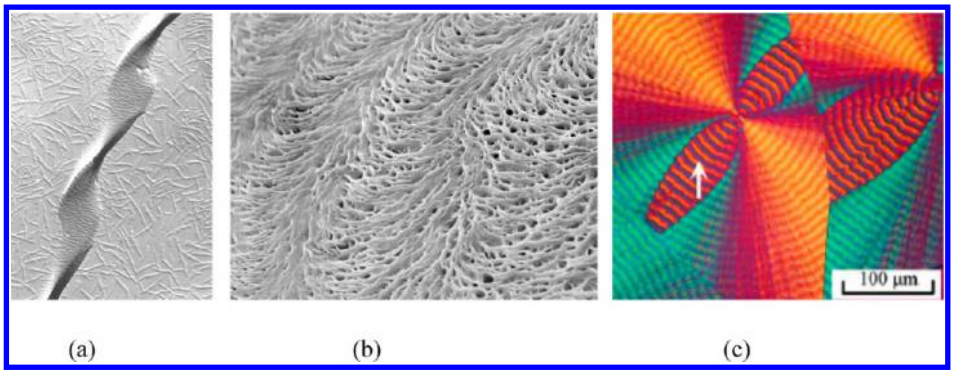


**Figure 15.** Manifestations of twisted morphology. (a) Double twisted single crystal of a main-chain chiral polyester, decorated with polyethylene vapors. (b) Surface pattern of a PE pellet slowly cooled from the melt; polyethylene spherulite. The spherulite center is located below the surface on the right side of the picture. (c) Polarizing optical micrograph of poly(hydroxyvalerate) isothermally crystallized at 70 °C. The white arrow indicates one of the eye-like regions with alternating positive and negative birefringent bands and opposite lamellar twist sense to the neighbor regions. Part a: reproduced with permission from ref 84. Part b: reproduced with permission from ref 107. Copyright 2005 Elsevier. Part c: reproduced with permission from ref 117.

growth by scratching a thin film of the polymer melt with an AFM tip.[110,111]

For $\alpha$-PLLA crystals, Ruan et al. could connect chain tilt and the sense of lamellar bending. In crystals grown edge-on by epitaxial crystallization on hexamethylbenzene, the stems are tilted to the lamellar fold surfaces. Further growth into the melt generates bent crystals. The sense of bending indicates that the fold surface at the obtuse angle is more crowded than at the acute angle.[112]

The usual picture of twisting lamellae is that of a symmetrical twisting helicoid with its axis parallel to the growth axis. In addition, "the crystal rotation is continuous and regular".[113] In the achiral PE, chirality results from the chain tilt sense and induces both left-handed and right-handed lamellar twist. This simple scheme explains satisfactorily the optical banding in spherulites examined in polarizing microscopy as well as the regular surface pattern of for example polyethylene spherulites revealed by scanning electron microscopy. This pattern is generated when oblique, twisting lamellae reach the surface of the pellet (Figure 15b).[106] However, many more lamellar shapes are conceivable and can be generated by any one or any combination of different features: strength, orientation, or imbalance of surface stresses, imbalance in the size of the lamella "halves" on opposite sides of the growth axis due to growth on a support (cf. Figure 14c), or an underlying lamella in a screw dislocation. In PE lamellae, surface stresses exerted transverse to the growth direction generate a bending of the lamellae additional to the stresses that induce lamellar twisting: when seen end-on, the lamellae have the shape of an "S".[38,114] Different illustrations of such departures from simple lamellar twist have been modeled with, for example, rubber strips either partly protected and soaked in solvents[108] or by gluing two prestretched rubber sheets, cutting out strips at different angles, and letting the composite strips mechanically relax.[105] The growth pattern and/or the lamellar orientation may thus differ from the more standard scheme of radial twisting helicoids. According to Woo et al., such departures and original lamellar orientations take place quasi-systematically in polymer spherulites. Disturbingly, the (mostly atomic force microscopy) pictures of well-known and well-investigated polymers are interpreted in terms of morphologies that may not account for the optical properties of the spherulites.[115] Along the same line, an investigation by nanofocus X-ray diffraction of spherulites of poly(propylene adipate) suggests that the lamellae are helical strips that wind around a radial, cylindrical axis. This model maintains the continuous winding but is considered as "breaking the paradigm of the polymer spherulite microstructure".[116] It remains to establish the exact lamellar shape (that could be one of the models produced by soaking rubber strips) and what type of underlying stresses and stress asymmetries are at play in this specific material.

The impact of the strength, orientation, and imbalance of surface stresses is a complex issue. It can be investigated by analysis of the lamellar twist sense. Lamellar twist can be right-handed or left-handed and, therefore, introduces an additional and often unexpected morphological chirality in polymer science. As already indicated, achiral polymers such as PE can form right-handed or left-handed lamellae—the defining feature has been recognized in PE as being the stem tilt in the lamellae. However, what about chiral polymers? The molecular chirality is transferred to the conformation: the chains adopt a given right or left helicity. This chirality exists also in the crystal structure. Is this chirality transferred to the next and final structural level, the lamellar shape? Since several polymers are available in their two enantiomeric forms, crystalline polymers are well suited to tackle this "issue of a century standing".[118] In other words, is the lamellar twist connected to the crystalline core, as is expected for low molecular weight materials or for the $\beta$ sheets of polypeptides and fibrous proteins?[119] Or does the lamellar twist result from the fold surfaces features? Various investigations specifically devoted to answer this question did not provide a clear answer.[120] Indications that there is no correlation did exist. For example, in a series of chiral polyesters (Figure 15a), there is an "odd−even" effect: changing the length of the aliphatic segment by one methylene unit reverses the lamellar twist sense.[121]

The final and conclusive experimental evidence was provided by an investigation of poly[(*R*)-3-hydroxyvalerate] spherulites.[122] This polyester has a chiral helical conformation and the helices pack in a *near*-tetragonal unit cell. Because of this *near*-symmetry of the unit cell, the growth rates along the *a*- and *b*-axes are nearly similar. The spherulites are therefore made of sectors in which either the *a*- or *b*-axes are radial—a unique example in polymer science for low symmetry unit cells



DOI: 10.1021/acs.macromol.7b00907
*Macromolecules* 2017, 50, 5995−6025

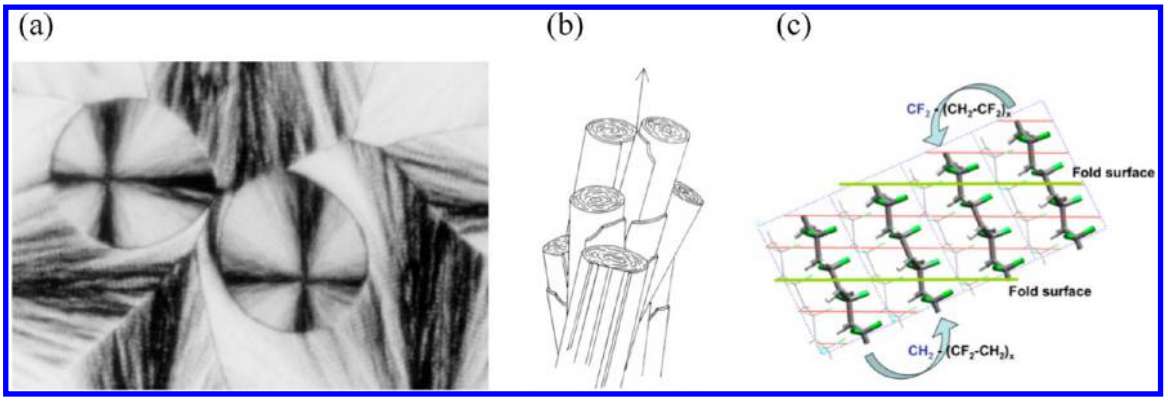


**Figure 16.** Scrolled morphology lamellae in γ-PVDF spherulites. (a) Optical micrograph (polarizing microscope) of two γ-PVDF sherulites surrounded by larger α-PVDF spherulites. The black and white extinction rings indicating lamellar twisting are best seen in the horizontal arm of the left α-PVDF spherulite. (b) The initial drawing of Vaughan illustrating the scrolled lamellae revealed by etching. (c) The parallel conformational crankshafts in the γ-PVDF crystal structure generate folds with different chemical constitutions on opposite lamellar surfaces. Part b: reproduced with permission from ref 125. Copyright 1993 Springer.

(Figure 15c). The lamellar twist sense is found to be *different* in these sectors. Within *one* spherulite of a *chiral* polymer, the *two opposite* lamellar twist senses coexist, and they depend on the radial growth direction. This leaves as the only origin of lamellar twist the fold surface stresses, that is, of the fold structures differences that, however, themselves, depend on the molecular and helix chirality.

In a different experiment, a similar lamellar twist reversal has been used as a morphological probe to evaluate the nature and orientation of the stresses associated with the fold bulkiness in a series of random copolymers of poly[(*R*)-3-hydroxybutyrate-*co*-(*R*)-3-hydroxyvalerate). In spite of their bulkier side chains, the valerate units are incorporated in the crystal lattice but because of their size they are also preferentially rejected in the fold surface. When their concentration exceeds a threshold value (14%—but only 2% for the bulkier hexanoate), the lamellar twist sense is reversed: the overcrowding changes the orientation of the stresses in the fold surface.[123,124]

The origin of surface stresses in unconventional scrolled lamellar shapes is amenable to an even more precise molecular analysis. Two examples are worth being mentioned. One is the gamma phase of PVDF. γ-PVDF crystallizes at high crystallization temperatures together with the alpha phase (α-PVDF) (Figure 16a). In the γ-PVDF spherulites, as observed by Vaughan, the lamellae are scrolled, with the scroll axis radial (Figure 16b).[125] Twisting supposes the existence of a 2-fold axis parallel to the radial growth direction. Scrolling is expected when no such 2-fold symmetry exists. Such a 2-fold axis exists for α-PVDF, but not for γ-PVDF. The scrolling results from a difference in fold volume in opposite sides of the lamella. As seen in Figure 16c, the structure of γ-PVDF is polar: the stems are parallel, and the crankshaft geometry brings similar main chain atoms to the (tilted) surface of the lamella. As a result of this polarity, the *chemical* constitution of the folds is different. On one lamellar surface, even for identical folds, there is one extra $CH_2$ and on the other one extra $CF_2$. The small difference in fold volume (10 $Å^3$ for a fold volume of ≈300 $Å^3$) generates a small splay of the stems (≈0.04°) that, when repeated nearly $10^4$ times, results in the observed lamellar scroll.[19,107]

Even−even polyamides and, namely, PA66 single crystals grown from solution display a similar and tighter scrolling. The morphology information is even more telling because different morphologies are observed. When crystallized at the same crystallization temperature, the single crystals are flat, scrolled, and flat again for increasing annealing temperatures used to generate the self-seeds. This morphology sequence must be related to the corresponding increase in lamellar thickness and the possibility to form acid and amine folds, as illustrated in Figure 17 for the cyclic monomer and dimer.[126] Flat crystals

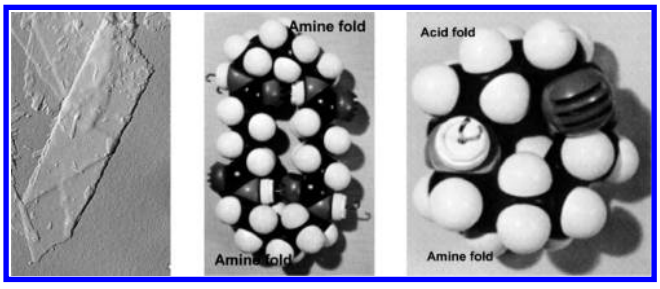


**Figure 17.** (a) A scrolled crystal of polyamide 66 formed at 172 °C in a dilute solution of glycerin that becomes flat when deposited on the substrate carbon film. The scroll diameter is 350 nm. (b) Possible structure of the cyclic PA66 dimer displaying two amine folds. (c) Possible structure of the cyclic PA66 monomer displaying an acid and an amine fold. Part a: reproduced with permission from ref 127. Copyright 2004 Wiley-VCH. Parts b and c: reproduced with permission from ref 126. Copyright 1969 Elsevier.

would then correspond to identical folds on opposite fold surfaces, whereas scrolled crystals signal the existence of amine and acid folds on opposite fold surfaces. The larger difference in volume would explain the tighter scroll diameter.[127]

The scrolled crystals of γ-PVDF and PA66 help analyze the nature and extent of the molecular features that generate the *unbalanced* surface stresses. In both cases, the information provided by the crystal structure helps track the folds' different volumes linked with chemical differences. As such, these two studies represent the only morphologies for which the origin of the unbalanced surface stresses can be quantified: 10 $Å^3$ out of nearly 300 $Å^3$ for PVDF, two methyl units (≈70 $Å^3$) for the tighter PA66 scrolls. Different fold volumes or encumbrances linked with conformational features are more difficult or virtually impossible to establish. The impact of differences in surface stresses can also be illustrated by designing triblock copolymers in which the central B block is crystalline and the


DOI: 10.1021/acs.macromol.7b00907
*Macromolecules* 2017, 50, 5995−6025

amorphous blocks A and C are incompatible and segregate on opposite surfaces of the lamellae upon crystallization of block B. The resulting lamellar morphology is, in this specific case, scrolled.[128] The local deviations from strict crystallography of the crystalline core are even smaller than for the PVDF and PA66 cases. In all these cases, the deviations are revealed only because of their cumulative impact and the resulting nonplanar lamellar morphology that helps reveal these local otherwise undetectable interactions.

At this stage, it may be worth underlining the fact that very different lamellar morphologies are amenable to a single and coherent cause, namely, the existence of surface stresses associated with overcrowding of the fold surface. The various manifestations and the experimental support provided by the recent studies are a delayed tribute to the concluding words of Keith and Padden's paper in 1984 about their "postulate": "...It is for this reason that in the main text the suggested differences in degrees of overcrowding at opposite surfaces is advanced as postulate rather than a demonstrable premise. It is believed that this postulate commands attention because deductions based upon it appear to represent a significant advance in interpretation of diverse and hitherto unexplained morphological observations in a reasonably coherent way".[108]

To conclude, the analysis of the structure and morphology of crystalline polymers has represented a considerable challenge because several structural levels are involved. Elucidation of each level and the connections and interactions up and down the hierarchical ladder—from the unit cell to the spherulites—is a continuing and challenging process. The elucidation of the interactions between the various structural scales amounts at times to forensic approaches that require testing different scenarios and evaluate the possible implication of potential "culprits": crystalline core, lamellar thickness, folds, reorganization during crystallization, etc. Many such "cases" have been solved sometimes after years of effort. Their understanding provides means to alter the spontaneous processes and generate new structures and properties. These insights provide a detailed background to evaluate the different crystallization theories that explain how these complex structures develop from the entangled polymer melt.

## ■ SUPRAMOLECULAR CRYSTALS

A modern and rapidly developing research area has recently emerged. Supramolecular chemistry and physics lead to newly designed and synthesized molecules which can be hierarchically self-assembled to form long-range ordered supralattices. These supralattices can also be viewed as the formation of supramolecular crystals. Before describing in detail supramolecular crystals, one needs to clearly define what supramolecular crystals are and how they differ from polymer crystals considered so far.

Polymer crystals are not different from any other type of crystals. They are homogeneous solids with basic motifs constituted by atoms, molecules, ions, or clusters. These identical motifs build up highly and periodically ordered crystal lattices with exactly the same arrangement over three directions in the real space.[129] In crystals, motifs are the smallest building blocks that repeat themselves in crystal lattices. A crystal possesses three principal orders: long-range positional, bond-orientational, and molecular orientational orders. These orders apply down to the atomic level: every atom is located at a specific space position that is orderly repeated. In supramolecular crystals, the highly ordered supramolecular lattices extend also periodically along the three directions in real space. But their building blocks (corresponding to "motifs" in normal crystals) are at least nanoscale and are constructed of molecules and/or clusters. Within the building blocks, those atoms, molecules, and/or clusters may not have specific space positions at a subnanometer scale, and thus, the repetition scheme may not exist within the building blocks. Therefore, in a supramolecular crystal, the positional, bond-orientational, and molecular orientational long-range orders are only meaningful at the length scale of the building block level. Therefore, lattices that are constructed based on the repeatability of such building blocks are categorized as supramolecular crystals.[130] Note that the globular protein crystals that are also built of large units do not belong to this category, since in those crystals each atomic position in the proteins is perfectly defined to fit to the repetition scheme.

A simple example of supramolecular crystal formation is the nanophase separation process due to the immiscibility between components in systems such as diblock copolymers with two immiscible blocks. Generally speaking, all the crystallographic methods can be utilized to investigate the structure of supramolecular crystals. X-ray and/or electron diffraction experiments help obtain correlation functions generated by density functions of these ordered structures to determine crystal lattices based on the Bragg equation in its reciprocal lattice. Note that a reciprocal lattice is a Fourier transformation of its corresponding ordered structure in real space, while construct a density function from a correlation in a reciprocal lattice is impossible. The length scale of these crystals ranges from sub-10 nm (various nanophase separated ordered structures) to micrometers (such as so-called "colloidal crystals").

One of the most recent examples in supramolecular crystals is the finding of Frank−Kasper phases in soft matter materials. Frank−Kasper phases were originally found in metal alloys in which metal atoms with different radii and electronic states pack into spherical phases.[131,132] These phases include the Frank lattice (an icosahedron with a coordination number of 12) and the Kasper lattices (with higher coordination numbers of 14, 15, and 16). Some high-temperature superconductors belong to these phases. Stabilization of these phases in metal alloys results from both geometric factors and the tendency to enhance low orbital electron sharing due to fewer surface contacts among the atoms.

In organic/hybrid molecules, the Frank−Kasper phases observed so far are the A15 (space group of $Pm\bar{3}n$) and sigma (space group $P4_2/mnm$) phases and dodecagonal quasicrystals. Reports include small molecule surfactants,[133−138] block copolymers,[139−144] liquid crystals,[145,146] dendrimers,[147−150] colloidal particles,[151] molecular giant tetrahedra,[152,153] and very recently a series of giant surfactants.[154] In contrast to metal alloys that use atomic spheres with different sizes and electronic states as the motifs, these supralattices are built up with molecules of a single size. Spherical building blocks of different sizes are constructed during the first step of self-assembly process, and the motifs further organize into supralattices, during a so-called hierarchical self-assembly process. The Frank−Kasper supralattices reported so far have two different spherical building blocks with similar size (the ratio of their diameters is not too different). Further investigations show that it is possible to find more varied Frank−Kasper phases with larger size differences of the



DOI: 10.1021/acs.macromol.7b00907
Macromolecules 2017, 50, 5995−6025

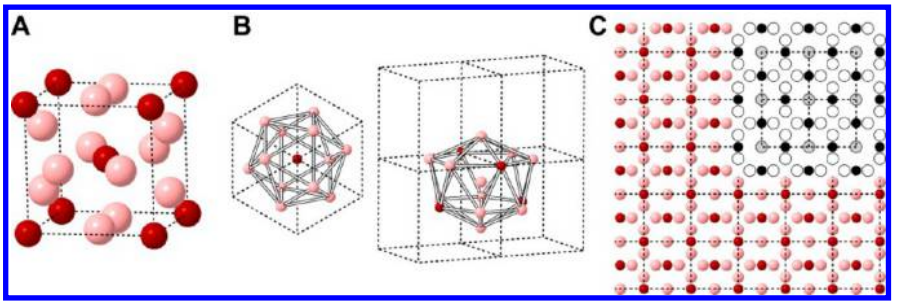


**Figure 18.** Schematic illustration of the A15 phase. (A) In an A15 cubic unit cell, the red and pink colors represent different coordination environments. (B) Schemes of CN = 12 (the red sphere) and CN = 14 (the pink sphere) coordination environments in the A15 lattice. (C) 2D projection of the A15 lattice along the ⟨001⟩ direction. The inset shows a $4^4$ tiling number along the $z$-axis. The spheres located in sparse layers ($z$/4 and $3z$/4) are shown by gray circles, and the spheres in the dense layers are shown by black and white circles ($z$/2 and $z$). Reproduced with permission from ref 152. Copyright 2015 AAAS.

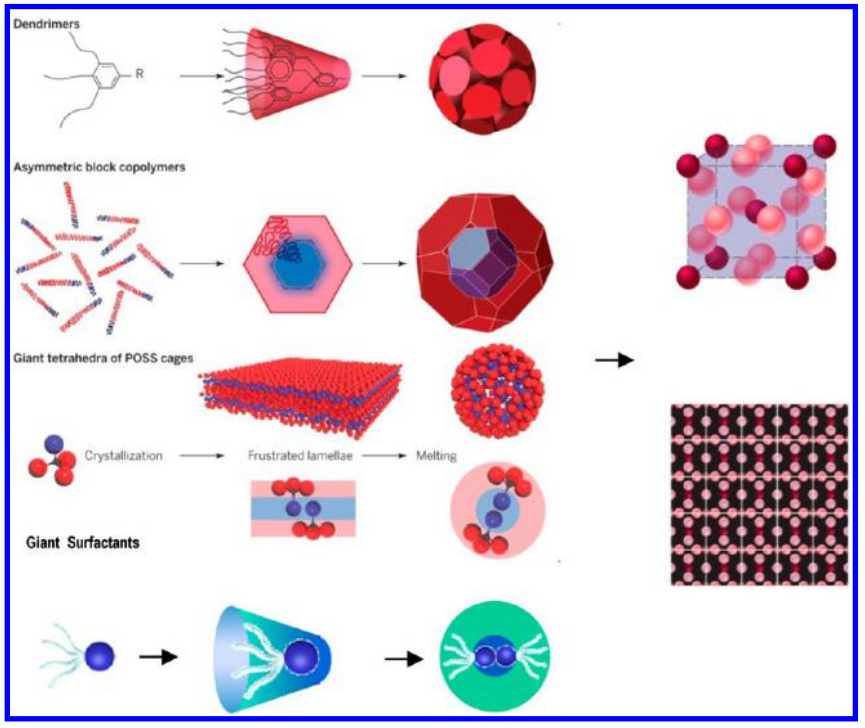


**Figure 19.** Several different molecular designs of dendrimers, block copolymers, giant tetrahedra, and giant surfactants. All of them are involved in hierarchal self-assembly processes. First, these molecules self-assemble into spherical building blocks via different interactions. The spherical building blocks then construct a supramolecular crystal with a Frank−Kasper A15 phase lattice. Reproduced with permission from ref 153. Copyright 2015 AAAS.

spherical building blocks, such as the z phase. Work along this line is in progress, and further developments are anticipated.

Let us examine the A15 phase in supramolecules in more detail. In metal alloys such as $Cr_3Si$, the A15 phase possesses an $A_3B$ stoichiometry with a cubic unit cell. As shown in Figure 18A, a typical cubic unit cell consists of six A units (pale-red spheres) in 14-fold Kasper polyhedra and, as shown in Figure 18B, two B units (dark-red spheres) in 12-fold icosahedral coordination with a space group of $Pm\bar{3}n$ ($O_h^3$). The projection of the spherical atoms seen along the ⟨001⟩ direction displays a regular two-dimensional (2D) $4^4$ tiling number (Figure 18C) (4).

Figure 19 summarizes four different types of supramolecules which construct those A15 phases via hieratical self-assembly processes.[153] It is evident that for these materials the pathways and mechanisms to form spherical building blocks are quite different, yet all these four spherical building blocks adopt the same A15 lattice packing scheme. Within all of these spherical building blocks, no long-range order exists among the atoms, molecules, and/or clusters, and thus they are supramolecular crystals.

When a self-assembly process of supramolecules takes place in thin films, its overall free energy must be minimized by balancing enthalpy and entropy of the system. A specific phenomenon may take place: the components with low surface energy would preferentially migrate to the free surface and the components with higher affinity close to the substrate.[155] In addition, the thickness is limited, and its size allows for the packing of only a few unit cells along the thickness normal direction. This size limitation may also result in confinements of molecular conformation within the thin films and near the film surfaces (usually contacted with the air) and interphases (usually contacted with substrates).


DOI: 10.1021/acs.macromol.7b00907
*Macromolecules* 2017, 50, 5995−6025

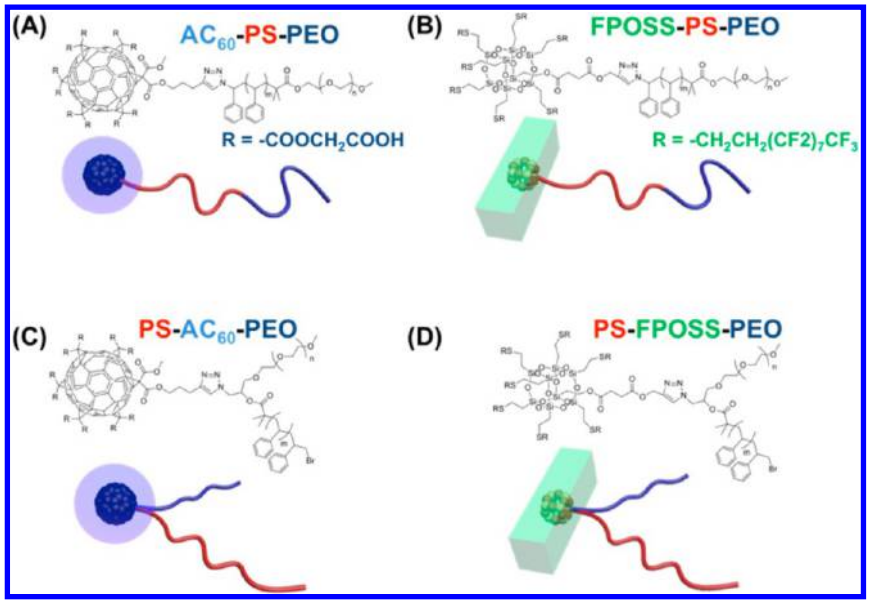


**Figure 20.** Molecular structures of giant surfactants: $AC_{60}$-PS-PEO (A), FPOSS-PS-PEO (B), PS-$AC_{60}$-PEO (C), and PS-FPOSS-PEO (D). Hydrophilic components are labeled in blue, hydrophobic components in red, and omniphobic components in green. Reproduced with permission from ref 156.

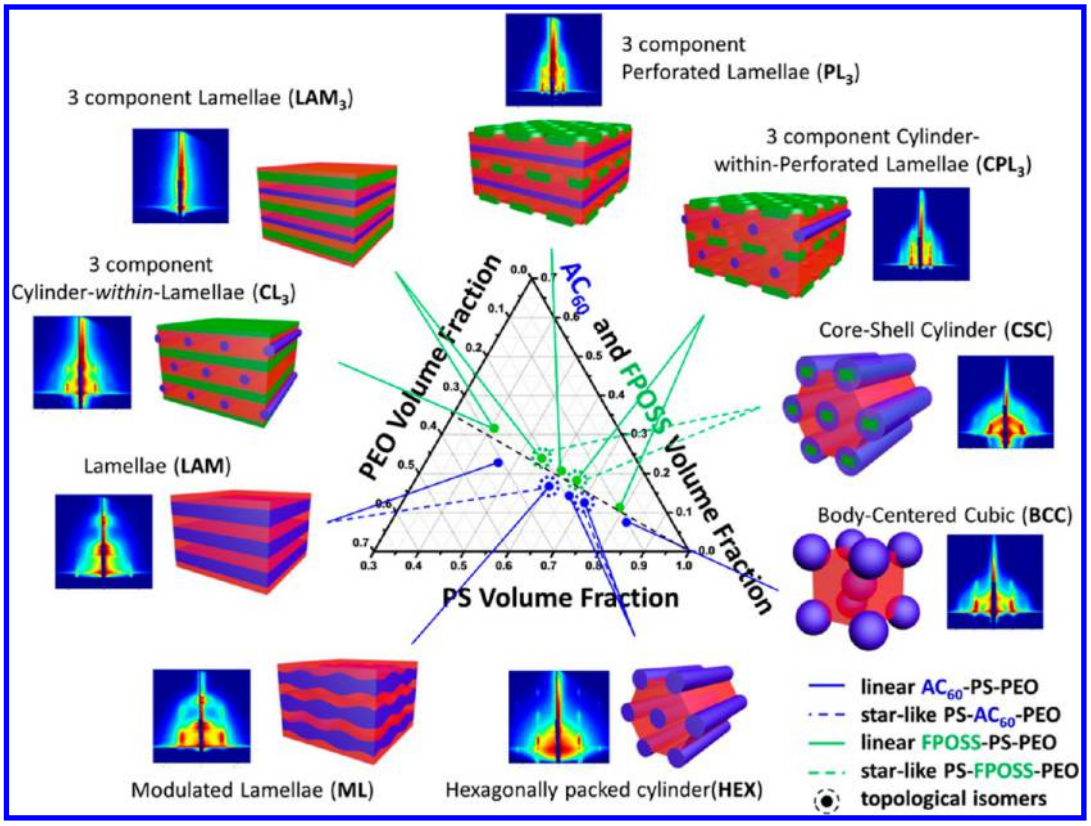


**Figure 21.** Ternary phase diagram of the three-component giant surfactants self-assembly in thin films. Self-assemblies of $AC_{60}$-based and FPOSS-based giant surfactants are depicted by blue and green lines, respectively. Each self-assembled phase is represented by the colored model and supported by the corresponding GIXRD pattern. Solid lines represent the linear giant surfactants, and the dashed lines represent the star-like ones. The black dashed line indicates compositions with the equal volume fraction of the molecular nanoparticles ($AC_{60}$ and FPOSS) and PEO. Reproduced with permission from ref 156.

An interesting molecular topological effect and space confinement impact on supramolecular crystallization in thin films has been investigated with different types of giant surfactants that have been specifically designed and synthesized. Distinct molecular topologies and different molecular nanoparticles surface functionalities of these giant surfactants include two molecular nanoparticles: hydrophilic, carboxylic acid-functionalized [60]fullerene ($AC_{60}$), and omniphobic, fluoro-functionalized polyhedral oligomeric silsesquioxane (FPOSS, see Figure 20) as heads of these giant surfactants



DOI: 10.1021/acs.macromol.7b00907
Macromolecules 2017, 50, 5995−6025

with different affinities with respect to the tail blocks.[156] The tails tethered are linear diblock copolymers of PEO-*block*-PS, and they are tethered at two different positions: at the PS end of the block (linear) and at the junction point of the diblock copolymer (star). These giant surfactants are two topological isomer pairs with almost identical chemical compositions but different architectures (Figure 20).

The ordered structure formations in thin films and the phase transitions of these giant surfactants can be monitored via grazing incidence X-ray scattering (GIXS) and bright field transmission electron microscopy. The phase structures vary widely by changing the tail length of the PS block with fixed length of the PEO block. In the series of giant surfactants with $AC_{60}$ head groups, relatively simple two-component morphologies are formed: PS domains and mixed $AC_{60}$/PEO domains. Whereas slight variations of the supramolecular crystal structures do exist for these two topological isomers, both exhibit a transition sequence of lamellar, modulated lamellar, hexagonal, and body-centered cubic phases (Figure 21), although different dimensions are observed. By contrast, the giant surfactants with FPOSS head groups form three-component morphologies. A sequence of undulated lamellar ($UL_3$), three-component lamellar ($LAM_3$), perforated lamellar ($PL_3$), and cylinder-*within*-perforated lamellar ($CPL_3$) structures is observed in three component structures with increasing tail length of the PS block.[156] Within each of the FPOSS-based giant surfactants, the topological isomers exhibit very different supramolecular crystal structures as shown in Figure 21. In order to explain the topological dependence of these phase behaviors, we utilize a stretching parameter of the PS blocks in these different structures to elucidate and quantitatively characterize the phase transitions.[156] The observed versatility of self-assembled morphologies suggests that carefully designed macromolecules can provide a variety of well-controlled supramolecular crystal structures. The size and the geometry of these supramolecular crystal structures can be further fine-tuned by specific molecular topologies in addition to the composition.

## POLYMER CRYSTALLIZATION MECHANISMS

When compared to crystallization processes of simple, small molecules, polymer crystallization takes place in much deeper supercooled liquids, and it is far away from thermodynamic equilibrium (supercooling is defined as the difference between an equilibrium melting temperature and the isothermal crystallization temperature). In classical nucleation theory, when a polymer is able to crystallize, the Gibbs free energy of the undercooled melt or solution under a constant pressure is always higher than that of the crystal solid. The traditional crystallization scheme describes the initial stage of crystallization as a crystal nucleus with a small volume and a large surface. During the formation of this nucleus, the volume free energy term of the nucleus is negative toward the overall Gibbs free energy and stabilizes the nucleus. The surface free energy term of the nucleus is positive in Gibbs free energy and thus destabilizes the nucleus. In the beginning, the surface free energy dominates and wins in the competition, leading to the formation of a free energy barrier. The driving force to overcome the free energy barrier and trigger the nucleation process (either primary or surface nucleation) originates from the thermal (density) fluctuations in the melt or solution.[157]

Beyond the general thermodynamic illustration of the crystallization process put forward by Gibbs and others, polymer crystallization process has a specific character. It represents a significant conformational change of linear polymers from a three-dimensional random coil conformation into chain-folded lamellar crystals. It is certain that the specific trajectory of an individual chain molecule during crystallization is very different from others. Nevertheless, we do not have a technique to monitor each chain molecule and "watch" how it crystallizes. An analytical theory thus takes a "mean-field" approach by simplifying the individual trajectories to become an average form, and the analytical theory sacrifices these molecular details. In addition, computer simulation may lead to catch up those individual trajectories and provide a visualized, phenomenological, and physical picture of polymer crystallization process. A number of simulations have also been performed that attempt to follow the fate of individual trajectories and the onset of chain folding prior to or during deposition on the growth front.[158−162]

Experimentally, in the past 60 years, a number of isothermal crystal growth (with pre-existing primary nuclei) experiments of semicrystalline polymers in the melt and solution at different crystallization temperatures (or supercoolings) have been investigated. The detailed descriptions of polymer crystallization rest for the most part on one hand on structural and morphological observations and on the other hand on scattering experimental results. These two approaches have led to dissimilar detailed microscopic kinetic models of polymer crystallization. Although some theoretical approach can provide certain satisfactory explanations for the experimentally observed results, no single theoretical approach can provide predictions of all the major experimental observations. These major experimental features include that: (1) Crystalline polymers exhibit linear growth rates (Figure 22a), and many of them show at least parts of the growth rate regimes (Figure 22b). (2) The lamellar thickness of the growing polymer crystals are proportional to the reciprocal supercooling, and for crystalline oligomer fractions, integral chain folding (IF) lamellar crystals are observed (Figure 22c). (3) When lamellar thickness is a constant, its linear growth rate is a unique function of the supercooling (Figure 22d). (4) Anisotropic or isotropic growth rates along different (*hkl*) growth directions in single crystals (Figures 22e). (5) Finally, the molecular mass dependence of the linear growth rates and molecular segregation phenomenon (Figure 22f).

Despite the heated debates over crystal-growth models and the validity and extent of chain folding, the best summaries and discussions of polymer crystallization were given by Gerhard Goldbeck-Wood in a discussion meeting in Gargnano in the year 2000 and also in an earlier publication.[163] The classical theories of crystallization rest on a scheme of "nucleation and growth" that has been widely applied for low molecular mass materials and emphasizes the impact of the crystal on its surrounding liquid. These views have been applied with a significant measure of success to the crystallization of polymers to account, in particular, for the variation of the average growth rate of lamellae as a function of undercooling. They assume that the relevant crystalline entities/units are the stems. These stems attach, more or less sequentially, on the growth front and reorganize. In this view, growth is controlled by the crystal growth face, and the whole process may be described as a single stage model. In brief, the first analytical theory was put forth by Hoffman and Lauritzen,[164,165] Hoffman et al.,[166,167] and Frank and Tosi.[168] Their physical mode was to describe a surface nucleation


DOI: 10.1021/acs.macromol.7b00907
*Macromolecules* 2017, 50, 5995−6025

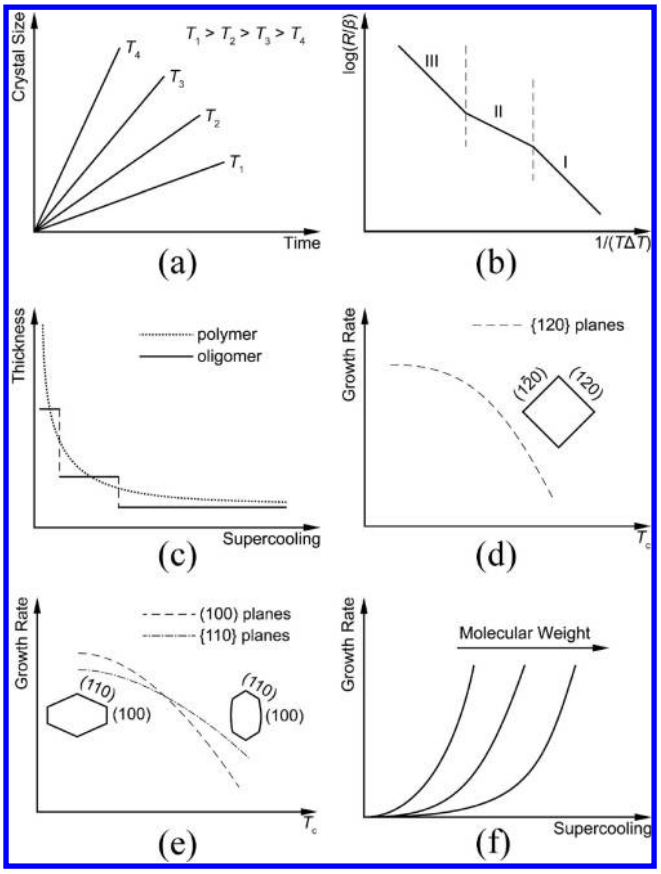


**Figure 22.** Schematic illustrations of the general features of polymer crystallization. (a) Linear crystal growth sizes at a constant temperature under isothermal crystallization experiments near and below the melting temperature. If the crystallization temperature is near and above the glass transition temperature, the trend will be reversed. (b) Relationships between logarithmic crystal growth rate ($R$) and $1/T\Delta T$, where the $\beta$ is the prefactor including an activation term, $T$ is the crystallization temperature, and $\Delta T$ is the supercooling based on classical nucleation theory. Growth regimes I, II, and III are based on experimental observations of PE (replotted with permission from Hoffman and Miller, 1997). (c) The lamellar thickness formed during crystallization is inversely proportional to supercooling. In oligomers, quantized changes in the lamellar thickness can be observed. (d) Only one relationship between growth rates and crystallization temperatures can be seen for isotropic single crystal habit (as in PEO). (e) Relationships between growth rates and crystallization temperatures along different crystallographic planes for anisotropic single crystal habit (as in PE). (f) Relationships between molecular masses and growth rates at different supercoolings. With decreasing molecular masses, the supercooling required for nucleation is reduced.[163] Reproduced with permission from ref 40. Copyright 2008 Elsevier.

process of polymer lamellar crystals with a clear enthalpic nucleation barrier associated with surface free energy countered with the bulk free energy by adding one stem at a time. There are four parameters to describe the surface nucleation process: the surface nucleation rate, the growth rate parallel to the growth plane that covers the growth front after surface nucleation which is called the lateral covering rate, the width of the growth front (the substrate length) which the nuclei and growth cover, and the growth rate normal to the growth plane. By establishing relationships among these four parameters, regime transitions can be revealed although these parameters are not all experimentally measurable. In order to explain new findings of polymer crystal growth behaviors, this theory has been under several modifications to reach an exquisite stage of details. It must be acknowledged that the long elaboration process has somewhat weakened its impact. As wisely and somewhat wittily stated by Doyle, referring to the LH theory, "the number of parameters in a complex theory may give the theory sufficient plasticity to fit a wide variety of scenarios".[169] Within the concept of surface nucleation mechanism, a few other crystallization modes and theories have also been proposed, which describe some specific features of polymer crystal growth. For example, Flory considers a first step with parallelization of chain segments involving changes in conformation followed by repeat units "falling" into crystallographic register. Multiple-path deposition within one stem on to a crystal growth surface was proposed by Point[170,171] in order to resolve the so-called "$\delta l$ catastrophy". To describe the molecular segregation during polymer crystal growth with broad molecular mass distributions, a molecular nucleation concept was proposed by Wunderlich.[172] A two-dimensional nucleation process was suggested to describe chain-sliding diffusion along the $c$-axis of the extended chain PE crystals with the hexagonal lattice at elevated pressures by Hikosaka.[173,174] An approach describing the rough surface growth of polymer crystals that possesses an entropic barrier (a "poisoning" mechanism) was proposed by Sadler,[175−179] Sadler and Gilmer,[180−182] and Ungar and Keller.[183] These developments lead to a reconsideration of the origin of the nucleation barrier that is attributed to both enthalpic and entropic terms.[184,185]

Polymer crystallization is however recognized as a multistage process that involves all or most of the following steps: conformational changes, liquid−liquid phase separation due to molecular mass distribution, chain folding, formation of aggregates or bundles, crystallographic packing, perfection (crystal and lamellar thickness), and further possible solid−solid phase transformations. The sequence, relative importance, or even existence of these different stages may depend on the polymer nature and crystallization conditions. Along this line, some models suggest that the melt becomes "structured" (at various stages and times) just prior to crystallization. These stages could be spinodal decomposition followed by crystallization,[186,187] formation of blocks that then form lamellae,[188−190] etc. Wide-angle X-ray diffraction and small-angle X-ray scattering results suggest that the melt becomes indeed organized on a large scale (small-angle X-ray scattering signal) prior to crystal building (wide-angle X-ray diffraction signal), which supports a spinodal decomposition. Also, diffraction data suggest that isotactic polyolefins adopt some form of helical conformation—thus preorganization—in the melt.[191] In addition, reorganization of lamellae behind the growth front is supported for several polymers (such as in the cases of PEO and PE) by their faster melting on heating: the crystal is not yet fully organized or has not yet reached its "stable" lamellar thickness.

Out of the various scenarios, the multistage model developed by Strobl is at present the most popular and most frequently used to interpret a wide range of experimental data. In the initial report, crystallization is described as a two-stage process in which "at first, an initial form of lower order builds up which then becomes stabilized to end in the final state with lamellar morphology... The initial structure is composed of crystal blocks in planar assemblies, which then fuse into a homogeneous lamella. The edge length of the blocks in chain


DOI: 10.1021/acs.macromol.7b00907
Macromolecules 2017, 50, 5995−6025

direction determines also the lamellar thickness. The size of the blocks corresponds to the minimum necessary to be stable".[192] This model of "granular substructure of lamellae" has been supported mostly by scattering, atomic force microscopy, and differential scanning calorimetry experimental data in a number of later reviews and publications.[185−187] The thermodynamic scheme rests in particular on extrapolation of the so-called "crystallization and melting lines" that correlate the inverse of lamellar thickness with melting, crystallization, and annealing temperatures.[190]

All the multistage scenarios describe a melt that becomes structured to some extent in the initial crystallization, in a process that "assists" crystallization and creates crystal "precursors" that later assemble to further reorganize or structure to form fully grown lamellae. An obvious difficulty of this approach is to evaluate the relationship and impact of the various (pre)organization stages on the final, global crystallization process and morphology. It should be stressed however that according to these views, growth results from an ordering process initiated and located outside the crystal.

Anticipating later developments, and quoting again Goldbeck-Wood,[163] the multistage models provide only limited links with the molecular level of information that can be and sometimes has been reached by an analysis of the crystal structure as developed in the present paper. Most of the information used in these models stems from global techniques (X-ray scattering, spectroscopic techniques, differential scanning calorimetry, etc.). Useful as they are, these techniques are little adapted to investigate a crystallization process that is very local and at any time affects only a very small fraction of the material investigated. With such a limitation, it is difficult to differentiate the crystalline and amorphous components.

Keeping in line with the present paper's emphasis on structure, a number of structural features of polymer crystals suggest that, in most cases, the interaction with the growth front of the polymer stems is by far the major determining factor in polymer crystallization. This forensic approach takes advantage of the many original and sometimes even unique features of the structure(s) and morphology(ies) of crystalline polymers, whether they are produced under "natural" and more artificial conditions. The structural and molecular markers reflect the diversity of polymer structures and conformations: molecular chirality, linear or helical stem shape, right- or left-handed helices in case of isotactic polyolefins, parallelism or antiparallelism of stems, crystal polymorphism, coexistence of chiral and racemic crystal structures for the polyolefins, etc. In many cases, appropriate crystallization conditions make it possible to gain a direct insight into the selection processes involved. The structural selection processes also translate into morphological features, e.g., crystal habits, lamellar twists in spherulites, and others. When considered together, these different markers provide more reliable clues to understand the polymer crystallization process than for example the less discriminative lamellae.

Several structural arguments have already been developed by two of the present authors to support a "nucleation and growth" type crystallization mechanism. Some of them are briefly recalled here. If a lamellar crystal is formed by ordering multiblocks fused together, the precursor blocks developing away from the growing crystal cannot foresee to what crystal polymorph at the growth front they will have to adapt to. When right- and left-handed helices are involved, reorganization of the blocks to adapt to the existing crystal structure (e.g., chiral $\beta$-it-PP) and racemic ($\alpha$-it-PP and $\gamma$-it-PP phases) would be tantamount to a "remedial" action. The helical hands need to be reversed, and/or the position of the stems should be modified to, for example, respect the sequence of layers made of right- and of left-handed helices in $\alpha$-it-PP and $\gamma$-it-PP. This is a major reshuffling of the whole structure that is inconsistent with the long-range organization revealed by the polymer morphology.

Both $\alpha$-it-PP and $\gamma$-it-PP phases provide another critical test for any model that assumes a pre-existing, presumably poorly organized phase. In $\alpha$-it-PP, a unique lamellar branching takes place, in which the plane of daughter lamellae is oriented at some 80° to their parent ones.[5] This branching is initiated by the deposition on the lateral *ac* faces of the elongated lamellae of helices of the same hand as the substrate ones rather than of opposite hand as required by the crystal structure.[6] In addition, this same (mis)orientation process becomes a systematic feature of the $\gamma$-it-PP phase.[7] As detailed earlier (see Figure 2), the crystal structure of $\gamma$-it-PP is made of (double) layers of *nonparallel* helices (*RR* and *LL*), with a stringent alternation of these double, antichiral layers. Such a structure with so many orientation and chirality constraints cannot be created by a reorganization of a precursor "block" made, most presumably, of *parallel* helices. It is more likely generated by a process of nucleation and growth in which the incoming stem "feels" the growth front surface topography and is attached or rejected depending on its chirality and orientation. Yet, the $\gamma$-it-PP overall crystallization characteristics (growth rate variation with supercooling, etc.) are "standard" and "normal" behavior and do not in any way make it possible to suspect the complexity of the structure. At the same time, this "normality" of the crystallization behavior questions the necessity to invoke a precursor phase and makes a strong case for a nucleation and growth-dominated crystallization process.

The importance of direct interaction with the growth front in crystal growth applies also when the polymer is deposited on a foreign, "artificial" substrate, namely, on nucleating agents. These interactions are best revealed for helical polymers, as illustrated in Figure 4. When the substrate periodicity matches the interstrand distance, the helical path (and not the chain axis) becomes oriented parallel to the substrate "grating". This helical path is tilted to the chain axis. In the form I of it-PBu, the structure is made, as in $\alpha$-it-PP, of alternating layers of right- and left-handed helices. Depending on the helical hand, right or left, in the first layer, two different chain orientations will be generated. As shown in Figure 4a, it is even possible to obtain multilamellar domains several tens of $\mu m^2$ with the same helix orientation, thus creating in effect a single crystal type unit cell orientation in a multilamellar crystalline domain. Here again, the structure is definitely controlled by the polymer/substrate exquisite interactions. As a corollary, since the major intermolecular interactions are van der Waals forces, the forces that acted in this nucleation and growth-type orientation process have an effective range of at most about 1 nm. This last figure fully justifies investigating crystallization processes via local structural features (helical hand, stem orientation (or *mis*orientation for $\alpha$-it-PP and $\gamma$-it-PP!) that remain embedded in the crystal morphology.

Polymer crystallization is intrinsically a complex process that implies generating order (or even several order types and length scales) starting from intertwined long random coils. Is this process amenable to a more elaborate analysis? We believe



DOI: 10.1021/acs.macromol.7b00907
*Macromolecules* 2017, 50, 5995−6025

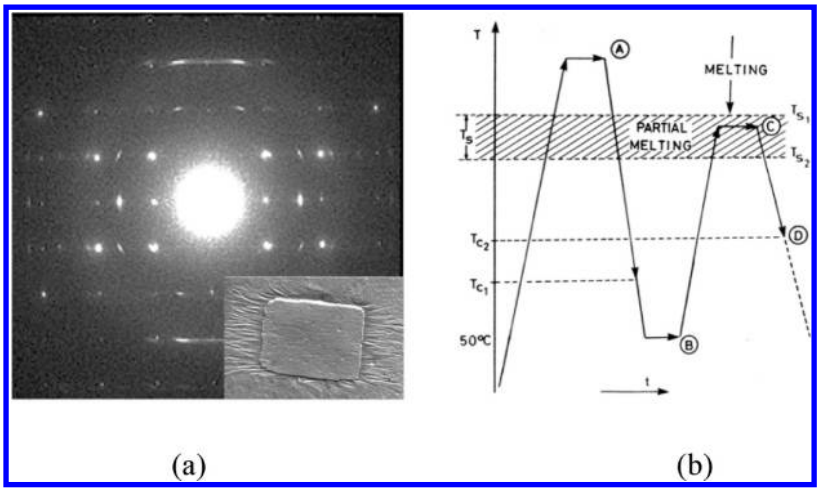


**Figure 23.** (a) Composite diffraction pattern of $\beta$-it-PP epitaxially crystallized on one of its nucleating agents, here dicyclohexylterephtalamide (DCHT). The sharp spots correspond to the DCHT and the arced reflections to $\beta$-it-PP. Note the dimension match between $\beta$-it-PP and the substrate along the chain axis (vertical). Inset: the trace of the DCHT single crystal (after its dissolution) on the film of it-PP. The further growth of $\beta$-it-PP lamellae in the melt after their nucleation on the NA crystal is vividly illustrated. (b) The thermal history used to produce self-seeds and establish the efficiency scale of nucleating agents. The final crystallization temperature (step D) depends on the partial melting temperature (step C) of a "standard" sample produced through steps A and B. Part a: reproduced with permission from ref 197. Part b: reproduced with permission from ref 200. Copyright 1993 John Wiley & Sons.

that the multiple selection processes required to generate a polymer crystal structure are such that an *a priori* selection process appears most efficient. The multiple selection processes on different length and time scales that take place during crystallization affect the growth kinetics. We have grouped them together and referred to them as the so-called nucleation barrier. Various experimental observations can monitor their effects on the nucleation barrier based on the structural and morphological evidence. The selection rules depend on how the similarities of effects arising from chemical structure, molecular conformation, molecular mass, and morphology can be sorted out in each selection process. Dissimilarities among these parameters result in a stronger "sorting out" process. The combination of these sorting processes in their free energy form creates a nucleation barrier that includes both enthalpic and entropic contributions. It is qualitatively expected that the traditional free energy enthalpic contribution dominates short-range interactions at smaller length scales and the entropic sorting processes at larger length scales. Although our understanding of solid state structures has progressed significantly, issues remain concerning the structure and dynamics of the supercooled melt in the bulk as well as near the interface and their effects on the nucleation and growth processes.

Any types of preorganization of the polymer melt in the vicinity of the growth front, such as mesomorphic-like or liquid-crystalline-like, imply merely parallelism of chains or segments. Of course, such a mechanism is consistent with the Gibbs rules stating that crystallization proceeds via intermediate metastable state(s), as first suggested by Ostwald to be the stage rule.[157] Such paths are well documented for PE crystallized under high pressure, and for some relatively rigid liquid-crystalline polymers. The pathways of these transformation sequences are usually well separated and identified by various experimental techniques. The less ordered mesophases, such as liquid crystals, possess highly symmetric morphologies, frequently hexagonal or, as illustrated in Figure 6b for the high-pressure PE lamellae, even rounded, very different from the more common asymmetric habits observed for PE crystallized in its stable, orthorhombic phase (Figures 7 and 8). These more symmetric shapes would be preserved and indicate a transient stage via a mesomorphic type organization.

## CRYSTALLIZATION PROCESSES IN SUPRAMOLECULAR CRYSTALS

To introduce the concept of "supramolecular crystallization", first and by far the most important notion is that the formed entities are crystals. In a supramolecular crystal, the positional, bond-orientational, and molecular orientational long-range orders are now only retained at the length scale of motif repetition, and these long-range orders are not necessary for the structures within the motifs at smaller length scales. In such a way, supramolecular lattices are constructed based on the repeatability of building blocks (motifs) to describe supramolecular crystals. When they form the supramolecular crystals, the formation mechanisms are identical with the classical descriptions of phase transformations. Namely, they are either nucleation and growth that illustrate a phase transition from a metastable state to an equilibrium state with a free energy barrier or spinodal decomposition that describes a phase transition from an unstable state to an equilibrium state without overcoming a free energy barrier. In addition, supramolecular crystallization is usually carried out cooperatively at different length scales as a hierarchical assembly process. The overall supramolecular crystal formation may thus require completion of several stages of sequential ordering structure formation, as illustrated in Figure 19. This may be best described to possess several separated steps of structure formations, and therefore, the free energy barrier, if it exists, is also partitioned into different stages to generate an energy landscape. A critical issue here is when the size of building blocks becomes increasingly larger with heavier masses; the dynamics of these building blocks may be more sluggish. Overcoming a free energy barrier or simply diffusing/moving to an equilibrium state by thermal (density) fluctuations becomes more difficult and time-consuming. The question is, how large does the building block have to be to stop this self-


DOI: 10.1021/acs.macromol.7b00907
*Macromolecules* 2017, 50, 5995−6025

assembly process? At what stage do we need to apply external force fields (such as mechanical, electric, or magnetic) to assist the building blocks movements and/or to overcome the barriers to assemble?

## MANIPULATING POLYMER CRYSTALLIZATION

Three specific topics in the field of polymer crystallization are of particular interest: one is related to practical industrial applications—nucleating agents—and two others are associated with nanoscience and engineering—homogeneous nucleation and polymer crystallization in nanoconfined environments.

**Nucleating Agents.** Crystalline polymers may differ widely by the ease with which they crystallize, as manifested by their growth rates. Maximum growth rates are, for example, for high density (linear) polyethylene >5000 mm/min, polyamide 66 1200 $\mu$m/min, polyamide 6 150 $\mu$m/min, and it-PP 20 $\mu$m/min.

Growth rates therefore set limitations on the overall crystallization rates that can be achieved for some commodity polymers. The most efficient way to overcome these limitations is to increase the number of nuclei, which in addition reduces the spherulite size, improves mechanical properties, and may, for highly divided nucleating agents, impart clarity to the molded parts.

The search for efficient nucleation agents has long been empirical and still is to some extent. In its most general acceptation, nucleation agents are any kind of material—low molecular weight crystalline particles or crystalline polymers—that provide a favorable, interacting substrate for the polymer nucleation. Deciphering the exact nature of these interactions has remained a considerable challenge for many years. The chemical and structural diversity of these materials and the fact that a given nucleating agent is efficient for structurally very different polymers (e.g., sodium benzoate for PE and it-PP) made it difficult to determine their mode of action. Also, the efficiency was usually investigated by global techniques—mostly differential scanning calorimetry analyses that determine the increase in crystallization temperature of the nucleated polymer cooled from the melt at some fixed rate.

Analysis of the interactions requires a *much closer* look at the interface. This can be achieved by using thin layers of the polymer and the nucleating agent that are examined by electron diffraction (crystal or morphology epitaxial growths).[82] The electron diffraction patterns (cf. Figure 23a) combine sharp nucleating agent spots and arced polymer ones. The combined pattern provides all the information needed to characterize the polymer/nucleating agent structural relationship: relative orientation of the two lattices and nature of the contact planes. A number of studies using this approach have helped determine that the polymer/nucleation agent interactions are mostly of epitaxial character. The interacting crystal surfaces have complementary structural/topographic features at the unit cell level, and this favorable interaction is repeated over the interface—thus the criterion of dimensional lattice match.[82] These requirements are illustrated in Figure 9c for the interface between it-PP ($\alpha$ phase) and the polymeric nucleation agent isotactic poly(vinylcyclohexane) (it-PVCH).[62] The profiles of the (100) plane of it-PVCH crystals and the (110) plane of $\alpha$-it-PP crystal display similar ripples. The matching of lattice dimensions is nearly perfect: 0.65 nm along the chain axis and ≈2.19 nm normal to it. The disregistry is thus nearly zero, whereas epitaxy is still possible when the matching lattice parameters at the interface differ by up to 10–15%.

Numerous interactions between a variety of polymers (PE, it-PP, st-PP, PET, polyamides, PLLA, etc.) and a variety of organic or mineral nucleation agents (e.g., talc) or polymers (e.g., polytetrafluoroethylene, PTFE) have been analyzed: nature of the contact planes, relative orientations of the cells, etc.[193] The polymer structure at the interface can be determined at the individual stem level by AFM after dissolution of the substrate.[194] The AFM image illustrates the pattern of methyl groups in the *ac* contact face of $\alpha$-it-PP[195] and the alternation of right- and left-handed helices in the syndiotactic st-PP stable crystal phase.[196] They also confirm the frustrated nature of the $\beta$-it-PP crystal structure.[197]

The nucleation of it-PP to generate its $\beta$-it-PP polymorph is very active.[198] A number of nucleation agents of different nature (minerals, liquid-crystalline polymers, polystyrene and acrylamides, etc.) can be found in the literature. It is fair to say, however, that their efficiency and, even more problematic, their $\beta$-it-PP specificity have not yet been explained in molecular or structural terms.

The efficiency of nucleating agents must be scaled versus an "ideally" nucleated polymer melt. This is possible in crystalline polymers since the crystalline entities—the lamellae—generate a highly dispersed system, actually at the ten or several tens of nanometers scale (in the range of lamellar thickness). When the crystalline samples are heated close to their melting temperature, the vast majority of the crystals are molten (over ≈99%). This melting generates multiple stable lamellar fragments that, on subsequent cooling, act as seeds for nucleation and growth. This "self-seeding" procedure is well-known in solution crystallization. It can also be adapted to polymer melts by using "standard" thermal histories (Figure 23).[199,200] More importantly, it helps generate an "ideally" nucleated polymer that fixes the ultimate goal when searching for new nucleation agents. For it-PP, the self-seeding procedure makes it possible to reach $10^{12}$–$10^{14}$ nuclei/cm$^3$ as compared to a "spontaneous" $10^6$ nuclei/cm$^3$ (generated spherulite size is smaller than 1 $\mu$m as compared to the spontaneous 100 $\mu$m).[199,200]

One limitation of this efficiency scale, not mentioned in the initial work, needs be emphasized. Depending on the quality of the structural matching, some nucleating agents may become active only at relatively low temperatures, below the higher crystallization temperatures potentially achievable. If highly dispersed, as would be the case for clarifying agents, their efficiency measured by the increase in crystallization temperature would not reflect the actual state (spherulite size) of the material.

The dispersion of the nucleation agents is a major factor in defining their efficiency. The most effective way to reach such dispersion is to generate "physical gels" of the nucleation agents.[199,200] The nucleation agents first dissolved in the molten polymer phase separate and crystallize before the onset of heterogeneous nucleation. The fibrillar nature results from highly anisotropic intermolecular forces in the crystal structure. Typically, these molecules have hydrogen bonds oriented in one direction only. In addition, these H bonds are "shielded" by side chains that provide the interacting interfaces with the polymer. This structural scheme was first encountered in sorbitol derivatives. The fibrils are ≈1 nm in cross section, which generates 4m$^2$/cm$^3$ of nucleation interface for a 1% nucleation agent concentration.[201] This same pattern has been



DOI: 10.1021/acs.macromol.7b00907
Macromolecules 2017, 50, 5995–6025

used to develop other highly efficient nucleation agents. Derivatives of 1,3,5-benzenetrisamides appear to provide a wide range of possibilities. They crystallize in the form of thin columnar supramolecular structures and are therefore classified as clarifying agents.[202] Their nucleating activity and phase specificity for e.g. $\alpha$-it-PP or $\beta$-it-PP can be tuned by appropriate selection of the lateral side chains. In a recent development, a family of 2,4,6-trimethyl-1,3,5-benzenetrisamides has been introduced that is efficient at concentrations as low as $3 \times 10^{-5}$ wt %.[203] In a parallel and similar approach, melt-miscible oxalamide-based nucleating agents have been tested—again for it-PP. The directionality of the H-bonds is maintained in these systems that, however, cannot produce the "columns" of the trisamides or sorbitol since the hydrogen bonding generates a sheet structure, much like in nylons.[204] Further research will probably concentrate on the dispersion issue and elaborate on the schemes developed so far. A clear alternative is to rely on nanodispersed materials—especially on carbon nanotubes that combine dispersion, elongated shape, and anisotropic properties. Oriented crystallization of PE on nanotubes has been documented and results in the formation of "nano-hybrid shish kebabs".[205,206]

Development of nucleation agents that impart different mechanical properties to the material is also a major industrial concern. Most immediate is the control of the crystal polymorphism, as is the case for $\beta$-it-PP (with higher impact strength, etc.) shown in Figure 23. Generation of controlled morphologies (lamellar structure and orientation) may also impart desired anisotropies of properties. In conventional injection molding the growth of lamellae is oriented perpendicular to the mold injection direction as a result of nucleation on "shishes" generated by shear near the mold walls slip. Because of their fibrillar nature, the clarifying nucleating agents are prone to being oriented in the molding process also away from the walls, in the interior of the mold. Lamellar growth on their surface may generate a much improved overall lamellar orientation.[207,208] To the exact opposite, a recently patented nucleation agent generates polyethylene lamellae that are oriented *parallel* to the molding injection direction.[209] In the present case, the elongated nucleation agent crystals are again oriented parallel to the flow direction, but the agent induces lamellae that are also oriented parallel to that injection direction, which results in enhanced stiffness of the parts.

The design of nucleating agents has been and remains a major scientific and industrial concern. The economic stakes are very high: reduced processing costs, improved and adapted properties of the final material. The development of metallocene catalysts has resulted in a variety of polyolefins with improved or more suited physical and/or mechanical properties. This is for example the case of copolymers of ethylene and olefins with longer alkyl side chain (pentene, hexene, etc.). As a rule, these copolymers have lower melting points and, contrary to polyethylene, have much reduced growth rates, which calls for the use of nucleation agents.

The discovery of nucleating agents has been mostly empirical—trial and error has been the rule for decades and probably will remain in use for some time. Significant progress has been made in the understanding of the polymer/NA epitaxial interactions although the experimental tools are less adapted when the nucleation agent is in the liquid-crystalline state or is intrinsically highly dispersed as in clarifying agents. It is to be hoped that the insights provided by fundamental developments will introduce a part of "educated guess" in the future trial and error searches for better nucleation agents. In a paper published very recently a different strategy to reach unprecedented levels of dispersion of the nucleating agent/species has been disclosed.[210] Specifically, a Ziegler Natta catalyst is used first in a reactor granule technology to synthesize a sequence of it-PVCH followed by a sequence of it-PP. The particles of iPP thus embody the nucleating agent and the dispersion of the latter is determined by the catalyst dispersion. Upon fast crystallization, a-iPP (rather than the usual mesomorphic phase) is generated, with nodules sized in the 20 nm range − significantly lower values than reached with "conventional" nucleating or even clarifying agents. The material thus produced has "outstanding and unexpected high mechanical strength and modulus as well as high ductility, flexibility and good transparency due to its nodular morphology".[210]

**Homogeneous Nucleation and Crystallization in Confined Space.** At the extreme opposite of the above concerns, a great deal of effort has been devoted to understand homogeneous nucleation. Crystallization is usually heterogeneously nucleated by impurities or nucleating agents. On the contrary, homogeneous nucleation in a "pure", nuclei-free melt results from fluctuations at high undercooling that generate ordered domains or "baby nuclei" of sufficient size to induce growth. In practice, homogeneous nucleation is frequently hidden since, upon cooling, heterogeneous nucleation and growth "eat up" the melt before it reaches the Tc domain where homogeneous nucleation becomes operative. Its investigation therefore remains mostly an academic concern, although thin films and fast cooling processes may result in homogeneous nucleation.

The classical means to investigate homogeneous nucleation is to physically limit the "spread" of spherulites, i.e., to investigate highly divided materials, in which growth induced by heterogeneous nucleation is physically *confined* within small domains. The standard "droplet experiment", in which the number of droplets far exceeds the number of heterogeneities and leaves nuclei-free droplets, has been used for decades to investigate these phenomena and to locate the Tc domain over which homogeneous nucleation becomes effective—in polymers, typically several tens of degrees below the heterogeneous nucleation range.[211] A similar dispersed state can be reached by a liquid−liquid phase separation in polymer/poor solvent solutions.[212] For bulk systems, generation of small domains is solely achieved in specifically processed polymer blends[213,214] or in blend laminates with nanometer-thin plies.[215] In many cases, it appears that nucleation is not really "homogeneous" but is induced by local molecular orientations generated by for example the domain walls, in an "interface-assisted" crystallization.[213] In the phase-separated PE droplets, the lamellae grow parallel to the droplet surface, suggesting a preferred molecular orientation normal to the droplet interface.[212] The polymer decoration technique illustrated in Figure 12 provides another example of nucleation of a germ-free polymer "melt", in the present case condensed PE vapors.[216] In this case, "homogeneous" nucleation is "assisted" by the presence of folds of the substrate lamellae and reproduces/highlights their azimuthal orientation. The molecules are also in-plane, as they lie parallel to the fold surface "interface". This specific orientation may explain the presence of short stretches of lamellae normal to the main orientation in bulk polyethylene,[216] and more generally be relevant to the observed,



DOI: 10.1021/acs.macromol.7b00907
*Macromolecules* 2017, 50, 5995−6025

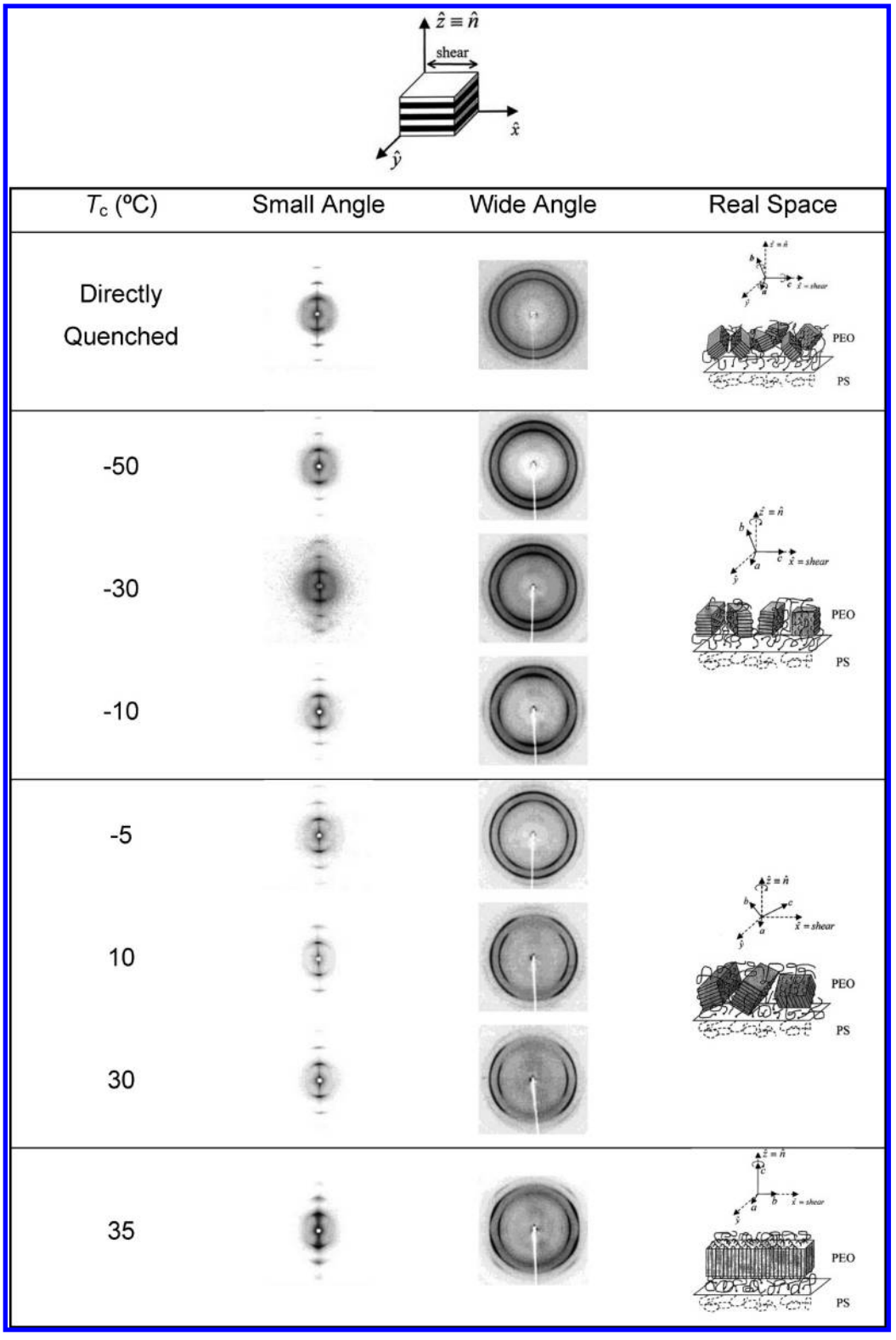


**Figure 24.** Small-angle X-ray scattering and wide-angle X-ray diffraction results for a lamella-forming PEO-*block*-PS diblock copolymer after the samples were mechanically sheared and isothermally crystallized at different temperatures. All the two-dimensional patterns were taken along the *x* direction of the samples, and the mechanical geometry of the sample is also shown. The schematics represent the crystal orientation changes in real space at different crystallization temperatures ($T_c$).[220] Reproduced with permission from ref 40. Copyright 2008 Elsevier.

similar stem orientation (to be described shortly) for highly divided systems after deep quench.

For *bulk* polymers, i.e., in the absence of nanoconfinement, homogeneous nucleation can only be reached for polymers with intrinsically slow growth rates (e.g., it-PS) that can be quenched to the glassy state. Studies on highly divided systems have confirmed that the undercooling reached depends on the size of the "droplet" or small domain. In poly(ethylene oxide)



DOI: 10.1021/acs.macromol.7b00907
*Macromolecules* 2017, 50, 5995−6025

droplets deposited on a thin polystyrene film 3−8 μm in size, namely, in the absence of nanoconfinement, homogeneous nucleation takes place in the in the −3 to −10 °C range. Furthermore, the nucleation rate scales with the volume of the crystallizable domain, indicating that homogeneous nucleation in the bulk of the droplets is observed.[216] In the much smaller domains of PEO−PS block copolymers, homogeneous crystallization takes place at down to ≈−25 to −30 °C.

The recent advent of ultrafast chip calorimetry has provided new means to investigate this whole field, as summarized in a recent contribution by Schick and Androsch.[218] Polymer nucleation at low temperature and crystallization kinetics can now be investigated also for "processing relevant cooling conditions".[219] Some major insights gained from these studies and as summarized in Schick and Androsch's review deal with the determination of cooling rates that suppress crystallization and nucleation, the analysis of the kinetics of homogeneous crystal nucleation (it is "fastest slightly above the glass transition temperature"), reorganization, and melting. In addition, annealing of a vitrified crystallizable polymer helps follow the formation of homogeneous nuclei. The authors also indicate that nucleation needs much faster local transport terms than usually considered in the so-called transport term of polymer crystallization theories.[168] Further developments are to be expected from the insights accessible via these ultrafast techniques.

**Crystallization in Confined Space. Structural Investigations.** Homogeneous nucleation and subsequent growth are best investigated not under microconfinement, but under nanoconfinement, since the impact of heterogeneous nucleation becomes marginal. Crystallization in confined space has gained considerable interest as a result of the development of block copolymers that associate an amorphous and a crystallizable sequence. Because of the familiar phase separation of the sequences, polymer crystallization takes place under nanometer sized confined environments at different dimensions: in thin films, in cylinders, and even in spheres (as two-, one-, and zero-dimensional growths, respectively). In addition to the polymer crystallization in the bulk, dimension control of polymer crystallization introduces new parameters, such as surface tension and substrate interactions and others. These parameters may significantly affect the crystal orientations, crystallinities, and structures of these polymers.

Many approaches are available to create confined environments. Inorganic matrices, alternating immiscible polymer thin film produced via extrusion, crystalline−amorphous diblock copolymers, and many other methods help achieve confinements of precisely controlled size and shape. Here we illustrate and focus on a convenient and effective approach that uses crystalline−amorphous diblock copolymers. Various ordered phase morphologies, such as lamellae, double gyroid, cylinders, and spheres, have been found in flexible, immiscible diblock copolymers on a nanometer length scale. These nanophase-separated structures become templates that confine the crystallizable blocks. If the glass transition temperature of the amorphous blocks is lower than the melting/crystallization temperatures of the crystalline blocks, the confinement is soft. The confinement becomes hard when the amorphous blocks vitrify prior to the crystallization; i.e., the order−disorder transition temperature of the block copolymer is higher than the glass transition temperature of the amorphous blocks that is further higher than the crystallization temperature of the crystalline blocks. The polymer crystallization under a hard nanoconfinement is achieved. The detailed confined structures are either one-dimensional (lamellae),[220−231] two-dimensional (cylinders),[232−234] or three-dimensional (spheres).[217,235−240]

Using a one-dimensional confinement as an example, the major issues are: (i) How are the crystals oriented in this nanoconfinement? (ii) When is the confinement condition released? (iii) At which length scale will this confinement not be felt by polymer crystallization? PEO-*block*-PS diblock copolymers were adopted in the investigations.[220] Based on combined two-dimensional small-angle X-ray scattering and wide-angle X-ray diffraction experiments, the crystal orientation (the *c*-axis of the PEO crystals) within the nanoscale confined lamellae changes in a complex sequence. It goes from random to perpendicular, then to inclined, and finally to parallel to the lamellar surface normal with increasing crystallization temperature, as shown in Figure 24 at a confinement scale of 8.8 nm. If however this one-dimensional nanoconfinement is released from 8.8 to 23.3 nm using different molecular masses of PEO-*block*-PS diblock copolymers, the crystallization temperature domain in which the *c*-axis is inclined becomes narrower, indicating a confinement size effect on the crystal orientation of the PEO crystals. This result suggests that when the size of confinement (in this case one-dimensional) becomes large enough, the homogeneous orientation of the *c*-axis in the PEO crystals would disappear.

Based on nucleation theory, different crystal orientations under the nanoconfined crystallization can be qualitatively explained via several aspects. First, under the 1D nanoconfined environment, the polymer melt may possess anisotropic thermal-density fluctuation, namely, along the confined direction may exhibit different behavior compared with nonconfined direction in a one-dimensional confined space. Therefore, the ability to overcome nucleation barrier may be varied.[227] Second, the crystallization in 1D confinement is governed by both primary nucleation and crystal growth processes. The free energy expressions must not only include the traditional bulk and surface free energies but also include a term for the energy resulting from the 1D confinement. Therefore, the PEO crystals with a specific orientation of the *c*-axis at each crystallization temperature must possess a local free energy minimum due to the effect of their neighboring PS glassy layers. Furthermore, the polymer crystallization is always kinetically governed by developing the maximum crystallinity in the fastest pathway under nanoconfined environment.

## ■ PERSPECTIVES AND CONCLUSION

Polymer crystals and crystallization are a wide field as they cover different levels of organization at length scales ranging from submolecular to morphology and, needless to say, their broad and various industrial applications. The personal "grooves" followed in the present account have touched on several aspects of this wide field but have left aside many important aspects. Among a number of such issues, only two aspects will be mentioned here, while being aware of the fact that this does not do full justice to many other fields and topics.

The invention of ultrahigh modulus PE fibers from precursor systems with limited entanglements (concentrated gels) has its roots in the initial observations of shish kebabs produced in stirred polymer solutions. It is one of the most spectacular scientific achievements and industrial development in the field of crystalline polymers.[241,242] A recent extension of



DOI: 10.1021/acs.macromol.7b00907
*Macromolecules* 2017, 50, 5995−6025

the underlying concept of reduced entanglements has led to the industrial production of ultrahigh molecular mass ($M_w$ > $10^4$ kDa) and at the same time disentangled PE. When sintered and stretched near their melting temperature, they lead to "unprecedented high-modulus high-strength tapes and films" via an industrially more tractable, solvent-free route. Tensile moduli >165 GPa could be reached, and biaxial drawing could be achieved for solvent-free materials.[243] This recent development illustrates how the contribution of innovative chemistry can push further a clever scientific means to manipulate the polymer structure and reach near "ultimate" properties. These different scientific and industrial breakthroughs deserve developments in their own right.

Another recent development is the newer and challenging field of plastic electronics and semiconducting polymers (SCP) such as regioregular poly(alkylthiphenes), the substituted poly(*p*-phenylenevinylene)s, and polyfluorenes. The anisotropy of their charge transport and light emission properties impose a full control of the structural order at multiple length scales[244−248] and, more specifically, their orientation and biorientation, as illustrated in a recent review.[249] These functional materials are widely used for the fabrication of electronic devices such as organic field effect transistors (OFETs)[250] and polymer solar cells (PSCs).[251] Among SCPs, regioregular poly(3-alkylthiophene)s (P3ATs) combine (relative) ease of processing (linked with the hairy rod character conferred by the alkyl side chains) with high charge carrier mobility. The charge transport is mostly intrachain along the conjugated chain axis thiophene units whereas interchain transport is linked with the $\pi-\pi$ interactions. Orientation is reached by using various techniques that may imply friction forces (e.g., rubbing) or by taking advantage of the orienting properties of polymer films or via epitaxial interactions with inorganic or organic substrates.[252,253] In the present structural context, these oriented materials help determine the influence of the side chains structure on the main chain organization of the poly(3-hexylthiophene) (P3HT). For the rigid P3HT epitaxially crystallized films helped establish the onset of chain folding depending on the chain length. For lower molecular weight (≤7.3 kDa), the crystals of P3HT are paraffin-like with extended chains. For higher molecular weight (≥18.8 kDa), chain folding intervenes, and lamellar structures are produced with alternation of crystalline cores and amorphous interlamellar layers.[91] Orientation and structuring processes help to take advantage of the intrinsically anisotropic properties of these materials, such as emitting polarized light. One potential application of highly oriented SCP layers lies in the replacement of conventional backlights in liquid crystal displays by polarized light emitting devices[254] as illustrated for P3HT, "a workhorse among conjugated semiconducting polymers".[255]

Even in their "spontaneous" form, polymer crystals and crystallization are a challenging research field. Some structural issues have been solved only after decades. The chirality issue in spherulites has been an "issue of a century long-standing", in the words of Andrew Keller. After 60 years of active research, an enormous amount of experimental results and investigation topics are available in the literature. To understand and master such a varied knowledge is extremely difficult. This is why reinventing this knowledge appears to become frequent in this field. However, in many cases, "new" is merely rediscovering the "old". "New" may also result from the development of new experimental tools—the major contributions of ultrafast DSC and near-field microscopies have been underlined in this contribution. The impact of molecular modeling and molecular simulation appears more contrasted. Molecular modeling and its earlier version, namely model building, have become a significant additional tool in (static) structure analysis (cf. the determination of the double helix of DNA and the $\alpha$ helix of proteins). Molecular simulation as a means to analyze dynamic processes taking place in polymer crystallization appears at present more limited. Polymer crystallization rests on short-range interactions (mostly, van der Waals forces) but generate a long-range order. This long-range order may include sorting out helical hands in polyolefins—a process associated in one case at least with widely different stem orientations ($\gamma$-it-PP). Generating or even simply reproducing such processes is beyond the present capabilities of molecular simulation. This structural complexity also underlines the need of "forensic" analyses based on detailed structural investigations, as illustrated in this contribution.

When looking at what is ahead, one must not forget that polymer crystals and crystallization are critically associated with many industrial products. The tendency of polymer academic researches to progressively diverge from industrial applications is alarming, since after all industry provides the research base and in certain ways the research platform for developing polymer science and engineering. Young researchers should establish close connections with industrial research, which implies emphasis on applications and material properties. As just indicated, the body of knowledge and the manipulation of morphologies (by control of nucleation and orienting processes) developed for the "common" polymers will be of great help in the field of functional/intelligent polymers. Because of these newer developments and the widespread use of crystalline polymers, we have a clear obligation to maintain and further develop our understanding of these materials.

Along another line, the polymer field must also definitely strengthen its interdisciplinary research activities in the broader context of materials and bioscience engineering. The section devoted to supramolecular structures developed in this Perspective illustrates one possible and promising such development. Many more bridges remain to be established.

From a general scientific point of view, polymer crystals and crystallization are an important part of the wider field of structure and phase transitions in condensed matter physics. Even though the theoretical and practical fundamentals have been established, what is the future for this field? We still have many issues and topics left unsolved—especially the most difficult ones. Yet, scientific research aims at understanding atomic and molecular structures and states as the first principles in materials—nature or man-made. Polymers serve as unique materials in many cases to understanding their crystals and crystallization processes. First is that polymer crystals usually are far away from thermodynamic equilibrium, and crystallization takes place in deep supercooled metastable states. Because of their flexible molecular shape, the polymer crystallization also involves a nature of entropy, in addition to enthalpy driven process. When polymer crystallization takes place in a space that is not three-dimensionally large in sizes, anisotropic behaviors of polymer crystals may dominate. As the space becomes small enough to reach molecular scale, the statistical "mean field" of theoretical approaches breaks down, and the single polymer crystallizes and becomes a "sudden-change event". The central question is whether we need a new crystallization theory? Current available theories and/or



DOI: 10.1021/acs.macromol.7b00907
*Macromolecules* 2017, 50, 5995−6025

models provide physical molecular images of how polymer crystallization takes place, and they are not able to predict crystallization behavior of polymers. Yet, new theories and simulations based on different conditions and environments are awaited for many physical principles to be further developed.

## AUTHOR INFORMATION


### Corresponding Author

*E-mail scheng@uakron.edu (S.Z.D.C.).

### ORCID

Toshikazu Miyoshi: 0000-0001-8344-9687

Stephen Z. D. Cheng: 0000-0003-1448-0546


### Notes

The authors declare no competing financial interest.

### Biographies

Bernard Lotz was born in Alsace, France, where he has spent most of his research career at the Centre de Recherches sur les Macromolecules, which became later the Institut Charles Sadron (ICS), a laboratory owned and run by the French Centre National de la Recherche Scientifique (CNRS). He is currently Emeritus Directeur de Recherche at CNRS. He has held various positions as visiting scientist and visiting professor at several American and Japanese Universities and Research Institutes. His research interests include the phase transitions, structure and morphology of crystalline polymers and biopolymers, and block copolymers. He has authored or coauthored over 300 research papers, reviews, and book chapters.

Toshikazu Miyoshi obtained his Ph.D in Chemistry (1997) at Kyoto University, Japan. After postdoctoral work at Institute of Polymer Research Dresden, Germany, he joined National Institute of Advanced Technology and Industrial Science (AIST), Japan, in 2000. He joined the department of polymer science at the University of Akron as an associate professor in 2010. His research interests include development of solid-state NMR techniques and their application to semicrystalline and glassy polymers, self-assembly, and biomaterials.

Stephen Z. D. Cheng received his Ph.D. degree at Rensselaer Polytechnic Institute at Troy, NY, in 1985. His research interests are in the area of chemistry, physics, and engineering of polymers and advanced functional materials including ordered structure, morphology, phase transition thermodynamics, kinetics, and molecular motions. His recent interests in particular are focusing on nanohybrid materials with different molecular chemical structures and physical topologies, architectures, and interactions and their assemblies in the bulk, solution, and thin films. He is also active in developing researches of conducting polymers, photovoltaics, polymer optics, and photonics. He currently holds the R. C. Musson & Trustees Professor and serves as the Dean of the College of Polymer Science and Polymer Engineering at the University of Akron. He is the recipient of Presidential Young Investigator Award (1991), John H. Dillon Medal (APS, 1995), Mettler-Toledo Award (NATAS, 1999), TA-Instrument Award (ICTAC, 2004), PMSE Cooperative Research Award (ACS, 2005), Polymer Physics Prize (APS, 2013), SPSJ International Award (Society of Polymer Science, Japan, 2017), and other awards and recognitions. Cheng has been a Fellow of AAAS and APS and an Honorable Fellow of Chinese Chemical Society. He has been elected as a member of the National Academic of Engineering of US (2008).

## ACKNOWLEDGMENTS

This work was supported by National Science Foundation (DMR-1409972).

## REFERENCES


(1) Lovinger, A. J. Foreword in *Phase Transitions in Polymers: The Rule of Metastable States*; Elsevier: 2008.

(2) Wasanasuk, K.; Tashiro, K.; Hanesaka, M.; Ohhara, T.; Kurihara, K.; Kuroki, R.; Tamada, T.; Ozeki, T.; Kanamoto, T. Crystal Structure Analysis of Poly(L-lactic Acid) r Form On the basis of the 2-Dimensional Wide-Angle Synchrotron X-ray and Neutron Diffraction Measurements. *Macromolecules* **2011**, *44*, 6441−6452.

(3) Wasanasuk, K.; Tashiro, K. Crystal structure and disorder in Poly(L-lactic acid) $\delta$ form ($\alpha'$ form) and the phase transition mechanism to the ordered $\alpha$ form. *Polymer* **2011**, *52*, 6097−6109.

(4) Sasaki, S.; Asakura, T. Helix Distortion and Crystal Structure of the $\alpha$-Form of Poly(L-lactide). *Macromolecules* **2003**, *36*, 8385−8390.

(5) Khoury, F. The spherulitic crystallization of isotactic polypropylene from solution: Evolution of monoclinic spherulites from dendritic chain-folded crystal precursors. *J. Res. Natl. Bur. Stand., Sect. A* **1966**, *70*, 29−61.




DOI: 10.1021/acs.macromol.7b00907
*Macromolecules* 2017, 50, 5995−6025

(6) Lotz, B.; Wittmann, J. C. The molecular origin of lamellar branching in the $\alpha$ (monoclinic) form of isotactic polypropylene. *J. Polym. Sci., Part B: Polym. Phys.* **1986**, *24*, 1541−1558.
(7) Brückner, S.; Valdo Meille, S. Non-parallel chains in crystalline $\gamma$-isotactic polypropylene. *Nature* **1989**, *340*, 455.
(8) Kressler, J. In *Polypropylene, an A-Z. reference*; Karger-Kocsis, J., Ed.; Kluwer Publishers: 1999.
(9) Lotz, B.; Graff, S.; Straupé, C.; Wittmann, J. C. Single crystals of $\gamma$ phase isotactic polypropylene: combined diffraction and morphological support for a structure with non-parallel chains. *Polymer* **1991**, *32*, 2902−2910.
(10) Cao, Y.; Van Horn, R. M.; Tsai, C. C.; Graham, M. J.; Jeong, K.-U.; Wang, B. J.; Auriemma, F.; De Rosa, C.; Lotz, B.; Cheng, S. Z. D. Epitaxially dominated crystalline morphology of the gamma-phase in isotactic polypropylene. *Macromolecules* **2009**, *42*, 4758−4768.
(11) Rieger, B.; Mu, X.; Mallin, D. T.; Rausch, M. D.; Chien, J. C. W. Degree of Stereochemical control of rac-Et[Ind]2ZrC12/MAO catalyst and properties of anisotactic polypropylenes. *Macromolecules* **1990**, *23*, 3559−3568.
(12) Auriemma, F.; De Rosa, C. Crystallization of metallocene-made isotactic polypropylene: Disordered modifications intermediate between the $\alpha$ and $\gamma$ forms. *Macromolecules* **2002**, *35*, 9057−9068.
(13) De Rosa, C.; Auriemma, F.; Circelli, T.; Waymouth, R. M. Crystallization of the $\alpha$ and $\gamma$ forms of isotactic polypropylene as a tool to test the degree of segregation of defects in the polymer chains. *Macromolecules* **2002**, *35*, 3622−3629.
(14) Toulouse, G. Theory of the frustration effect in spin glasses. *Commun. Phys.* **1977**, *3*, 115−119.
(15) Sadoc, J.-F.; Mosseri, R. In *Geometrical Frustration*; Cambridge University Press: 1999.
(16) Lotz, B. Frustration and frustrated crystal structures in polymers and biopolymers. *Macromolecules* **2012**, *45*, 2175−2189.
(17) Puterman, M.; Kolpak, F. J.; Blackwell, J.; Lando, J. B. X-Ray Structure determination of isotactic poly(2-vinylpyridine). *J. Polym. Sci., Polym. Phys. Ed.* **1977**, *15*, 805−819.
(18) Okihara, T.; Cartier, L.; Alberda van Ekenstein, G. O. R.; Lotza, B. Frustration and single crystal morphology of isotactic poly(2-vinylpyridine). *Polymer* **1999**, *40*, 1−11.
(19) Lotz, B.; Kopp, S.; Dorset, D. L. Sur une structure originale de polymères en conformation helicoïdale $3_1$ ou $3_2$. *C. R. Acad. Sci.(Paris)* **1994**, *319*, 187−192.
(20) Meille, S. V.; Ferro, D. R.; Brückner, S.; Lovinger, A. J.; Padden, F. J. Structure of $\beta$ isotactic polypropylene: A long-standing structural puzzle. *Macromolecules* **1994**, *27*, 2615−2622.
(21) Durand, D.; Doucet, J.; Livolant, F. A study of the structure of highly concentrated phases of DNA by X-ray diffraction. *J. Phys. II* **1992**, *2*, 1769−1783.
(22) Livolant, F.; Leforestier, A. Condensed phases of DNA: Structures and phase transitions. *Prog. Polym. Sci.* **1996**, *21*, 1115−1164.
(23) Kornyshev, A. A.; Leikin, S. Theory of interaction between helical molecules. *J. Chem. Phys.* **1997**, *107*, 3656−3674. Correction: *J. Chem. Phys.* **1998**, *108*, 7035.
(24) Petraccone, V.; Pirozzi, B.; Meille, S. V. Analysis of chain folding in crystalline isotactic polypropylene. The implications of tacticity and crystallographic symmetry. *Polymer* **1986**, *27*, 1665−1668.
(25) Ruan, J.; Thierry, A.; Lotz, B. A low symmetry structure of isotactic poly(4-methyl-pentene-1), form II. An illustration of the impact of chain folding on polymer crystal structure and unit-cell symmetry. *Polymer* **2006**, *47*, 5478−5493.
(26) Tashiro, K.; Hu, J.; Wang, H.; Hanesaka, M.; Saiani, A. Refinement of the Crystal Structures of Forms I and II of Isotactic Polybutene-1 and a Proposal of Phase Transition Mechanism between Them. *Macromolecules* **2016**, *49*, 1392−1404.
(27) Mathieu, C.; Stocker, W.; Thierry, A.; Wittmann, J. C.; Lotz, B. Epitaxy of isotactic poly(1-butene): new substrates, impact and attempt at recognition of helix orientation in form I′ by AFM. *Polymer* **2001**, *42*, 7033−7047.
(28) Lovinger, A. J.; Lotz, B.; Davis, D. D.; Padden, F. J. Structure and defects in fully syndiotactic polypropylene. *Macromolecules* **1993**, *26*, 3494−3503.
(29) Zhou, W.; Weng, X.; Jin, S.; Rastogi, S.; Lovinger, A. J.; Lotz, B.; Cheng, S. Z. D. Chain orientation and defects in lamellar single crystals of syndiotactic polypropylene fractions. *Macromolecules* **2003**, *36*, 9485−9491.
(30) Jaccodine, R. Observations of spiral growth steps in ethylene polymer. *Nature* **1955**, *176*, 305−306.
(31) Keller, A. A note on single crystals in polymers: Evidence of a folded-chain configuration. *Philos. Mag.* **1957**, *2*, 1171−1175.
(32) Till, P. H., Jr. The growth of single crystals of linear polyethylene. *J. Polym. Sci.* **1957**, *24*, 301−306.
(33) Fischer, E. W. Stufen- und spiralförmiges kristallwachstum bei hochpolymeren. *Z. Naturforsch., A: Phys. Sci.* **1957**, *12*, 753−754.
(34) Geil, P. H. *Polymer Single Crystals*; Wiley-Interscience: New York, 1963.
(35) Keller, A. Polymer crystals. *Rep. Prog. Phys.* **1968**, *31*, 623−704.
(36) Wunderlich, B. *Macromolecular Physics*; Academy Press: New York, 1973; Vol. *I*.
(37) Khoury, F.; Passaglia, E. The morphology of crystalline synthetic polymers. In *Treatise on Solid State Chemistry*; Hannay, N. B., Ed.; Plenum Press: New York, 1976; Vol. *3*, Chapter 6.
(38) Bassett, D. C. *Principles of Polymer Morphology*; Cambridge University Press: Cambridge, 1981.
(39) Cheng, S. Z. D.; Li, C. Y. Structure and formation of polymer single crystal textures. *Mater. Sci. Forum* **2002**, *408-412*, 25−38.
(40) Cheng, S. Z. D. *Phase Transitions in Polymer Transitions: The Rule of Metastable States*; Elsevier: 2008.
(41) Shcherbina, M. A.; Ungar, G. Analysis of crystal habits bounded by asymmetrically curved faces: Polyethylene oxide oligomers and poly(vinylidene fluoride). *Polymer* **2007**, *48*, 2087−2097.
(42) Shcherbina, M. A.; Ungar, G. Asymmetric curvatures of growth faces of polymer crystals. *Macromolecules* **2007**, *40*, 402−405.
(43) Keith, H. D.; Padden, F. J., Jr; Lotz, B.; Wittmann, J. C. Asymmetries of habit in polyethylene crystals grown from the melt. *Macromolecules* **1989**, *22*, 2230−2238.
(44) DiCorleto, J. A.; Bassett, D. C. On circular crystals of polyethylene. *Polymer* **1990**, *31*, 1971−1977.
(45) Khoury, F. Organization of macromolecules in the condensed phase: General discussion. *Faraday Discuss. Chem. Soc.* **1979**, *68*, 404−405.
(46) Khoury, F.; Bolz, L. H. Scanning transmission electron microscopy of polyethylene crystals. *Proc. - Annu. Meet., Electron Microsc. Soc. Am.* **1980**, *38*, 242−245.
(47) Khoury, F.; Bolz, L. The lateral growth habits and sectored character of polyethylene crystals. *Bull. Am. Phys. Soc.* **1989**, *30*, 493.
(48) Organ, S. J.; Keller, A. Solution crystallization of polyethylene at high temperatures. Part 1. Lateral crystal habits. *J. Mater. Sci.* **1985**, *20*, 1571−1585.
(49) Organ, S. J.; Keller, A. Solution crystallization of polyethylene at high temperatures. Part 2. Three-dimensional crystal morphology and melting behavior. *J. Mater. Sci.* **1985**, *20*, 1586−1601.
(50) Organ, S. J.; Keller, A. Solution crystallization of polyethylene at high temperatures. Part 3. The fold lengths. *J. Mater. Sci.* **1985**, *20*, 1602−1615.
(51) Toda, A. Growth of polyethylene single crystals from the melt: Change in lateral habit and regime I-II transition. *Colloid Polym. Sci.* **1992**, *270*, 667−681.
(52) Toda, A. Growth mode and curved lateral habits of polyethylene single crystals. *Faraday Discuss.* **1993**, *95*, 129−143.
(53) Toda, A.; Keller, A. Growth of polyethylene single crystals from the melt: Morphology. *Colloid Polym. Sci.* **1993**, *271*, 328−342.
(54) Passaglia, E.; Khoury, F. Crystal-growth kinetics and the lateral habits of polyethylene crystals. *Polymer* **1984**, *25*, 631−644.
(55) Kovacs, A. J.; Gonthier, A. Crystallization and fusion of self-seeded polymers. II. Growth rate, morphology, and isothermal thickening of single crystals of low molecular weight poly(ethylene oxide) fractions. *Kolloid Z. Z. Polym.* **1972**, *250*, 530−551.


DOI: 10.1021/acs.macromol.7b00907
*Macromolecules* 2017, 50, 5995−6025

(56) Kovacs, A. J.; Gonthier, A.; Straupé, C. J. Isothermal growth, thickening, and melting of poly(ethylene oxide) single crystals in the bulk. *J. Polym. Sci., Polym. Symp.* **1975**, *50*, 283−325.
(57) Kovacs, A. J.; Straupé, C.; Gonthier, A. Isothermal growth, thickening, and melting of poly(ethylene oxide) single crystals in the bulk. II. *J. Polym. Sci., Polym. Symp.* **1977**, *59*, 31−54.
(58) Kovacs, A. J.; Straupé, C. Isothermal growth, thickening, and melting of poly(ethylene oxide) single crystals in the bulk. Part 4. Dependence of pathological crystal habits on temperature and thermal history. *Faraday Discuss. Chem. Soc.* **1979**, *68*, 225−238.
(59) Kovacs, A. J.; Straupé, C. Isothermal growth, thickening, and melting of poly(ethylene oxide) single crystals in the bulk. III. Bilayer crystals and the effect of chain ends. *J. Cryst. Growth* **1980**, *48*, 210−226.
(60) Cheng, S. Z. D.; Chen, J. H. Nonintegral and integral folding crystal growth in low- molecular mass poly(ethylene oxide) fractions. III. Linear crystal growth rates and crystal morphology. *J. Polym. Sci., Part B: Polym. Phys.* **1991**, *29*, 311−327.
(61) Alcazar, D.; Thierry, A.; Schultz, P.; Kawaguchi, A.; Cheng, S. Z. D.; Lotz, B. Determination of the extent of lateral spread and secondary nucleation density in polymer single crystal growth. *Macromolecules* **2006**, *39*, 9120−9131.
(62) Alcazar, D.; Ruan, J.; Thierry, A.; Lotz, B. Structural matching between the polymeric nucleating agent isotactic poly-(vinylcyclohexane and isotactic polypropylene. *Macromolecules* **2006**, *39*, 2832−2840.
(63) Kopp, S.; Wittmann, J. C.; Lotz, B. Phase II to phase I crystal transformation in polybutene-1 single crystals: a reinvestigation. *J. Mater. Sci.* **1994**, *29*, 6159−6166.
(64) Tashiro, K.; Hu, J.; Wang, H.; Hanesaka, M.; Saiani, A. Refinement of the Crystal Structures of Forms I and II of Isotactic Polybutene-1 and a Proposal of Phase Transition Mechanism between Them. *Macromolecules* **2016**, *49*, 1392−1404.
(65) Lotz, B.; Mathieu, C.; Thierry, A.; Lovinger, A. J.; De Rosa, C.; Ruiz de Ballesteros, O.; Auriemma, F. Chirality constraints in crystal-crystal transformations: isotactic poly(1-Butene) versus syndiotactic polypropylene. *Macromolecules* **1998**, *31*, 9253−9257.
(66) Wasanasuk, K.; Tashiro, K. Structural Regularization in the Crystallization from the Glass or Melt of Poly(L-lactic Acid) Viewed from the Temperature-Dependent and Time-Resolved Measurements of FTIR and Wide-Angle/Small-Angle X-ray Scatterings. *Macromolecules* **2011**, *44*, 9650−9660.
(67) Di Lorenzo, M. L. Crystallization behavior of poly(L-lactic acid). *Eur. Polym. J.* **2005**, *41*, 569−575.
(68) Kawai, T.; Rahman, N.; Matsuba, G.; Nishida, K.; Kanaya, T.; Nakano, M.; Okamoto, H.; Kawada, J.; Usuki, A.; Honma, N.; Nakajima, K.; Matsuda, M. Crystallization and Melting Behavior of Poly(L-lactic acid). *Macromolecules* **2007**, *40*, 9463−9469.
(69) Cho, T. Y.; Strobl, G. Temperature dependent variations in the lamellar structure of poly(L-lactide). *Polymer* **2006**, *47*, 1036−1043.
(70) Lotz, B. Single crystals of the frustrated $\beta$-phase and genesis of the disordered $\alpha'$-phase of poly(L-lactic acid). *ACS Macro Lett.* **2015**, *4*, 602−605.
(71) Wittmann, J. C.; Grayer, V.; Lotz, B.; Smith, P.; Lommerts, B. J. Solid-solid phase transition in a perfectly alternating ethylene-carbon monoxide copolymer. *Polym. Prep. Am. Chem. Soc. Div. Polym. Chem.* **1995**, *36*, 257−258.
(72) Storks, K. H. An electron-diffraction examination of some linear high polymers. *J. Am. Chem. Soc.* **1938**, *60*, 1753−1761.
(73) Point, J. J. Enroulement hélicoïdal dans les sphérolithes de polyéthylène. *Bulletin de la Classe des Sciences, Académie Royale de Belgique* **1955**, *41*, 982−990.
(74) Keith, H. D.; Padden, F. J., Jr. The optical behavior of spherulites in crystalline polymers. Part I. Calculation of theoretical extinction patterns in spherulites with twisting crystalline orientation. *J. Polym. Sci.* **1959**, *39*, 101−122.
(75) Keith, H. D.; Padden, F. J., Jr. The optical behavior of spherulites in crystalline polymers. Part II. The growth and structure of the spherulites. *J. Polym. Sci.* **1959**, *39*, 123−138.
(76) Keller, A. Investigations on banded spherulites. *J. Polym. Sci.* **1959**, *39*, 151−173.
(77) Price, F. P. Extinction patterns of polymer spherulites. *J. Polym. Sci.* **1959**, *39*, 139−150.
(78) Fischer, E. W.; Lorenz, R. Über fehlordnungen in polyäthylen-einkristallen. *Colloid Polym. Sci.* **1963**, *189*, 97−110.
(79) Kobayashi, K. In *Kobunshi no Bussei (Properties of Polymers)*; Nakajima, A., Tadokoro, H., Tsuruta, T., Yuki, H., Ohtsu, T., Eds.; Kagakudojin: Kyoto, 1962; Chapter 11.
(80) Wittmann, J. C.; Lotz, B. Crystallization of paraffins and polyethylene from the "vapor phase". A new surface decoration technique for polymer crystals. *Makromol. Chem., Rapid Commun.* **1982**, *3*, 733−738.
(81) Wittmann, J. C.; Lotz, B. Polymer decoration: the orientation of polymer folds as revealed by the crystallization of polymer vapors. *J. Polym. Sci., Polym. Phys. Ed.* **1985**, *23*, 205−226.
(82) Wittmann, J. C.; Lotz, B. Epitaxial crystallization of polymers on organic and polymeric substrates. *Prog. Polym. Sci.* **1990**, *15*, 909−948.
(83) Chen, J. H.; Cheng, S. Z. D.; Wu, S. S.; Lotz, B.; Wittmann, J. C. Polymer decoration study in chain folding behavior of solution-grown poly(ethylene oxide) crystals. *J. Polym. Sci., Part B: Polym. Phys.* **1995**, *33*, 1851−1855.
(84) Li, C. Y.; Yan, D.; Cheng, S. Z. D.; Bai, F.; He, T.; Chien, L.-C.; Harris, F. W.; Lotz, B. Double-twisted helical lamellar crystals in a synthetic main-chain chiral polyester similar to biological polymers. *Macromolecules* **1999**, *32*, 524−527.
(85) Li, C. Y.; Cheng, S. Z. D.; Ge, J. J.; Bai, F.; Zhang, J. Z.; Mann, I. K.; Harris, F. W.; Chien, L.-C.; Yan, D.; He, T.; Lotz, B. Double twist in helical polymer "soft" crystals. *Phys. Rev. Lett.* **1999**, *83*, 4558−4561.
(86) Li, C. Y.; Cheng, S. Z. D.; Ge, J. J.; Bai, F.; Zhang, J. Z.; Mann, I. K.; Chien, L.-C.; Harris, F. W.; Lotz, B. Molecular orientations in flat-elongated and helical lamellar crystals of a main-chain nonracemic chiral polyester. *J. Am. Chem. Soc.* **2000**, *122*, 72−79.
(87) Kumaki, J.; Kawauchi, T.; Yashima, E. Two-dimensional folded chain crystals of a synthetic polymer in a Langmuir− Blodgett film. *J. Am. Chem. Soc.* **2005**, *127*, 5788.
(88) Mullin, N.; Hobbs, J. K. Direct imaging of polyethylene films at single-chain resolution with torsional tapping atomic force microscopy. *Phys. Rev. Lett.* **2011**, *107*, 197801.
(89) Savage, R. C.; Mullin, N.; Hobbs, J. K. Molecular Conformation at the Crystal−Amorphous Interface in Polyethylene. *Macromolecules* **2015**, *48*, 6160−6165.
(90) Ho, R.-M.; Cheng, S. Z. D.; Hsiao, B. S.; Gardner, K. H. Crystal morphology and phase identification in poly(aryl ether ketone)s and their copolymers. 1. Polymorphism in PEKK. *Macromolecules* **1994**, *27*, 2136−2140.
(91) Brinkmann, M.; Rannou, P. Effect of Molecular Weight on the Structure and Morphology of Oriented Thin Films of Regioregular Poly(3-hexylthiophene) Grown by Directional Epitaxial Solidification. *Adv. Funct. Mater.* **2007**, *17*, 101.
(92) Mena-Osteritz, E.; Meyer, A.; Langeveld-Voss, B. M. W.; Janssen, R. A.J.; Meijer, E. W.; Bäuerle, P. Two-Dimensional Crystals of Poly(3-Alkyl-Thiophenes)s: Direct Visualization of Polymer Folds in Submolecular Resolution. *Angew. Chem., Int. Ed.* **2000**, *39* (15), 2679−2684.
(93) Hong, Y.-l.; Chen, W.; Yuan, S.; Kang, J.; Miyoshi, T. Chain Trajectory of Semicrystalline Polymers As Revealed by Solid-State NMR Spectroscopy. *ACS Macro Lett.* **2016**, *5*, 355−358.
(94) Hong, Y.; Miyoshi, T. Chain-Folding Structure of a Semicrystalline Polymer in Bulk Crystals Determined by $^{13}C$-$^{13}C$ Double Quantum NMR. *ACS Macro Lett.* **2013**, *2*, 501−505.
(95) Hong, Y.-l.; Yuan, S.; Li, Z.; Ke, Y.; Nozaki, K.; Miyoshi, T. Three-Dimensional Conformation of Folded Polymers in Single Crystals. *Phys. Rev. Lett.* **2015**, *115*, 168301.
(96) Hong, Y-l.; Miyoshi, T. Elucidation of the Chain-Folding Structures of a Semi-crystalline Polymer in Single Crystals by Solid-state NMR Spectroscopy. *ACS Macro Lett.* **2014**, *3*, 556−559.


DOI: 10.1021/acs.macromol.7b00907
*Macromolecules* 2017, 50, 5995−6025

(97) Hong, Y-l.; Koga, T.; Miyoshi, T. Chain Trajectory and Crystallization Mechanism of Semicrystalline Polymer in Melt- and Solution-Grown Crystals as Studied by $^{13}C$-$^{13}C$ Double Quantum NMR. *Macromolecules* **2015**, *48*, 3282−3293.
(98) Li, Z.; Hong, Y-l.; Yuan, S.; Kang, J.; Kamimura, A.; Otsubo, A.; Miyoshi, T. Determinaiton of Chain Folding Structure of Isotactic-Polypropylene Melt-Grown $\alpha$ Crystals by $^{13}C$-$^{13}C$ Double Quantum NMR and Selective Isotopic Labeling. *Macromolecules* **2015**, *48*, 5752−5760.
(99) Yuan, S.; Li, Z.; Hong, Y-l.; Kang, J.; Kamimura, A.; Otsubo, A.; Miyoshi, T. Folding of Polymer Chains in the Early Stage of Crystallization. *ACS Macro Lett.* **2015**, *4*, 1382−1385.
(100) Yuan, S.; Li, Z.; Kang, J.; Hong, Y.; Kamimura, A.; Otsubo, A.; Miyoshi, T. Determination of Local Packing Structure of Mesomorphic Form of Isotactic Polypropylene by Solid-State NMR. *ACS Macro Lett.* **2015**, *4*, 143−146.
(101) Kang, J.; Yuan, S.; Hong, Y-l.; Chen, W.; Kamimura, A.; Otsubo, A.; Miyoshi, T. Unfolding of Isotactic Poly(propylene) under Uniaxial Stretching. *ACS Macro Lett.* **2016**, *5*, 65−68.
(102) Chen, W.; Wang, S.; Zhang, W.; Hong, Y-l.; Miyoshi, T. Molecular Structural Basis for Stereocomplex Formation of Poly-(Lactide)s in Dilute Solution. *ACS Macro Lett.* **2015**, *4*, 1264−1267.
(103) Shtukenberg, A. G.; Punin, Y. O.; Gunn, E.; Kahr, B. Spherulites. *Chem. Rev.* **2012**, *112*, 1805−1838.
(104) Lustiger, A.; Lotz, B.; Duff, T. S. The morphology of the spherulitic surface in polyethylene. *J. Polym. Sci., Part B: Polym. Phys.* **1989**, *27*, 561−579.
(105) Armon, S.; Efrati, E.; Kupferman, R.; Sharon, E. Geometry and Mechanics in the Opening of Chiral Seed Pods. *Science* **2011**, *333*, 1726−1730.
(106) Shtukenberg, A. G.; Punin, Y. O.; Gujral, A.; Kahr, B. Growth Actuated Bending and Twisting of Single Crystals. *Angew. Chem., Int. Ed.* **2014**, *53*, 672−699.
(107) Lotz, B.; Cheng, S. Z. D. A critical assessment of unbalanced surface stresses as the mechanical origin of twisting and scrolling of polymer crystals. *Polymer* **2005**, *46*, 577−610.
(108) Keith, H. D.; Padden, F. P., Jr Twisting orientation and the role of transient states in polymer crystallization. *Polymer* **1984**, *25*, 28−42.
(109) Boudet, A.; Kubin, L. P. Electron-microscopy observations of fold domain boundaries in polyethylene single-crystals. *J. Microsc. Spectrosc. Electron.* **1980**, *5*, 187−200.
(110) Maillard, D.; Prud'homme, R. E. Chirality Information Transfer in Polylactides: From Main-Chain Chirality to Lamella Curvature. *Macromolecules* **2006**, *39*, 4272−4275.
(111) Maillard, D.; Prud'homme, R. E. Crystallization of Ultrathin Films of Polylactides: From Chain Chirality to Lamella Curvature and Twisting. *Macromolecules* **2008**, *41*, 1705−1712.
(112) Wang, F.-D.; Ruan, J.; Huang, Y.-F.; Su, A.-C. Stem Tilt in the Contact Plane of Epitaxially Grown Polylactide Lamellae and Its Direct Correlation with Lamellar Bending. *Macromolecules* **2011**, *44*, 4335−4341.
(113) Rosenthal, M.; Bar, G.; Burghammer, M.; Ivanov, D. A. On the Nature of Chirality Imparted to Achiral Polymers by the Crystallization Process. *Angew. Chem.* **2011**, *123*, 9043−9047.
(114) Bassett, D. C. *Principles of Polymer Morphology*; Cambridg-eUniversity Press: Cambridge, 1981.
(115) Woo, E. M.; Lugito, G. Origins of periodic bands in polymer spherulites. *Eur. Polym. J.* **2015**, *71*, 27−60.
(116) Rosenthal, M.; Hernandez, J. J.; Odarchenko, Y. I.; Soccio, M.; Lotti, N.; Di Cola, E.; Burghammer, M.; Ivanov, D. A. Non-Radial Growth of Helical Homopolymer Crystals: Breaking the Paradigm of the Polymer Spherulite Microstructure. *Macromol. Rapid Commun.* **2013**, *34*, 1815−1819.
(117) Ye, H.-M.; Xu, J.; Guo, B.-H.; Iwata, T. Left- or Right-Handed Lamellar Twists in Poly[(R)-3-hydroxyvalerate] Banded Spherulite: Dependence on Growth Axis. *Macromolecules* **2009**, *42*, 694−701.
(118) Singfield, K. L.; Hobbs, J. K.; Keller, A. Correlation between main chain chirality and crystal twist direction in polymer spherulites. *J. Cryst. Growth* **1998**, *183*, 683−689.
(119) Lotz, B.; Gonthier-Vassal, A.; Brack, A.; Magoshi, J. Twisted single crystals of Bombyx mori silk fibroin and related model polypeptides with $\beta$ structure. A correlation with the twist of the $\beta$ sheets in globular proteins. *J. Mol. Biol.* **1982**, *156*, 345−357.
(120) Saracovan, I.; Cox, J. K.; Revol, J. F.; St. John Manley, R.; Brown, G. R. Optically active polyethers. 3. On the relationship between main-chain chirality and the lamellar morphology of solution-grown single crystals. *Macromolecules* **1999**, *32*, 717−725.
(121) Li, C. Y.; Cheng, S. Z. D.; Weng, X.; Ge, J. J.; Bai, F.; Zhang, J. Z.; Calhoun, B. H.; Harris, F. W.; Chien, L. C.; Lotz, B. Left or right, it is a matter of one methylene unit. *J. Am. Chem. Soc.* **2001**, *123*, 2462−2463.
(122) Ye, H.-M.; Xu, J.; Guo, B.-H.; Iwata, T. *Macromolecules* **2009**, *42* (3), 694−701.
(123) Wang, Z.; Li, Y.; Yang, J.; Gou, Q.; Wu, Y.; Wu, X.; Liu, P.; Gu, Q. Twisting of Lamellar Crystals in Poly(3-hydroxybutyrate-co-3-hydroxyvalerate) Ring-Banded Spherulites. *Macromolecules* **2010**, *43*, 4441−4444.
(124) Ye, H.-M.; Wang, J.-S.; Tang, S.; Xu, J.; Feng, X.-Q.; Guo, B.-H.; Xie, X.-M.; Zhou, J.-J.; Li, L.; Wu, Q.; Chen, G.-Q. Surface Stress Effects on the Bending Direction and Twisting Chirality of Lamellar Crystals of Chiral Polymer. *Macromolecules* **2010**, *43*, 5762−5770.
(125) Vaughan. Etching and morphology of poly(vinylidene fluoride. A.S. *J. Mater. Sci.* **1993**, *28*, 1805−1813.
(126) Frayer, P. D.; Koenig, J. L.; Lando, J. B. Infrared studies of chain folding in polymers. *J. Macromol. Sci., Part B: Phys.* **1969**, *3*, 329−335.
(127) Cai, W.; Li, C. Y.; Li, L.; Lotz, B.; Keating, M.; Marks, D. Submicrometer scroll/tubular lamellar crystals of Nylon 6,6. *Adv. Mater.* **2004**, *16*, 600−605.
(128) Xiong, H. M.; Chen, C. K.; Lee, K.; Van Horn, R. M.; Liu, Z.; Ren, B.; Quirk, R. P.; Thomas, E. L.; Lotz, B.; Ho, R. M.; Zhang, W. B.; Cheng, S. Z. D. Scrolled Polymer Single Crystals Driven by Unbalanced Surface Stresses: Rational Design and Experimental Evidence. *Macromolecules* **2011**, *44*, 7758−7766.
(129) Benz, K.-W.; Neumann, W. *Introduction to Crystal Growth and Characterization*; Wiley-VCH: Weinheim, 2014.
(130) Dong, X.-H.; Hsu, C.-H.; Li, Y.; Yue, K.; Huang, M.; Liu, H.; Sun, H.-J.; Wang, J.; Zhang, W.-B.; Lotz, B.; Cheng, S. Z. D. Supramolelar crystals and crystallization with nano-size motifs of giant molecules. *Adv. Polym. Sci.* **2016**, *276*, 183−213.
(131) Frank, F. C.; Kasper, J. S. Complex alloy structures regarded as sphere packings. I. Definitions and basic principles. *Acta Crystallogr.* **1958**, *11*, 184−190.
(132) Frank, F. C.; Kasper, J. S. Complex alloy structures regarded as sphere packings. II. Analysis and classification of representative structures. *Acta Crystallogr.* **1959**, *12*, 483−499.
(133) Che, S.; Garcia-Bennett, A. E.; Yokoi, T.; Sakamoto, K.; Kunieda, H.; Terasaki, O.; Tatsumi, T. A novel anionic surfactant templating route for synthesizing mesoporous silica with unique structure. *Nat. Mater.* **2003**, *2*, 801−805.
(134) Han, L.; Che, S. Anionic surfactant templated mesoporous silicas (AMSs). *Chem. Soc. Rev.* **2013**, *42*, 3740−3752.
(135) Gao, C.; Qiu, H.; Zeng, W.; Sakamoto, Y.; Terasaki, O.; Sakamoto, K.; Chen, Q.; Che, S. Formation mechanism of anionic surfactant-templated mesoporous silica. *Chem. Mater.* **2006**, *18*, 3904−3914.
(136) Tolbert, S. H. Mesoporous silica: Holey quasicrystals. *Nat. Mater.* **2012**, *11*, 749−751.
(137) Gao, C.; Sakamoto, Y.; Terasaki, O.; Cen, Q.; Che, S. Formation of diverse mesophases templated by a diprotic anionic surfactant. *Chem. - Eur. J.* **2008**, *14*, 11423−11428.
(138) Kim, S. A.; Jeong, K.-J.; Yethiraj, A.; Mahanthappa, M. K. Low-symmetry sphere packings of simple surfactant micelles induced by ionic sphericity. *Proc. Natl. Acad. Sci. U. S. A.* **2017**, *114*, 4072−4077.


DOI: 10.1021/acs.macromol.7b00907
*Macromolecules* 2017, 50, 5995−6025

(139) Lee, S.; Bluemle, M. J.; Bates, F. S. Discovery of a Frank-Kasper sigma Phase in Sphere-Forming Block Copolymer Melts. *Science* **2010**, *330*, 349−353.
(140) Lee, S.; Leighton, C.; Bates, F. S. Sphericity and symmetry breaking in the formation of Frank-Kasper phases from one component materials. *Proc. Natl. Acad. Sci. U. S. A.* **2014**, *111*, 17723−17731.
(141) Hayashida, K.; Dotera, T.; Takano, A.; Matsushita, Y. Polymeric quasicrystal: Mesoscopic quasicrystalline tiling in ABC star polymers. *Phys. Rev. Lett.* **2007**, *98*, 195502.
(142) Zhang, J.; Bates, F. S. Dodecagonal quasicrystalline morphology in a poly(styrene-b-isoprene-b- styrene-b-ethylene oxide) tetrablock terpolymer. *J. Am. Chem. Soc.* **2012**, *134*, 7636−7639.
(143) Chanpuriya, S.; Kim, K.; Zhang, J.; Lee, S.; Arora, A.; Dorfman, K. D.; Delaney, K. T.; Fredrickson, G. H.; Bates, F. S. Cornucopia of Nanoscale Ordered Phases in Sphere-Forming Tetrablock Terpolymers. *ACS Nano* **2016**, *10*, 4961−4972.
(144) Gillard, T. M.; Lee, S.; Bates, F. S. Dodecagonal quasicrystalline order in a diblock copolymer melt. *Proc. Natl. Acad. Sci. U. S. A.* **2016**, *113*, 5167−5172.
(145) Cheng, X. H.; Diele, S.; Tschierske, C. Molecular design of liquid-crystalline block molecules: Semifluorinated pentaerythritol tetrabenzoates exhibiting lamellar, columnar, and cubic mesophases. *Angew. Chem., Int. Ed.* **2000**, *39*, 592−595.
(146) Ungar, G.; Zeng, X. B. Frank-Kasper, quasicrystalline and related phases in liquid crystals. *Soft Matter* **2005**, *1*, 95−106.
(147) Hudson, S. D.; Jung, H. T.; Percec, V.; Cho, W. D.; Johansson, G.; Ungar, G.; Balagurusamy, V. S. K. Direct Visualization of Individual Cylindrical and Spherical Supramolecular Dendrimers. *Science* **1997**, *278*, 449−452.
(148) Ungar, G.; Liu, Y. S.; Zeng, X. B.; Percec, V.; Cho, W. D. Giant Supramolecular Liquid Crystal Lattice. *Science* **2003**, *299*, 1208−1211.
(149) Rosen, B. M.; Wilson, C. J.; Wilson, D. A.; Peterca, M.; Imam, M. R.; Percec, V. Dendron-Mediated Self-Assembly, Disassembly, and Self-Organization of Complex Systems. *Chem. Rev.* **2009**, *109*, 6275−6540.
(150) Sun, H. J.; Zhang, S. D.; Percec, V. From structure to function via complex supramolecular dendrimer systems. *Chem. Soc. Rev.* **2015**, *44*, 3900−3923.
(151) Shevchenko, E. V.; Talapin, D. V.; Kotov, N. A.; O'Brien, S.; Murray, C. B. Structural diversity in binary nanoparticle superlattices. *Nature* **2006**, *439*, 55−59.
(152) Huang, M. J.; Hsu, C. H.; Wang, J.; Mei, S.; Dong, X. H.; Li, Y. W.; Li, M. X.; Liu, H.; Zhang, W.; Aida, T. Z.; Zhang, W. B.; Yue, K.; Cheng, S. Z. D. Selective assemblies of giant tetrahedra via precisely controlled positional interactions. *Science* **2015**, *348*, 424−428.
(153) Yang, S. Supramolecular lattices from tetrahedral nanobuilding blocks. *Science* **2015**, *348*, 396−397.
(154) Yue, K.; Huang, M. J.; Marson, R. L.; He, J. L.; Huang, J. H.; Zhou, Z.; Wang, J.; Liu, C.; Yan, X. S.; Wu, K.; Guo, Z. H.; Liu, H.; Zhang, W.; Ni, P. H.; Wesdemiotis, C.; Zhang, W. B.; Glotzer, S. C.; Cheng, S. Z. D. Geometry induced sequence of nanoscale Frank-Kasper and quasicrystal mesophases in giant surfactants. *Proc. Natl. Acad. Sci. U. S. A.* **2016**, *113*, 14195−14200.
(155) Hsieh, I. F.; Sun, H.-J.; Fu, Q.; Lotz, B.; Cavicchi, K. A.; Cheng, S. Z. D. Phase structural formation and oscillation in polystyrene-block-polydimethylsiloxane thin films. *Soft Matter* **2012**, *8*, 7937−7944.
(156) Hsu, C.-H.; Dong, X.-H.; Lin, Z.; Ni, B.; Lu, P.; Jiang, Z.; Tian, D.; Shi, A.-C.; Thomas, E. L.; Cheng, S. Z. D. Tunable Affinity and Molecular Architecture Lead to Diverse Self-Assembled Supramolecular Structures in Thin Films. *ACS Nano* **2016**, *10*, 919−929.
(157) Cheng, S. Z. D. Phase transitions in Polymers. In *The Role of Metastability*; Elsevier: 2008.
(158) *Simulation Methods for Polymers*; Kotelyanskii, M., Theodorou, D. N., Eds.; CRC Press: 2004.
(159) Goldbeck-Wood, G. Simulation of polymer crystallization kinetics with the Sadler/Gilmer model. *Polymer* **1990**, *31*, 586−592.
(160) Waheed, N.; Lavine, M. S.; Rutledge, G. C. Molecular simulation of crystal growth in n-eicosane. *J. Chem. Phys.* **2002**, *116*, 2301−2309.
(161) Hu, W. Chain folding in polymer melt crystallization studied by dynamic Monte Carlo simulations. *J. Chem. Phys.* **2001**, *115*, 4395−4401.
(162) Liu, C.; Muthukumar, M. Langevin dynamics simulations of early-stage polymer nucleation and crystallization. *J. Chem. Phys.* **1998**, *109*, 2536−2542.
(163) Armitstead, K.; Goldbeck-Wood, G. Polymer crystallization theories. *Adv. Polym. Sci.* **1992**, *100*, 221.
(164) Hoffman, J. D.; Lauritzen, J. I., Jr. Crystallization of bulk polymers with chain folding-Theory of growth of lamellar spherulites. *J. Res. Natl. Bur. Stand., Sect. A* **1961**, *65A*, 297.
(165) Lauritzen, J. I., Jr.; Hoffman, J. D. Extension of theory of growth of chain-folded polymer crystals to large undercoolings. *J. Appl. Phys.* **1973**, *44*, 4340.
(166) Hoffman, J. D.; Frolen, L. J.; Ross, G. S.; Lauritzen, J. I., Jr. Growth-rate of spherulites and axialites from melt in polyethylene fractions-regime-1 and regime-2 crystallization. *J. Res. Natl. Bur. Stand., Sect. A* **1975**, *79A*, 671.
(167) Hoffman, J. D.; Davis, G. T.; Lauritzen, J. I., Jr. In *Treatise on Solid State Chemistry*; Hannay, N. B., Ed.; Plenum: New York; 1976; Vol. *3*, Chapter 7, pp 497− 614.
(168) Frank, F. C.; Tosi, M. On the theory of polymer crystallization. *Proc. R. Soc. London, Ser. A* **1961**, *263*, 323 (Frank & Tosi 1961).
(169) Doye, J. P. K. Computer simulations of the mechanism of thickness selection in polymer crystals. *Polymer* **2000**, *41*, 8857−8867.
(170) Point, J. J. Reconsideration of kinetic theories of polymer crystal growth with chain folding. *Faraday Discuss. Chem. Soc.* **1979**, *68*, 167.
(171) Point, J. J. A new theoretical approach of the secondary nucleation at high supercooling. *Macromolecules* **1979**, *12*, 770.
(172) Wunderlich, B. Crystal nucleation, growth, annealing. In *Macromolecular Physics*; Academic Press: New York, 1976; Vol. *2*.
(173) Hikosaka, M. Unified theory of nucleation of folded-chain crystals and extended-chain crystals of linear-chain polymers. *Polymer* **1987**, *28*, 1257.
(174) Hikosaka, M. Unified theory of nucleation of folded-chain crystals (FCCs) and extended-chain crystals (ECCs) of linear-chain polymers: 2. Origin of FCC and ECC. *Polymer* **1990**, *31*, 458.
(175) Sadler, D. M. When is a nucleation theory not a nucleation theory? *Polym. Commun.* **1986**, *27*, 140.
(176) Sadler, D. M. New explanation for chain folding in polymers. *Nature* **1987**, *326*, 174.
(177) Sadler, D. M. On the growth of two dimensional crystals: 2. Assessment of kinetic theories of crystallization of polymers. *Polymer* **1987**, *28*, 1440.
(178) Sadler, D. M.; Gilmer, G. H. Preferred fold lengths in polymer crystals: predictions of minima in growth rates. *Polym. Commun.* **1987**, *28*, 242.
(179) Sadler, D. M. On the growth of two dimensional crystals. I. Fluctuations and the relation of step free energies to morphology. *J. Chem. Phys.* **1987**, *87*, 1771.
(180) Sadler, D. M.; Gilmer, G. H. A model for chain folding in polymer crystals: rough growth faces are consistent with the observed growth rates. *Polymer* **1984**, *25*, 1446−1452.
(181) Sadler, D. M.; Gilmer, G. H. Rate-Theory Model of Polymer Crystallization. *Phys. Rev. Lett.* **1986**, *56*, 2708.
(182) Sadler, D. M.; Gilmer, G. H. Selection of lamellar thickness in polymer crystal growth: A rate-theory model. *Phys. Rev. B: Condens. Matter Mater. Phys.* **1988**, *38*, 5684.
(183) Ungar, G.; Keller, A. Time-resolved synchrotron X-ray study of chain-folded crystallization of long paraffins. *Polymer* **1986**, *27*, 1835.


DOI: 10.1021/acs.macromol.7b00907
*Macromolecules* 2017, 50, 5995−6025

(184) Cheng, S. Z. D.; Lotz, B. Nucleation control in polymer crystallization: structural and morphological probes in different length- and time-scales for selection processes. *Philos. Trans. R. Soc., A* **2003**, *361*, 517−537.
(185) Cheng, S. Z. D.; Lotz, B. Enthalpic and entropic origins of nucleation barriers during polymer crystallization: the Hoffman-Lauritzen theory and beyond. *Polymer* **2005**, *46*, 8662−8681.
(186) Olmsted, P. D.; Poon, W. C. K.; McLeish, T. C. B.; Terrill, N. J.; Ryan, A. J. Spinodal-assisted crystallization in polymer melts. *Phys. Rev. Lett.* **1998**, *81*, 373.
(187) Imai, M.; Mori, K.; Mizukami, T.; Kaji, K.; Kanaya, T. Structural formation of poly(ethylene terephthalate) during the induction period of crystallization: 2. Kinetic analysis based on the theories of phase separation. *Polymer* **1992**, *33*, 4457−4462.
(188) Strobl, G. From the melt via mesomorphic and granular crystalline layers to lamellar crystallites: A major route followed in polymer crystallization? *Eur. Phys. J. E: Soft Matter Biol. Phys.* **2000**, *3*, 165−184.
(189) Strobl, G. A thermodynamic multiphase scheme treating polymer crystallization and melting. *Eur. Phys. J. E: Soft Matter Biol. Phys.* **2005**, *18*, 295−309.
(190) Strobl, G. Crystallization and melting of bulk polymers: new observations, conclusions and a thermodynamic scheme. *Prog. Polym. Sci.* **2006**, *31*, 398.
(191) Kim, M. H.; Londono, J. D.; Habenschuss, A. Structure of molten stereoregular polyolefins with different side-chain sizes: Linear polyethylene, polypropylene, poly (1-butene), and poly (4-methyl-1-pentene). *J. Polym. Sci., Part B: Polym. Phys.* **2000**, *38*, 2480−2485.
(192) Heck, B.; Hugel, T.; Iijima, M.; Strobl, G. Steps in the formation of the partially crystalline state. *Polymer* **2000**, *41*, 8839−8848.
(193) Thierry, A.; Lotz, B. In *Handbook of Polymer Crystallization*; Piorkowska, E., Rutledge, G., Eds.; Wiley: Hoboken, NJ, 2013; Chapter 8, pp237−264.
(194) Lotz, B. Analysis and observation of polymer crystal structures at the individual stem level. *Adv. Polym. Sci.* **2005**, *180*, 17−44.
(195) Stocker, W.; Magonov, S. N.; Cantow, H. J.; Wittmann, J. C.; Lotz, B. Contact faces of epitaxially crystallized and phase isotactic polypropylene observed by atomic force microscopy. *Macromolecules* **1993**, *26*, 5915−5923.
(196) Stocker, W.; Schumacher, M.; Graff, S.; Lang, J.; Wittmann, J. C.; Lovinger, A. J.; Lotz, B. Direct observation of right and left helical hands of syndiotactic polypropylene by atomic force microscopy. *Macromolecules* **1994**, *27*, 6948−6955.
(197) Stocker, W.; Schumacher, M.; Graff, S.; Thierry, A.; Wittmann, J. C.; Lotz, B. Epitaxial crystallization and AFM investigation of a frustrated polymer structure: Isotactic poly(propylene), $\beta$ phase. *Macromolecules* **1998**, *31*, 807−814.
(198) Housmans, J.-W.; Gahleitner, M.; Peters, G. W. M.; Meijer, H. E. H. Structure−property relations in molded, nucleated isotactic polypropylene. *Polymer* **2009**, *50*, 2304−2319.
(199) Fillon, B.; Lotz, B.; Thierry, A.; Wittmann, J. C. Self-nucleation and enhanced nucleation of polymers. Definition of a convenient calorimetric "efficiency scale" and evaluation of nucleating additives in isotactic polypropylene ($\alpha$ phase). *J. Polym. Sci., Part B: Polym. Phys.* **1993**, *31*, 1395−1405.
(200) Fillon, B.; et al. Self-seeding and Recrystallization of Isotactic Polypropylene (a phase) Investigated by Differential Scanning Calorimetry. *J. Polym. Sci., Part B: Polym. Phys.* **1993**, *31*, 1383−1393.
(201) Thierry, A.; Straupé, C.; Lotz, B.; Wittmann, J. C. Physical gelation: a path towards "ideal" dispersion of additives in polymers. *Polym. Commun.* **1990**, *31*, 299−301.
(202) Schmidt, M.; Wittmann, J. J.; Kress, R.; Schneider, D.; Steuernagel, S.; Schmidt, H.-W.; Senker, J. Crystal Structure of a Highly Efficient Clarifying Agent for Isotactic Polypropylene. *Cryst. Growth Des.* **2012**, *12*, 2543−2551.
(203) Abraham, F.; Kress, R.; Smith, P.; Schmidt, H.-W. A New Class of Ultra-Efficient Supramolecular Nucleating Agents for Isotactic Polypropylene. *Macromol. Chem. Phys.* **2013**, *214*, 17−24.
(204) Deshmukh, Y. S.; Wilsens, C. H. R. M.; Leoné, N.; Portale, G.; Harings, J. A. W.; Rastogi, S. Melt-miscible Oxalamide Based Nucleating Agents and Their Nuclation Efficiency in Isotactic polypropylene. *Ind. Eng. Chem. Res.* **2016**, *55*, 11756−11766.
(205) Li, L.; Li, B.; Hood, M. A.; Li, C. Y. Carbon nanotube induced polymer crystallization: The formation of nanohybrid shish−kebabs. *Polymer* **2009**, *50*, 953−965.
(206) Li, C. Y.; Li, L.; Cai, W.; Kodjie, S. L.; Tenneti, K. K. Nanohybrid shish-kebabs: Periodically functionalized carbon nanotubes. *Adv. Mater.* **2005**, *17*, 1198−1202.
(207) Luo, B.; Li, H.; Zhang, Y.; Xue, F.; Guan, P.; Zhao, J.; Zhou, C.; Zhang, W.; Li, J.; Huo, H.; Shi, D.; Yu, D.; Jiang, S. Wall Slip Effect on Shear-Induced Crystallization Behavior of Isotactic Polypropylene Containing $\beta$-Nucleating Agent. *Ind. Eng. Chem. Res.* **2014**, *53*, 13513−13521.
(208) Balzano, L.; Rastogi, S.; Peters, G. W. M. Flow Induced Crystallization in Isotactic Polypropylene-1,3:2,4-Bis(3,4-dimethylbenzilidene)sorbitol Blends: Implications on Morphology of Shear and Phase Separation. *Macromolecules* **2008**, *41*, 399−408.
(209) *Leaflet on Milliken's Hyperform HPN 210 M*; Milliken Company: Spartanburg, SC.
(210) De Rosa, C.; Auriemma, F.; Tarallo, O.; Di Girolamo, R.; Troisi, E. M.; Esposito, S.; Liguori, D.; Piemontesi, F.; Vitale, G.; Morini, G. Tailoring properties of polypropylene in the polymerization reactor using polymeric nucleating agents as prepolymer on the Ziegler-Natta catalyst granule. *Polym. Chem.* **2017**, *8*, 655.
(211) Koutsky, J. A.; Walton, A. G.; Baer, E. Nucleation of polymer droplets. *J. Appl. Phys.* **1967**, *38*, 1832−1839.
(212) Schaaf, P.; Lotz, B.; Wittmann, J. C. Liquid-liquid phase separation and crystallization in binary polymer systems. *Polymer* **1987**, *28*, 193−200.
(213) He, Z.; Shi, W.; Chen, F.; Liu, W.; Liang, Y.; Han, C. C. Effective Morphology Control in an Immiscible Crystalline/Crystalline Blend by Artificially Selected Viscoelastic Phase Separation Pathways. *Macromolecules* **2014**, *47*, 1741−1748.
(214) Sánchez, M. S.; Mathot, V.; Poel, G. V.; Groeninckx, G.; Bruls, W. Crystallization of polyamide confined in sub-micrometer droplets dispersed in a molten polyethylene matrix. *J. Polym. Sci., Part B: Polym. Phys.* **2006**, *44*, 815−825.
(215) Wang, H.; Keum, J. K.; Hiltner, A.; Baer, E.; Freeman, B.; Rozanski, A.; Galeski, A. Confined crystallization of polyethylene oxide in nanolayer assemblies. *Science* **2009**, *323*, 757−760.
(216) Wittmann, J. C.; Hodge, A. M.; Lotz, B. Epitaxial crystallization of polymers onto benzoic acid: polyethylene and paraffins, aliphatic polyesters, and polyamides. *J. Polym. Sci., Polym. Phys. Ed.* **1983**, *21*, 2495−2509.
(217) Massa, M. V.; Dalnoki-Veress, K. Homogeneous crystallization of poly(ethylene oxide) confined to droplets: the dependence of the crystal nucleation rate on length scale and temperature. *Phys. Rev. Lett.* **2004**, *92*, 255509.
(218) Schick, C.; Androsch, R. New Insights into Polymer Crystallization by Fast Scanning Chip Calorimetry. In *Fast Scanning Calorimetry*; Schick, C., Mathot, V., Eds.; Springer: pp 463−535.
(219) Rhoades, A. M.; Williams, J. L.; Androsch, R. Crystallization kinetics of polyamide 66 at processing-relevant cooling conditions and high supercooling. *Thermochim. Acta* **2015**, *603*, 103−109.
(220) Zhu, L.; Cheng, S. Z. D.; Calhoun, B. H.; Ge, Q.; Quirk, R. P.; Thomas, E. L.; Hsiao, B. S.; Yeh, F.; Lotz, B. Crystallization Temperature-Dependent Crystal Orientations within Nanoscale Confined Lamellae of a Self-Assembled Crystalline−Amorphous Diblock Copolymer. *J. Am. Chem. Soc.* **2000**, *122*, 5957−5967.
(221) Li, C. Y.; Ge, J. J.; Bai, F.; Calhoun, B. H.; Harris, F. W.; Cheng, S. Z. D.; Chien, L.-C.; Lotz, B.; Keith, H. D. Early-Stage Formation of Helical Single Crystals and Their Confined Growth in Thin Film. *Macromolecules* **2001**, *34*, 3634−3641.
(222) Zhu, L.; Calhoun, B. H.; Ge, Q.; Quirk, R. P.; Cheng, S. Z. D.; Thomas, E. L.; Hsiao, B. S.; Yeh, F.; Liu, L.; Lotz, B. Initial-Stage Growth Controlled Crystal Orientations in Nanoconfined Lamellae of


DOI: 10.1021/acs.macromol.7b00907
*Macromolecules* 2017, 50, 5995−6025

a Self-Assembled Crystalline−Amorphous Diblock Copolymer. *Macromolecules* **2001**, *34*, 1244−1251.
(223) Zhu, L.; Cheng, S. Z. D.; Calhoun, B. H.; Ge, Q.; Quirk, R. P.; Thomas, E. L.; Hsiao, B. S.; Yeh, F.; Lotz, B. Phase structures and morphologies determined by self-organization, vitrification, and crystallization: confined crystallization in an ordered lamellar phase of PEO-b-PS diblock copolymer. *Polymer* **2001**, *42*, 5829−5839.
(224) Zhu, L.; Mimnaugh, B. R.; Ge, Q.; Quirk, R. P.; Cheng, S. Z. D.; Thomas, E. L.; Lotz, B.; Hsiao, B. S.; Yeh, F.; Liu, L. Hard and soft confinement effects on polymer crystallization in microphase separated cylinder-forming PEO-b-PS/PS blends. *Polymer* **2001**, *42*, 9121−9131.
(225) Loo, Y.-L.; Register, R. A.; Ryan, A. J. Modes of Crystallization in Block Copolymer Microdomains: Breakout, Templated, and Confined. *Macromolecules* **2002**, *35*, 2365−2374.
(226) Zhu, L.; Cheng, S. Z. D.; Huang, P.; Ge, Q.; Quirk, R. P.; Thomas, E. L.; Lotz, B.; Hsiao, B. S.; Yeh, F.; Liu, L. Nanoconfined Polymer Crystallization in the Hexagonally Perforated Layers of a Self-Assembled PS-b-PEO Diblock Copolymer. *Adv. Mater. (Weinheim, Ger.)* **2002**, *14*, 31−34.
(227) Zhu, L.; Huang, P.; Chen, W. Y.; Ge, Q.; Quirk, R. P.; Cheng, S. Z. D.; Thomas, E. L.; Lotz, B.; Hsiao, B. S.; Yeh, F.; Liu, L. Nanotailored Crystalline Morphology in Hexagonally Perforated Layers of a Self-Assembled PS-b-PEO Diblock Copolymer. *Macromolecules* **2002**, *35*, 3553−3562.
(228) Huang, P.; Zhu, L.; Guo, Y.; Ge, Q.; Jing, A. J.; Chen, W. Y.; Quirk, R. P.; Cheng, S. Z. D.; Thomas, E. L.; Lotz, B.; Hsiao, B. S.; Avila-Orta, C. A.; Sics, I. Confinement Size Effect on Crystal Orientation Changes of Poly(ethylene oxide) Blocks in Poly(ethylene oxide)-b-polystyrene Diblock Copolymers. *Macromolecules* **2004**, *37*, 3689−3698.
(229) Hsiao, M.-S.; Chen, W. Y.; Zheng, J. X.; Van Horn, R. M.; Quirk, R. P.; Ivanov, D. A.; Thomas, E. L.; Lotz, B.; Cheng, S. Z. D. Poly(ethylene oxide) Crystallization within a One-Dimensional Defect-Free Confinement on the Nanoscale. *Macromolecules* **2008**, *41*, 4794−4801.
(230) Hsiao, M.-S.; Zheng, J. X.; Leng, S.; Van Horn, R. M.; Quirk, R. P.; Thomas, E. L.; Chen, H.-L.; Hsiao, B. S.; Rong, L.; Lotz, B.; Cheng, S. Z. D. Crystal Orientation Change and Its Origin in One-Dimensional Nanoconfinement Constructed by Polystyrene-block-poly(ethylene oxide) Single Crystal Mats. *Macromolecules* **2008**, *41*, 8114−8123.
(231) Hsiao, M.-S.; Zheng, J. X.; Van Horn, R. M.; Quirk, R. P.; Thomas, E. L.; Chen, H.-L.; Lotz, B.; Cheng, S. Z. D. Poly(ethylene oxide) Crystal Orientation Change under 1D Nanoscale Confinement using Polystyrene-block-poly(ethylene oxide) Copolymers: Confined Dimension and Reduced Tethering Density Effects. *Macromolecules* **2009**, *42*, 8343−8352.
(232) Quiram, D. J.; Register, R. A.; Marchand, G. R.; Adamson, D. H. Chain Orientation in Block Copolymers Exhibiting Cylindrically Confined Crystallization. *Macromolecules* **1998**, *31*, 4891−4898.
(233) Huang, P.; Guo, Y.; Quirk, R. P.; Ruan, J.; Lotz, B.; Thomas, E. L.; Hsiao, B. S.; Avila-Orta, C. A.; Sics, I.; Cheng, S. Z. D. Comparison of poly(ethylene oxide) crystal orientations and crystallization behaviors in nano-confined cylinders constructed by a poly(ethylene oxide)-b-polystyrene diblock copolymer and a blend of poly(ethylene oxide)-b-polystyrene and polystyrene. *Polymer* **2006**, *47*, 5457−5466.
(234) Huang, P.; Zheng, J. X.; Leng, S.; Van Horn, R. M.; Jeong, K.-U.; Guo, Y.; Quirk, R. P.; Cheng, S. Z. D.; Lotz, B.; Thomas, E. L.; Hsiao, B. S. Poly(ethylene oxide) Crystal Orientation Changes in an Inverse Hexagonal Cylindrical Phase Morphology Constructed by a Poly(ethylene oxide)-block-polystyrene Diblock Copolymer. *Macromolecules* **2007**, *40*, 526−534.
(235) Loo, Y.-L.; Register, R. A.; Ryan, A. J. Polymer Crystallization in 25-nm Spheres. *Phys. Rev. Lett.* **2000**, *84*, 4120−4123.
(236) Massa, M. V.; Carvalho, J. L.; Dalnoki-Veress, K. Confinement Effects in Polymer Crystal Nucleation from the Bulk to Few-Chain Systems. *Phys. Rev. Lett.* **2006**, *97*, 247802.
(237) Carvalho, J. L.; Dalnoki-Veress, K. Surface nucleation in the crystallisation of polyethylene droplets. *Eur. Phys. J. E: Soft Matter Biol. Phys.* **2011**, *34*, 6.
(238) Loo, Y.-L.; Register, R. A.; Ryan, A. J.; Dee, G. T. Polymer Crystallization Confined in One, Two, or Three Dimensions. *Macromolecules* **2001**, *34*, 8968−8977.
(239) Sun, L.; Zhu, L.; Ge, Q.; Quirk, R. P.; Xue, C.; Cheng, S. Z. D.; Hsiao, B. S.; Avila-Orta, C. A.; Sics, I.; Cantino, M. E. Comparison of crystallization kinetics in various nanoconfined geometries. *Polymer* **2004**, *45*, 2931−2939.
(240) Kim, D.-Y.; Nayek, P.; Kim, S.; Ha, K. S.; Jo, M. H.; Hsu, C.-H.; Cao, Y.; Cheng, S. Z. D.; Lee, S. H.; Jeong, K.-U. Suppressed Crystallization of Rod-Disc Molecule by Surface Anchoring Confinement. *Cryst. Growth Des.* **2013**, *13*, 1309−1315.
(241) Smith, P.; Lemstra, P. J. US Patent 4344908, 1982.
(242) Lemstra, P. L.; Kirschbaum, R. Speciality products based on commodity polymers. *Polymer* **1985**, *26*, 1372−1384.
(243) Rastogi, S.; Yao, Y.; Ronca, S.; Bos, S.; van der Eem, J. Unprecedented high-modulus high-strength tapes and Films of ultrahigh molecular weight polyethylene via solvent-free route. *Macromolecules* **2011**, *44*, 5558−5568.
(244) Crossland, E. J. W.; Tremel, K.; Fischer, F.; Rahimi, K.; Reiter, G.; Steiner, U.; Ludwigs, S. Anisotropic Charge Transport in Spherulitic Poly (3-hexylthiophene) Films. *Adv. Mater.* **2012**, *24*, 839.
(245) Jimison, L. H.; Toney, M. F.; McCulloch, I.; Heeney, M.; Salleo. Charge-Transport Anisotropy Due to Grain Boundaries in Directionally Crystallized Thin Films of Regioregular Poly (3-hexylthiophene). A. *Adv. Mater.* **2009**, *21*, 1568.
(246) Grell, M.; Bradley, D. D. C. Polarized luminescence from oriented molecular materials. *Adv. Mater.* **1999**, *11*, 895.
(247) Banach, M. J.; Friend, R. H.; Sirringhaus, H. Influence of the molecular weight on the thermotropic alignment of thin liquid crystalline polyfluorene copolymer films. *Macromolecules* **2003**, *36*, 2838.
(248) Zheng, Z.; Yim, K.-H.; Saifullah, M. S. M.; Welland, M. E.; Friend, R. H.; Kim, J.-S.; Huck, W. T. S. Uniaxial alignment of liquid-crystalline conjugated polymers by nanoconfinement. *Nano Lett.* **2007**, *7*, 987.
(249) Brinkmann, M. Structure in thin films of $\pi$-conjugated semiconductors from the perspective of transmission electron microscopy. In *Conjugated Polymers and Oligomers: Structural and Soft Matter Aspects*; World Scientific: 2017.
(250) Salleo, A. Charge transport in polymeric transistors. *Mater. Today* **2007**, *10*, 38−45.
(251) Sirringhaus, H.; Brown, P. J.; Friend, R. H.; Nielsen, M. M.; Bechgaard, K.; Langeveld-Voss, B. M. W.; Spiering, A. J. H.; Janssen, R. A. J.; Meijer, E. W.; Herwig, P.; de Leeuw, D. M. Two-dimensional charge transport in self-organized, high-mobility conjugated polymers. *Nature* **1999**, *401*, 685−688.
(252) Brinkmann, M.; Wittmann, J.-C. Orientation of Regioregular Poly(3-hexylthiophene) by Directional Solidification: A Simple Method to Reveal the Semicrystalline Structure of a Conjugated Polymer. *Adv. Mater.* **2006**, *18*, 860.
(253) Brinkmann, M.; Hartmann, L.; Biniek, L.; Tremel, K.; Kayunkid, N. Orienting Semi-Conducting $\pi$-Conjugated Polymers. *Macromol. Rapid Commun.* **2014**, *35*, 9−26.
(254) Zheng, Z.; Yim, K.-H.; Saifullah, M. S. M.; Welland, M. E.; Friend, R. H.; Kim, J.-S.; Huck, W. T. S. Uniaxial alignment of liquid-crystalline conjugated polymers by nanoconfinement. *Nano Lett.* **2007**, *7*, 987.
(255) Brinkmann, M. Structure and Morphology Control in Thin Films of Regioregular Poly(3-hexylthiophene). *J. Polym. Sci., Part B: Polym. Phys.* **2011**, *49*, 1218−1233.



DOI: 10.1021/acs.macromol.7b00907
*Macromolecules* 2017, 50, 5995−6025